ISBN 978-82-471-2359-1 (printed ver.)
ISBN 978-82-471-2360-7 (electronic ver.)
ISSN 1503-8181

Doctoral theses at NTNU, 2010:191

Sara Paunonen

Influence of moisture on the performance of polyethylene coated solid fiberboard and boxes

Sara Paunonen

Doctoral Thesis

Doctoral theses at NTNU, 2010:191

NTNU
Norwegian University of
Science and Technology
Thesis for the degree of
philosophiae doctor
Faculty of Natural Sciences and Technology
Department of Chemical Engineering

NTNU
Norwegian University of
Science and Technology

NTNU
Norwegian University of
Science and Technology

Sara Paunonen

Influence of moisture on the performance of polyethylene coated solid fiberboard and boxes

Thesis for the degree of philosophiae doctor

Trondheim, October 2010

Norwegian University of
Science and Technology
Faculty of Natural Sciences and Technology
Department of Chemical Engineering

NTNU
Norwegian University of
Science and Technology

NTNU
Norwegian University of Science and Technology

Thesis for the degree of philosophiae doctor

Faculty of Natural Sciences and Technology
Department of Chemical Engineering

ISBN 978-82-471-2359-1 (printed ver.)
ISBN 978-82-471-2360-7 (electronic ver.)
ISSN 1503-8181

Doctoral Theses at NTNU, 2010:191

Printed by Tapir Uttrykk

Begynn! Bare på den måten kan det umulige bli mulig.
- Thomas Carlyle

ABSTRACT

Effects of moisture on the mechanical properties of one commercial solid fiberboard grade and on the compression strength of mill-fabricated transport boxes made from this material were studied. The solid fiberboard (1220 g/m^2) has four middle layers made of old corrugated container (OCC). The middle layers are strongly internally sized with rosin sizing. The outer layers on both sides are made of bleached machine finished kraft paper. The kraft paper has extrusion coated low-density polyethylene (LDPE) double-layer as moisture barrier. The six paper and paperboard layers are glued together in an industrial lamination process. The boxes have unusual design including double-panel walls and webbed corners, and they are used in wet and humid conditions for transporting fresh round fish. The transportation takes up to eight days at the ambient environment of 4°C and 90-100% RH. These conditions are taken as the framework of the study.

Results show that the LDPE coating considerably slows down the transverse moisture penetration. The in-plane diffusivity ($5.9 \cdot 10^{-10}$ m^2/s, 27°C, 50/90% RH) was determined with an integrated unsteady state moisture transport model and was found to be nine times higher than the transverse diffusivity through the PE layer. Based on the diffusivity, water vapor can theoretically affect 80 mm from the open unsealed board edge during transport. Experiments show that liquid water penetrates 40-50 mm during eight days. In the middle of the sheet the moisture content increases moderately, approximately 0.3 percentage points during transport. The packaging producer's main concern is thus to ensure that the open material edges are at least 80 mm away from the load bearing sections of the box. Due to uneven moisture penetration into the boxes, the average moisture of a box is a questionable measure of moisture pick-up. Instead one should consider the moisture content of the load bearing parts.

The role of the adhesion layers in bending stiffness of the solid paperboard was modeled with laminate models. Results show that the adhesion layers affect the mechanical properties of the combined board and need to be addressed in the models. Best agreement with the measured bending stiffness values was obtained by a 11-layer model, where the properties of the adhesion layers are taken from the paper-glue-paper sandwich tests. The PE and kraft paper are regarded as one layer in the model. With this model, the calculated bending stiffnesses are close to the measured reference at 50% RH in MD (difference 1%). In 90% RH and in MD the results are 14% lower. Neglecting the adhesion layers gives 5% lower values in 50% RH and 18% in 90% RH compared to the reference measurement in MD. In each of the cases, the difference from reference is larger for the CD material direction. Three thickness measurement techniques (ISO,

STFI, and SEM) were used to gather input data for the bending stiffness model. In this application, the ISO technique provided best results compared to the other techniques.

It was found that the top-to bottom failure of a box can be expressed as a critical vertical displacement that is independent of moisture content. Similar results have been previously discovered when studying simpler structures like corrugated board panels and regular slotted containers (RSC). This research indicates that the strain dependent failure criterion also applies on more complex box structures.

Keywords: paper laminates, solid fiberboard, moisture, mechanical properties, diffusivity, hygroexpansion, bending stiffness, box compression.

PREFACE

This thesis with the title “Influence of moisture on the performance of polyethylene coated solid fiberboard and boxes“ has been submitted for fulfilment of the Ph.D. degree at the Norwegian University of Science and Technology (NTNU). The work has been performed at the Biorefinery and Fiber Technology group at the Department of Chemical Engineering from May 2007 to June 2010. The period from August 2009 to January 2010 was spent at Innventia in Stockholm. Prof. Øyvind Weiby Gregersen has been the supervisor of this work. Dr. Johan Alfthan and Lic. Eng. Thomas Trost supervised the work at Innventia.

The work has been part of the FiBaPack project (Novel Fibre-Based Water Barrier Packaging of Fresh Fish and Agricultural Products), which was lead by Marianne Lenes, PFI AS. The project was financed by Peterson AS, The Foundation for Pulp and Paper Research Institute, Eka Chemicals AB, and The Research Council of Norway.

The work and the results are presented in the following three papers and in one report:

Paper A: Paunonen, S., Lenes, M. and Gregersen, Ø. (2010), Moisture content of polyethylene coated solid fiberboard after industrial lamination, Accepted for publication in the Packaging Technology and Science.

Paper B: Paunonen, S., Lenes, M. and Gregersen, Ø. (2010), Modeled and measured bending stiffness of polyethylene coated solid fiberboard, Accepted for publication in the Nordic Pulp and Paper Research Journal.

Paper C: Paunonen, S. and Gregersen, Ø. (2010), The effect of moisture content on compression strength of boxes made of solid fiberboard with polyethylene coating - An experimental study, Submitted to the Journal of Applied Packaging Research.

Report A: Paunonen, S. and Gregersen, Ø. (2010), Effect of polyethylene coating on in-plane hygroexpansion of solid fiberboard.

The author has done all the planning, the testing and the data analysis in Papers A-C and in Report A. In Paper B, the SEM pictures were taken by Per Olav Johnsen at PFI. The author has written all the papers. Øyvind Gregersen has taken part in the planning of the work, commented the results, and proof-read the manuscripts. Marianne Lenes proof-read Papers A-B.

Additional publications

- Paunonen, S. and Gregersen, Ø. (2010), Modelled and measured bending stiffness of polyethylene coated multi-layer paperboard at two moisture contents, Oral presentation, 6th International Symposium - Moisture and Creep Effects on Paper, Board and Containers, Madison, Wisconsin, USA.

ACKNOWLEDGEMENTS

This work was part of a large consortium project, which was lead and held together by Ms. Marianne Lenes at the Paper and Fibre Research Institute PFI in Trondheim. I thank PFI people for providing the equipment and the required training that I needed for my experiments. The financial support from Peterson AS, The Foundation for Pulp and Paper Research Institute, Eka Chemicals AB, and The Research Council of Norway is gratefully acknowledged.

I thank Ms. Gunvor Haga Levang at Peterson Emballage and Ms. Helle Kvam at Peterson Linerboard, both in Ranheim in Trondheim, for providing the materials to the research, and answering my questions concerning the production process.

I want to thank my supervisor prof. Øyvind Weiby Gregersen at Norwegian University of Science and Technology for the guidance throughout the work and proof-reading the papers and the thesis. The transformation from a process chemist to a paper physicist has required a lot of work, and at times the need for guidance has been substantial.

In scientific terms, my stay at Innventia in Stockholm was a necessary and beneficial period. Dr. Johan Alfthan, Lic. Eng. Thomas Trost, Dr. Jan-Erik Gustafsson and Tech. Lic. Petri Mäkelä formed a very pleasant, highly skilful and professional group to work with. I wouldn't have this thesis without your comments and support. Dr. Johan Alfthan and Lic. Eng. Thomas Trost are thanked for the careful proof-reading and commenting on the papers and the thesis.

The research institutes VTT and KCL in Finland allowed me to take a leave to pursue a Ph.D. I'm thankful for the encouragement I got from my colleagues at KCL to take the leap and start working with paper physics. I have many friends in Finland whom I always enjoy meeting while there. It has been proven many times that distance and time does not kill real friendship.

My fellow students and post-doc's at NTNU Biorefinery and fiber technology group: Asuka, Cathy, Collin, Galina, Janga, Klodian, Marco, Marius, Mihaela, Swarnima, Tuan-Anh, it is you who have made my every day. One could never hope for better colleagues and nicer environment to work in. I sincerely hope the very best for each of you in your lives. Many of you will scatter around the world after finishing your Ph.D. I hope that we will meet again.

Behind every great man and great woman there is mother. Thank you Mom for patiently listening to the latest happenings, success and sometimes great despair in my numerous projects. Once I listened to my Dad defending his thesis on satellite laser ranging systems. I will have him in my heart when I stand on the podium defending mine.

Science never happens in a vacuum, unattached from life. The scientific everyday work is done from the ever so personal foundation of emotions, attitudes, and beliefs. My years as a Ph.D. student in Trondheim have profoundly affected that foundation. I have had the great luck and the great joy to meet people who have changed my way of being, feeling and thinking. Thank you for coming into my life.

In Trondheim, 7th July 2010,

Sara Paunonen

TABLE OF CONTENTS

Chapter 1
INTRODUCTION

1.1 Motivation of the study

The Norwegian export of aquacultured salmon amounted to 740 000 tons in 2008 (Statistics Norway 2008). 86% of this amount is exported as fresh round fish mainly to the EU region by road transportation (Norwegian Seafood Council 2008). 32 million boxes are needed annually for the transportation. At present, the oil based expanded polystyrene (EPS) dominates as box material. Table 1–1 shows the share of different materials used in fresh fish boxes in the UK as an example.

Table 1–1: Estimated usage of wholesale fresh fish boxes in the UK (Seafish Industry Authority 1996).

Box material	Millions of boxes per year
Expanded polystyrene	14
Solid fiberboard	5
Corrugated plastic	0.6
Corrugated fiberboard	0.5

Specialized paper producers have a motivation to increase their market share in this business, especially since the present environmental movement favors the use of transport boxes made from renewable wood fiber over polystyrene boxes made from fossil raw materials. Developments in integrated transport and distribution systems with improved cold chain have opened the market for paper-based boxes that have good strength and ecological properties but suffer from relatively poor insulation properties. Usage of paper-based boxes also offers other benefits, for example substantial saving in space when the boxes are delivered and stored flat at the fish supplier's premises.

Wood fiber-based materials have the inherent ability to absorb environmental moisture, which weakens the mechanical properties of the material and the performance of the products made from it. Typical methods to shield the material against moisture include internal sizing, usage of wet strength agents, and application of various barrier coatings on the surface. To deliver the product intact to the receiver, the fish transport boxes need to resist high relative humidity and presence of water, and maintain its strength during the transportation.

Solid fiberboard is a paperboard grade that is converted from containerboards. It is a rigid, heavy, and impact resistant grade specially designed for packaging applications

where wet or greasy products are transported in humid environment. It is made in an industrial off-line laminator by gluing together several paper and paperboard plies. Solid fiberboard can be finished with a variety of lining papers and optionally with a polyethylene (PE) coating.

1.2 Objectives

This Ph.D. work concentrates on studying the effects of environmental factors during the transport of round fish on the mechanical properties of polyethylene coated solid fiberboard and on the performance of transport boxes converted from this material. One particular laminated solid fiberboard grade is studied. The box is of unusual, more complicated design compared to, for example, the well-known regular slotted containers.

Polyethylene coated fiberboard is a special packaging material which is inadequately studied. The material covers a large field of disciplines and complicated interactions: behavior of paper materials (paperboard layers), chemistry of polymers (polyethylene coating and adhesive used in lamination), interactions between paper and polymers (e.g., adhesion of polyethylene to the paper substrate in extrusion coating, and wetting and adhesion of glue components in lamination). In this work, the main focus is on the combined board behavior. When studying the properties of combined board, the explanations are often sought from the paperboard medium side, as paperboard accounts for the major part of the grammage of the solid fiberboard.

The major environmental factor studied is moisture in vapor and liquid form. Effects of temperature exposure are not studied. The material testing is done at a constant environment: two constant relative humidity levels (50% and 90% RH) and one temperature (23°C). The box testing is done at an atmosphere close to the actual climate of the transport (constant 4°C and 90% RH). Creep of the boxes at constant relative humidity (RH) is studied; creep in varying humidity is left out since the climate is constant during the transport. Studies of time-varying loadings on boxes are also excluded. The duration of the transport is eight days, which is often taken as the time frame of the experiments.

Scientifically the work brings together several tests and analyses into a single picture of how selected properties of a particular paperboard change and how a particular box type fails, when in contact with moisture. The role of the glue layer on the mechanical properties of the laminate is examined. The moisture resistance of polyethylene coating is identified. The practical contribution of the work is to find solutions and suggestions that aid in producing transport boxes with appropriate material and design choices that result in fulfilling the requirements of the intended use.

The contents of the work are divided into the following areas:

- Characterization of the rate of liquid water and water vapor penetration into the polyethylene coated fiberboard and the corresponding change in moisture content.

- Determination of the effect of moisture and glue layers on the bending stiffness of the laminated solid fiberboard. Bending stiffness is selected since it is a central structural property of packaging boards.
- Study of the moisture penetration into and the effects of moisture content on compression behavior of PE coated transport boxes during the simulated end-use situation.

1.3 Outline of the work

This thesis is organized in five chapters.

Chapter 1: Introduction.

Chapter 2: Literature. The solid fiberboard material and the converting operations to produce boxes are introduced. A lot is known about the fiber level phenomena that cause the wood fiber-based materials to be strongly affected by moisture. Chapter 2 introduces briefly these basics, and gives understanding and background on the phenomena observed when studying paperboard and paperboard boxes. Relevant literature on how exposure to environmental moisture and temperature affect the properties and behavior of polyethylene coated paper, solid fiberboard medium and solid board boxes, is reviewed.

Chapter 3: Materials and methods. The chapter gives an overview of the solid fiberboard grade studied in this work and of the experimental methods and analyses presented in the articles.

Chapter 4: Summary of the appended papers. This thesis is based on three articles and one report. The chapter summarizes the main findings.

Chapter 5: Conclusions. In this chapter conclusions are drawn from the results and suggestions are given for future work.

Chapter 2 BACKGROUND

2.1 Transport packaging

European Parliament and Council Directive 94/62/EC of 20 December 1994 on Packaging and Packaging Waste (EU 1994) defines the terms packaging and transport packaging as follows:

Packaging *shall mean all products made of any materials of any nature to be used for the containment, protection, handling, delivery and presentation of goods, from raw materials to processed goods, from the producer to the user or the consumer. 'Non-returnable' items used for the same purposes shall also be considered to constitute packaging. (EU, 1994).*

Transport packaging *or tertiary packaging, i.e. packaging conceived so as to facilitate handling and transport of a number of sales units or grouped packagings in order to prevent physical handling and transport damage. Transport packaging does not include road, rail, ship and air containers. (EU, 1994).*

In the case of transporting round fresh fish, no primary packages (sales package) or secondary packages (grouped sales packages) are used. Approximately 25 kg fresh fish is packed with 3-5 kg ice in a transport package. A number of transport packages are loaded on a standardized pallet, which is made of wood or plastic materials. The loaded pallet with an optional plastic wrap constitutes the unit cargo that is moved with, e.g., fork lifts.

2.1.1 Packaging functions

In general, the package contains and protects the product, provides convenience in handling and usage of it, informs and sells. It must also meet the economic and environmental requirements (Soroka 2009). These basic packaging functions have different emphasis depending on the level of the packaging (sales, grouped, transport packaging) and destination (consumer, industry).

The primary requirement for transport packages for fresh fish is to provide adequate protection against physical damage caused by deformation, humidity, water, vibration, mechanical shocks, temperature, tampering, and abrasion (Soroka 2009). In this study, the effects of relative humidity and liquid water on the compression strength of the box are studied.

2.1.2 Converting operations

Manufacture of any paper-based package comprises of certain converting operations that vary according to the product in question. Figure 2.1 shows the specific chain of operations for transport box manufacture from solid fiberboard sheets to filling at the customer. Lamination is an off-line process where several paperboard layers are glued together. The process is explained closer in Chapter 2.1.3. Most packages have printing that informs and sells the product. In the case of solid fiberboard (solidboard), the printing is done on the polyethylene coated paper with flexography technique before the lamination.

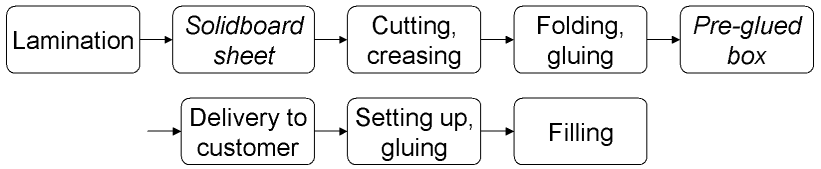

Figure 2.1: Converting operations to manufacture solid fiber boxes and operations at the customer.

Cutting and creasing (die-cutting) are essential operations in manufacturing a box. A box blank is cut from the sheet, and creasing lines that allow the box to be folded and erected in a controlled manner are pressed on the blank in the same operation. A flat bed cutting machine contains a plywood plate, with sharp cutting knifes and blunt creasing rules, that is pressed against a counter die, see Figure 2.2. A crease is formed when the blunt rule meets a groove. Sharp knifes cut the material. These two operations make a blank that is folded and pre-glued on relevant parts to make a box before the final setting up.

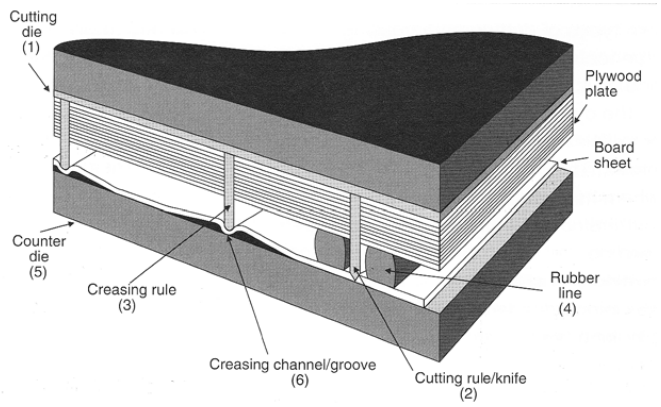

Figure 2.2: Flat bed cutting and creasing of a board sheet (Lahti et al. 2008).

Boxes are delivered flat to the customer. At the customer's premises, a machine erects the pre-glued collapsed box and glues the small flaps that hold the box in set-up position to be ready to be filled.

2.1.3 Solid fiberboard

Solid fiberboard is a stiff, puncture and water resistant paper-based packaging material, which consists of two or more plies of paperboard glued together. It varies in thickness from 0.8 mm to 4.5 mm and in grammage from 550 g/m^2 to 3000 g/m^2 (Kirwan 2005).

Containerboards are raw materials specially manufactured to produce solid fiberboard and corrugated fiberboard. In 2006, containerboard was the biggest grade by volume accounting for 31% (117.3 million tonnes) of the world's pulp and paper output (Mies et al. 2006). The production and consumption of solid fiberboard and corrugated fiberboard as combined board grades are not recorded. Statistics about packaging show that the production of solid fiberboard is marginal compared to corrugated board. In 2006, solid fiber boxes accounted for about 0.5% of U.S. total industry corrugated shipments (391.4 milliard m^2) (Mies et al. 2006).

Typical uses

Solid fiberboard covers a wide range of packaging and display applications ranging from packaging from meat, poultry and fish in boxes and trays to promotional trays and game boxes. Most often it is used as a distribution package (Kirwan 2005).

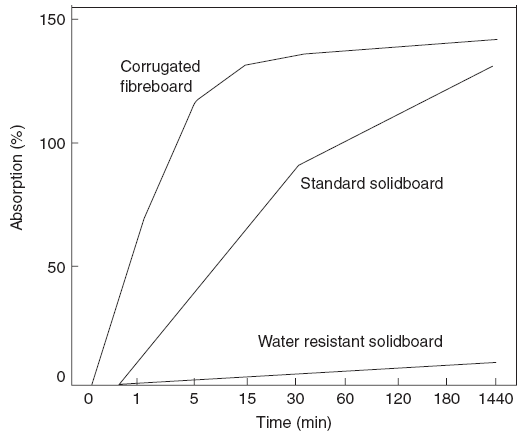

Figure 2.3: Water absorption [%] of standard solid fiberboard, water resistant solid fiberboard and corrugated fiberboard as a function of absorption time (Kirwan 2005).

The biggest advantage of solid fiberboard is the superior moisture resistance compared to corrugated fiberboard (Kirwan 2005). In Figure 2.3, the moisture absorption of standard and water resistant solid fiberboard and corrugated fiberboard are compared. Standard solid fiberboard is not PE coated, and its internal sizing is not so heavy as in the water resistant grade. The moisture resistance is achieved through internal sizing of the solid board medium and optionally by using polyethylene (PE) coated lining on one or both sides. At equal grammage, a box made of corrugated fiberboard has higher compression strength as a result of the increased thickness. At equal box compression strength, the solid fiber box will be heavier which means higher material costs. In

applications where frozen, chilled, ice-packed products are transported in moist or humid conditions and high puncture resistance and strength properties are required, the good properties of the solid board overcome these disadvantages.

Another advantage of fiber-based packages is that they are supplied flat to the customer which saves space in transportation and storage. A package is erected manually or with machines. Solid fiberboard containers are normally considered as one-trip packages. The materials in contact with victuals are controlled by legislation, regulations and standards. Fish boxes are combusted after the end-use.

Raw materials
The middle layers of solid fiberboard are made from recycled fibers. Moisture resistance is increased by hard sizing, and starch is used to increase strength. Additional liquid water and water vapor resistance is introduced by laminating PE coated kraft paper on one or both sides of the board. Typical grammage of the polyethylene layer is 15 g/m^2 (Kirwan 2005).

Lamination process
Thinner solid fiberboard grades are made on a multi-ply paperboard machine without gluing, but thicker grades are always manufactured by lamination. Two or more paperboard layers are laminated together to provide the necessary strength to meet the end-use requirements (Kirwan 2005).

Box design

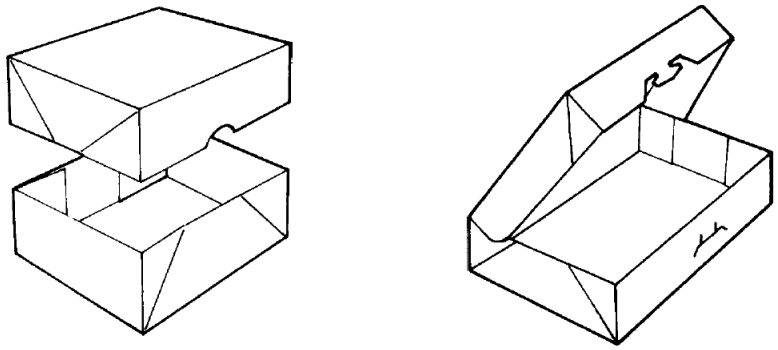

Figure 2.4: Two different box designs. Left: Separate base and full depth lid, Right: Integrated full depth hinged lid and base, hinged corners form a webbed corner (Kirwan 2005).

Round fresh fish is packed together with ice. Because the boxes need to be leak-proof, so called webbed corners are used. Webbed corners contain no cut material edges and gluings that could potentially let fluids leak out. The premium grade for this application type is the PE coated, hard sized solid fiberboard. Two examples of box designs are given in Figure 2.4. The principle of webbed corner can be seen in the figure on the right. The material foldings prevent leakage.

Polyethylene and extrusion coating

Polyethylene (PE) is the most widely used polymer for extrusion coating. Benefits of both paperboard and polyethylene can be joined by extrusion coating (see Table 2–1). This reasonably low cost plastic material is easy to process, and it has excellent moisture barrier and sealability properties (Cramm 1990).

Table 2–1: Advantages of paperboard and low-density polyethylene (Kuusipalo et al. 2008).

Paperboard	LDPE
Strength	Moisture barrier
Stiffness	Heat sealability
Printability	Suitable appearance (matt, gloss)
Permeability	Cleanness
Easy to handle	Inert
Economic	Easy to process
Easy to convert	No odor, no taste
Reliability	Transparent
Easy to recycle	Approved for food packaging
	Economic
	Easy to burn (recycling)

Polyethylene is manufactured by polymerization of ethene (Figure 2.5) by two basic mechanisms: free radical polymerization at high pressure and polymerization with organometallic catalysts (Ziegler-Natta polymerization) (Cramm 1990). The selected polymerization mechanism and manufacturing process conditions lead either to tightly packed linear polyethylene chains (high-density PE, HDPE) or branched chains (low-density PE, LDPE). Also linear low-density polyethylene exists (LLDPE), with a significant number of short branches instead of long chain branches of LDPE. The LDPE is the oldest and still the largest group of extrusion coating polymers due to the good processability properties. The usage of LDPE began late in the 1940's and its share is more than 80% of the total polymer consumption in coating (Vähälä and Grootel 2001). The normal amount of LDPE used as a coating is 10-25 g/m^2 (Kuusipalo and Lahtinen 2005).

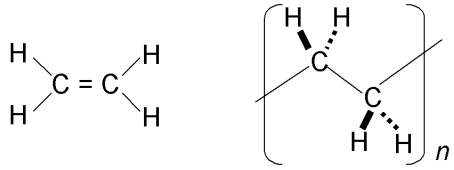

Figure 2.5: Ethene molecule and repeating unit of polyethylene.

Polyethylene is characterized by two properties: density (a measure of crystallinity) and melt index (a measure of molecular weight). Density is the primary characterization parameter for the moisture resistance, ability of the polymer to adhere to other polymers (heat sealing) and to some degree processability properties in extrusion. Melt index is a

measure of the ease of flow of the melt of a thermoplastic polymer, and it characterizes the extrusion properties (Cramm 1990). Four general density categories of PE for extrusion coating are shown in Table 2–2. The categories 0.917 and 0.923 are consider low density, 0.930 medium density, and 0.950 high density. The highly branched LDPE is the oldest and largest class of extrusion coating polymers (Kuusipalo et al. 2008).

Table 2–2: Density categories of polyethylenes for extrusion coating. The categories 0.917 g/m^3 and 0.923 g/m^3 are considered low density (LDPE) (Cramm 1990).

Density category [g/m^3]	Melt index range	End use
0.917	4-12	General purpose, Coating & Laminating, Good heat seal, High line speeds
0.923	3-10	General purpose, Coating & lamination, Board coating
0.930	6-10	Multi-wall bags, Boil-in-bags, Improved barrier
0.950	8-12	Spiral wound cans, Oil, fruit juices, Best barrier

The density of the PE polymer affects the properties of the extrusion coating, e.g., water vapor transmission rate (WVTR), minimum temperature needed for sealing, strength of the heat seal, tensile strength, and adhesion (Cramm 1990). Processing conditions during extrusion affect the density and melt index of the final coated polymer. The density of the polymer coating is lower than that of the unprocessed polymer due to incomplete crystallization after the extrusion. For calculations of water vapor penetration into PE coated materials, literature values on PE films should not thus be used to characterize PE coatings (Cramm 1990).

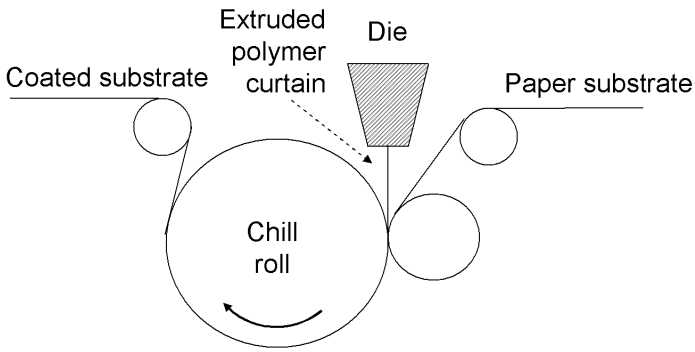

Figure 2.6: Principle of extrusion coating (redrawn from Cramm 1990).

In extrusion coating (Figure 2.6), a molten polymer is applied onto a moving web. The central part of the extruder is the die that forces the polymer melt to become a wide film. It also maintains the desired temperature, and controls the thickness and thickness profile of the polymer layer (Kuusipalo et al. 2008). In co-extrusion two (double-extrusion) or

more extruders melt the resins and lead them to a special die that simultaneously extrudes them to form one layer. Co-extrusion offers several advantages, e.g., better barrier properties due to less pinholes in the coating.

2.1.4 Overview of relevant board and box grades and their raw materials

The following definitions are adopted to consistently describe the materials that are studied and discussed in this thesis. The definitions are from Kouris (1996), unless otherwise stated. If there is no risk of confusion about the structure of the material, the term solid fiberboard, which emphasizes the laminated multi-layer structure, is sometimes replaced by the term solidboard in this thesis.

Combined board: A term to designate that two or more boards have been joined together by an adhesive. For example, a corrugated board or solid fiberboard is a combined board after having been passed through the corrugating or pasting machine.

Corrugated board: The structure formed by bonding one or more sheets of fluted corrugating medium to one or more flat facings of linerboards. When this consists of a single facing, it becomes single-face (wrapping material). If bonded on both sides, it becomes double-faced or single wall corrugated board. Similarly, double wall and triple wall corrugated boards are also produced.

Fiberboard: (1) General term to describe a board made from chemical wood pulp, waste papers, other waste materials, with or without the addition of chemicals. Its principal uses are for containers, and electrical products. (2) A term sometimes used to designate container boards in general, as well as trunk board and other products of this character. (3) Often a designation for vulcanized fiber.

Laminating: The operation of combining two or more layers of paper, paperboard, or other materials with an adhesive in such a way as to form a multi-ply paper product, the purpose generally being to increase thickness and rigidity or to impart special properties, for example, moisture- and grease-resistance.

OCC: Old corrugated containers.

Paperboard: One of the two broad subdivisions of paper (general term) the other being paper (specific term). The distinction between paperboard and paper is not sharp but, broadly speaking, paperboard has higher basis weight, is thicker, and more rigid than paper. In general, all sheets 304.8 μm (0.012 inch) or more in thickness are classified as paperboard. There are a number of exceptions based upon traditional nomenclature, e.g., corrugated medium or linerboard less than 304.8 μm is classified as paperboard.

RSC: Regular slotted container. The type of paperboard box most generally in use as the outer container in the shipment of a wide variety of articles. It is made from a single sheet of corrugated or solid fiberboard, slotted and scored. The two side edges are taped or stitched together leaving the end flaps to be folded inward when the box is closed.

Shipping container: A box made of corrugated board or solid fiberboard used as an outer container in the shipment of commodities. The most common style of container is the regular slotted container (RSC).

Solid board: A board made of the same material throughout as contrasted with a combination board where two or more stocks are used. A pasted board is not a solid board even though the same stock is used.

Solid fiber box: Rigid shipping container made of solid fiberboard, having closed faces and completely enclosing the contents. Designation as a box, as opposed to carton, infers that it meets requirements as an outer shipping container (Smook 1990).

Solid fiberboard: A pasted board used for fabricating shipping containers in which several layers of paperboard or containerboard are pasted together to make a thicker structure.

Solid fiberboard medium: A one-ply paperboard made of old corrugated containers (OCC) that is used as middle layer(s) in solid fiberboard. The term is used locally at the mill.

2.2 Moisture penetration into paper-based materials

2.2.1 Wood fibers and moisture content

Paper is a complex structure at multiple levels of length scales as is seen in Figure 2.7. A paper sheet is a network arrangement of fibers and fiber-fiber bonds that have certain occurrence and nature. The length of softwood fibers is 2-3 mm and thickness 0.03 mm, hardwood fibers are approximately 0.3-0.6 mm long and 0.03-0.13 mm thick (Engman et al. 1978). Individual fibers are composed of several layers of fibrils that surround the lumen inside the fiber. The different layers are distinguished by the differences in orientation of the cellulose microfibrils (Bristow and Kolseth 1986).

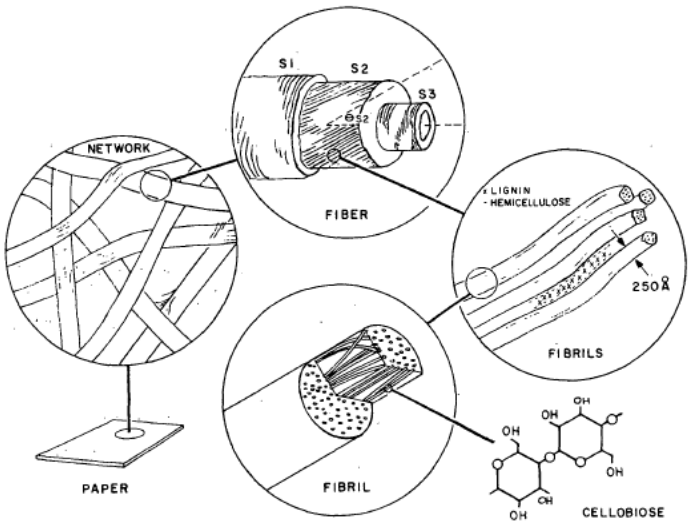

Figure 2.7: Complex structure of paper and internal organization of the fibers (Baum 1987)

The S1, S2 and S3 layers form the so called secondary wall of the fiber, and they consist of cellulose fibrils surrounded by a hemicellulose and lignin matrix. The fibrils are aligned almost parallel to the longitudinal fiber axis in the thick S2 layer. The three secondary layers are surrounded by a very thin primary wall consisting mainly of lignin (Bristow and Kolseth 1986). In wood, the fibers are 'glued' together by the middle lamella that consists of lignin. As a conclusion, cellulose provides the tensile stiffness and strength of fibers - and a tree, lignin surrounds the slender cellulose fibrils and prevents them from buckling, which brings the high compression strength of the wood (Bristow and Kolseth 1986). The underlying fine structure described above is often discarded, and the paper is treated as an engineering material with properties of a homogeneous continuum.

Water molecules interfere the hydrogen bonds between the chains of wood polymer molecules, and increase their mobility (Salmén 1993). Cellulose, lignin, and hemicelluloses show different sensitivity to water. The crystalline cellulose has neligible sorption capacity, while the amorphous and disordered regions of cellulose sorb water (Salmén 1993). Due to their higher hydroxyl content, the hemicelluloses have a higher sorption capacity compared to lignin. The water uptake of paper depends not only on the hygroscopic properties of the wood polymers, but also on the structural arrangement of the fiber network (density of paper) and the hygroscopicity of the paper surface (Salmén 1993), which is affected by the sizing and the extractives content of the pulp. The mechanical properties of paper depend mainly on how much water is residing inside the fibers. The amount of absorbed water is expressed as moisture content; the ratio between the amount of water and the total mass of moist paper.

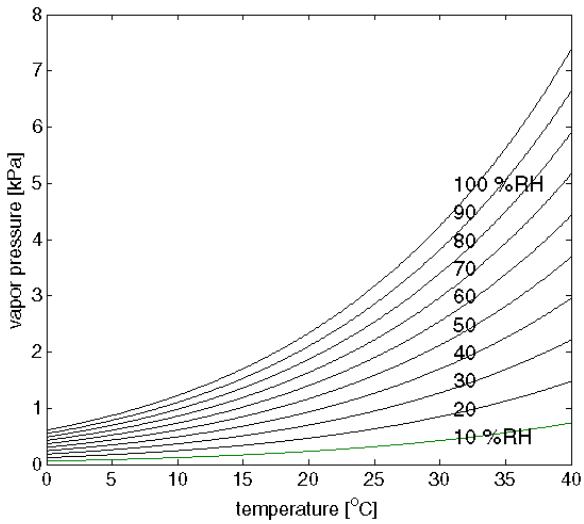

Figure 2.8: Saturation vapor pressure (100% RH) and vapor pressures at different relative humidities of moist air as a function of temperature. The graph is drawn with one variant of empirical Arden Buck equations (Buck 1981).

The ratio between the ambient partial pressure of the water vapor and the pressure of pure water at the same temperature (saturation vapor pressure) is called relative humidity, RH, of air (Castellan 1983). When multiplied by 100, it is the percent relative humidity, % RH. Figure 2.8 shows the relation between temperature, relative humidity and ambient vapor pressure.

Fiber, and as a consequence the man-made paper, tries to reach equilibrium with surrounding air. In that situation, the chemical potential of water is the same inside the paper and in the ambient air. When in equilibrium with the surrounding air, the moisture content of paper depends on the relative humidity of the air and the temperature (Niskanen 2008). Figure 2.9 shows the typical shape of the moisture content curve as a function of relative humidity. This curve is called the sorption curve of the material. The moisture content is different in adsorption and desorption. This hysteresis is connected to the hygroscopic nature of the fibers. Thermal energy is needed to remove water from the fibers, and energy is released when the fibers absorb water. This thermal energy (heat of sorption) changes the vapor pressure of the fibers between adsorption and desorption (Niskanen 2008).

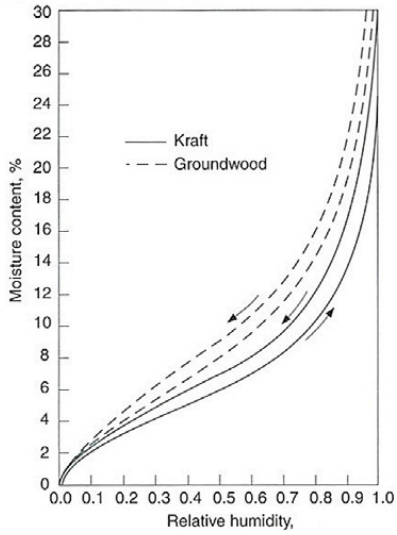

Figure 2.9: Moisture content of paper against relative humidity at the temperature 50°C (Niskanen 2008). Relative humidity is expressed as a ratio instead of a percentage.

2.2.2 Moisture transport in paper materials

Fibers lie in paper often in their collapsed condition, and form a porous structure of voids and fiber walls. Moisture transport into and inside this pore system is a complicated phenomenon comprising many moisture transport mechanisms that are affected by the environmental conditions and moisture content inside the paper. The permeability of paper increases as the moisture content increases (Niskanen 2008), unlike the permeability of polymer coating of solid fiberboard, as will be explained in Chapter

2.3.1. One classification of the occurring phenomena is given in Table 2–3. This chapter discusses the basics of capillary transport and diffusion.

Table 2–3: Possible mechanisms for moisture transport through paper according to Nilsson et al. (1993).

Transport mechanism	Transport phase	Place of transport	Dependence of transport coeff. on temperature	Dependence of transport coeff. on RH
Gas diffusion	Gas phase	The pores	Proportional to $T^{1.76}$	Independent (apart from effects of swelling)
Knudsen diffusion	Gas phase	Pores with diameters less than 100Å	Proportional to $T^{1.76}$	Independent (apart from effects of swelling)
Surface diffusion	Adsorbed phase	Surfaces of fibers		Increases with increasing RH
Bulk-solid diffusion	Adsorbed phase	Within the fibers		Increases with increasing RH
Capillary transport	Condensed phase	The pores		Only when pores are filled with water

Capillary transport

Meniscus flow of liquid water in thin capillaries in-between fibers and inside fibers is one of the main mechanisms of moisture transport. Roberts (2004) showed that the major fluid transport mechanism is the advancing of the wetting fluid along the channels formed by fiber overlaps, not the intuitive gradual filling of the pores. The basis of the capillary approach is the Lucas-Washburn equation (Washburn 1921):

$$h(t) = \left(\frac{r\gamma\cos\theta}{2\eta}\right)^{1/2}\sqrt{t} \qquad 2.1$$

where h = rise in a capillary [m] during time t [s], r = capillary radius [m], γ = surface tension of the liquid [N/m], θ = contact angle between liquid and the capillary wall [rad], η = viscosity of the liquid [Pa·s].

In early works, only single capillary models were used to describe the liquid imbibition. In later research, equivalent cases are sought for the porous materials and sets of cylindrical capillaries (Marmur and Cohen 1997). The capillary penetration approach is challenged by the complexity of the paper-void system. Modeling of the three-dimensional structure is challenging, but there has been attempts. The water penetration into paper can be simulated by first building a network representing the void system in paper with simplified elements, e.g., cubic pores and cylindrical throats, and then calculating how water enters the system of capillaries (Matthews 2000). An additional challenge posed on modeling is the concurrent swelling of fibers caused by liquid water and water vapor penetration, which changes the pore structure dynamically. Capillary

penetration models also neglect completely the amount of liquid that is transported by other processes, for example by diffusion.

Diffusion

The driving force of diffusion is the gradient in the moisture concentration in the fibers or in the partial pressure of water vapor in the pores. The phenomenon is described by Fick's first law (Castellan 1983). The diffusive flux J [g/m^{2}s] equals the concentration gradient $\frac{\partial c}{\partial x}$ [g/m^3/m] times a diffusion coefficient (moisture diffusivity) D [m^2/s]:

$$J = -D\frac{\partial c}{\partial x} \qquad 2.2$$

Table 2–3 lists different types and places of diffusion in porous materials. The exact order of occurrence of these types is not known when moisture is transported into and from paper materials. A different set of diffusion types is normally assumed for sorption and desorption.

From a practical point of view, diffusion in paper materials takes place from high vapor pressure (relative humidity) or water concentration to lower, and thus the overall or effective diffusivity resulting from all the diffusion processes in a fibrous pore system are considered. The effective moisture diffusivity is strongly affected by moisture content (Ramarao et al. 2003) and ambient temperature (Salminen 1988). The vapor diffusivity measured for kraft paperboard sheets is approximately constant up to relative humidity 60%, but increases sharply after this value (Rahhakrishnan et al. 2000, Massoquete et al. 2005). In drier sheets, the diffusion of water vapor in pores dominates, and operations that increase the tortuosity or reduce the pore volume, e.g., refining or wet pressing, tend to decrease the diffusivity. As the relative humidity increases, the moisture content dependent transport of condensed water becomes more important (Massoquete et al. 2005). Depending on the paper grade in question, the magnitude of the underlying diffusion phenomena varies, and the resulting overall dependency on relative humidity may deviate from this general trend (Ramarao et al. 2003). An extensive review on steady and unsteady state diffusion models assuming paper as a homogeneous material or a composite of fibers and voids is given in Ramarao et al. (2003).

The middle layers of the solid fiberboard studied in this study are strongly internally sized. For liquid water penetration into sized papers, it has been noticed that at short absorption times the water enters first the cavities on the surface before the absorption to the pore system commences (Bristow 1968). Further, the only mechanism of moisture transport is the diffusion flow within the fibers, no bulk or film fluid flow in inter-fiber or intra-fiber pores or lumen is observed (Roberts 2004).

2.2.3 Hygroexpansion

The phenomena described in Chapter 2.2.2 account for the moisture penetration into paper and the increase in moisture content. The penetrated water volume causes the

fibers to swell, which in turn makes the paper expand in three dimensions (Niskanen 2008). Fibers and paper shrink when the moisture content decreases. The transport boxes are stored in room temperature and relative humidity, but used in 4°C and 90% RH. Stability of the dimensions of paperboard are important parameters during converting and end-use of the boxes.

Several material properties of paper have responses analogous to the changes in relative humidity and temperature (Haslach and Abdullahi 1995). Haslach and Abdullahi (1995) studied thermal expansion of paper at constant relative humidity, and report thermo-expansive strains ~0.025% in the temperature range 25-55°C. Part of the strain observed as thermoexpansion is actually hygroexpansion, since the measurement occurred in constant RH. The following discussion concentrates on dimensional changes caused by changes in relative humidity.

In-plane hygroexpansive strain ε_h is measured as the change in length of the test piece between two equilibrium condition with relative humidity. Hygroexpansivity, or hygroexpansion coefficient of a material is defined as:

$$\beta = \frac{\varepsilon_h}{\Delta mc} \qquad 2.3$$

where β = hygroexpansivity [%/%], ε_h = hygroexpansive strain [%], Δmc = change in relative humidity [%]. Typical in-plane hygroexpansion coefficients for paper materials are in the ranges of 0.002-0.003%/% RH (MD) and 0.009-0.02%/% RH (CD) according to Kajanto and Niskanen (1996). Hygroexpansion is a linear function of moisture content as the experimental curves in Figure 2.10 show.

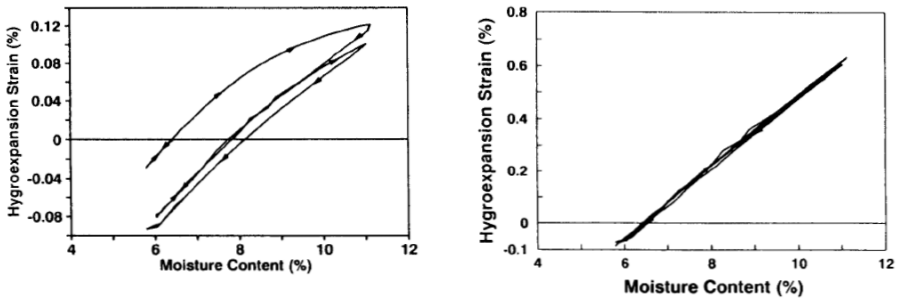

Figure 2.10: Relation between hygroexpansion and moisture content for machine made paper in MD direction (left) and in CD direction (left) (Uesaka 1991).

Drying conditions have a major impact on the hygroexpansive behavior of the sheet. When the paper sheet has been dried under restraint, which is the case for normal factory made papers in MD direction, it shows irreversible shrinkage under humidity cycling due to release of stresses that have been introduced during the drying (Uesaka 1991). Figure 2.10 shows the hygroexpansion of machine made paper in MD and CD directions. After

the internal strains created during manufacturing are released, the subsequent moisture cycling results in reversible shrinking and expansion of the sheet.

Moisture expansivity is directly proportional to the drying shrinkage (Figure 2.11) (Nordman 1958). The only affecting factor is the amount of drying shrinkage of the sheet, not the degree of beating or in what phase of the total drying the shrinkage took place.

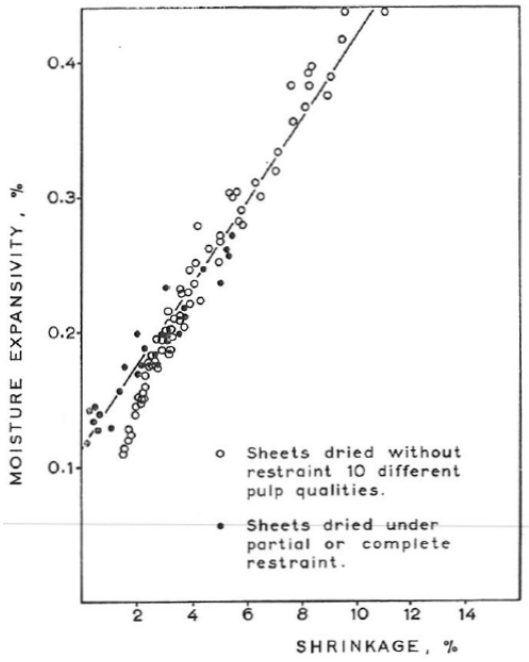

Figure 2.11: Hygroexpansive strain (from 20% to 60% RH) as a function of drying shrinkage (Nordman 1958).

The furnish composition, and the process of manufacturing the pulp and the paper has an effect on hygroexpansion. Drying of the pulp reduces the strength of the paper but increases its dimensional stability independent of the pulp type (Eklund 1969). Increasing number of dryings reduces the hygroexpansion (Eklund 1969). Coffin et al. (1999) simulated the recycling process by drying fibres, and found that the sheets from dried unbleached softwood fibers show smaller hygroexpansion than those made from virgin fibers. Water removal can increase irreversibly the bonding inside the fiberwall (hornification) (Niskanen 2008), and the same occurs in fiber recycling. If the once-dried pulp is beaten, hygroexpansivity increases again. In the experiment of Coffin et al. (1999) the once-dried refined sheets had the largest hygroexpansion. Comparisons of mechanical and chemical pulps can be found from, e.g., Nanri and Uesaka (1993). Non-filled sheets like solid board medium, show larger hygroexpansion than filled sheets in cross-machine direction due to filler particles interfering the fiber-fiber bonding (Lyne et

al. 1996). MD hygroexpansion is not affected by the filling of the sheet (Lyne et al. 1996). Hydrophobic sizing slows down the adsorption of moisture into fibers, and retards the rate of hygroexpansion (Niskanen 2008).

The joint hygroexpansion effect of layered sheets arises from the hygroexpansive properties of all the constituent layers. Lamination of paper with inert films restrain the hygroexpansion of paper whether the film is on the outside or between the paper layers (George 1958). If hygroexpansional properties of the layers in a laminate are different, out-of-plane stability problems emerge, e.g., curl or twist.

2.3 Moisture and temperature effects on solid fiberboard constituents and solid fiber boxes

The main function of the transport box is to resist mechanical loadings so that the contents reach the final destination in intact state. The boxes' ability to resist mechanical loading is affected by the ambient environment during the use. The main environmental loading variables relevant for packaging products are static and cyclic changes in ambient relative humidity and temperature, and presence of liquid penetrants like water.

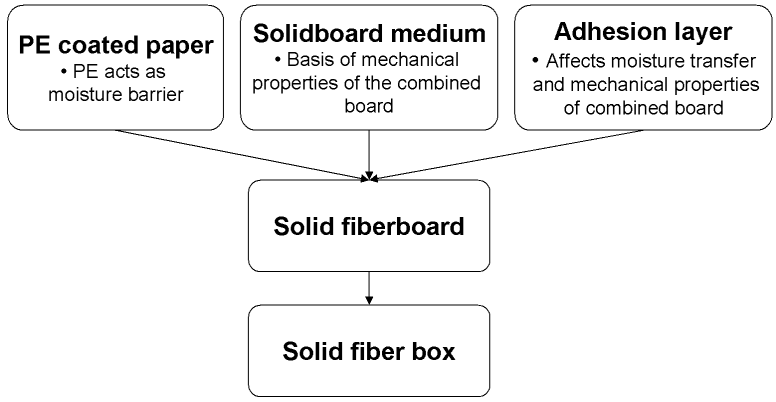

Figure 2.12: The roles of the solid fiberboard components on the behavior of the combined board.

The solid fiberboard constitutes of solid fiberboard medium made of recycled fiber and fillers, polyethylene coated kraft papers and polyvinyl acetate based glue in between the layers. Polyethylene acts as a moisture barrier restricting the transverse moisture transfer in the combined board, leaving the in-plane as the main direction of moisture penetration. Solid fiberboard medium layers make the biggest part of the grammage and thickness of the combined board. As a consequence, most of the mechanical properties of the solid fiberboard arise from the properties of the solid fiberboard medium layers. It is reasonable to believe that the adhesion layers have effects on the mechanical properties of the solid fiberboard, and that they also restrict the moisture transport inside the material. In the following, literature is surveyed on how environmental factors affect

the properties of the constituents and the solid fiber boxes (Figure 2.12). The adhesion layers and the combined solid fiberboards are not covered.

2.3.1 Polyethylene coated paper

The double-extruded polyethylene coating acts as a major obstacle for the transverse moisture transport to and from the solid fiberboard. A particular barrier material usually shows different resistance towards different penetrants; a good water vapor barrier polymer might be poor against, e.g., organic vapors, oil or grease. Actually in gas mixtures composed of water vapor and non-condensable gases (N_2, O_2, CO_2), each component of the mixture permeates individually without interactions through hydrophobic films like polyethylene (Rogers et al. 1957).

Barrier materials also have often different resistance towards gases and liquid water. Polarity of the molecule is a specific example of properties that results in good gas barrier but poor water barrier property, or vice versa. Polyethylene is a very non-polar polymer and has excellent, in the absence of pinholes almost perfect, barrier against liquid water but relatively poor gas barrier properties (Salame and Steingiser 1977).

This chapter first discusses the permeation of water vapor through polyethylene coating. The kraft paper substrate of the coating mainly acts as a carrier for the barrier properties, even if it has, along with other paper materials, its own barrier properties that differ greatly in magnitude and mechanism from polymer coatings. The water vapor transport through paper was discussed in Chapter 2.2.2. The rest of this chapter concentrates on PE coated papers. The measurement of water vapor transmission rate and the effect of polyethylene coating on the mechanical properties are presented.

Mechanisms of permeation through polyethylene

The two main mechanism of permeation through polyethylene coating are (Stannett 1973)

1. Laminar or viscous flow through pores, capillaries, pinholes and other defects in the PE film.
2. Activated diffusion through the (nonporous) PE film.

The simplest flow type through the pores can be described as viscous flow through a smooth-walled circular pipe. The volume of liquid being discharged can be expressed with the Poiseulle's formula (Castellan 1983) that includes viscosity of the permeant as a variable, which brings in the temperature dependency of the flow:

$$q = \frac{\pi r^4 \Delta p}{8 \eta \Delta x} \qquad 2.4$$

where q = volume of the penetrant passing through a capillary [m^3/s], r = radius of the capillary [m], Δp = pressure drop across the capillary [Pa], η = viscosity of the permeant [Pas], Δp = length of the capillary [m]. In flow type of permeation, the pressure drop across the film is the driving force of the permeation regardless of the permeant. In packaging applications, there is often no pressure difference, only difference in partial

pressure of water in air. In the absence of pressure difference, the flow through pinholes can be modelled as diffusional flow (Stannett 1973).

When there is a difference in partial pressure, water vapor molecules will transfer across the pinhole-free polymer film by activated diffusion. The phenomena occurring during the transfer are as follows (Yamauchi and Murakami 2002).

1. The vapor dissolves in the film on one surface.
2. The dissolved water molecules diffuse through the film under a concentration gradient. Only small concentrations of water molecules prevail within the polymer (Klute and Franklin 1958).
3. The diffused molecules evaporate (desorp) from the surface from the low concentration side.

Salame and Steingiser (1977) name the adsorption of the permeant into the polymer surface as the first step preceding the solubility phase. The rate of transmission depends thus on the solubility of penetrant in the polymer and the diffusion constant of the penetrant through the polymer. This diffusion type permeation follows the Fick's first law:

$$q = -D\frac{dc}{dx} \qquad 2.5$$

where q = gas flux through the film [mol/m^{2}s], D = diffusion coefficient [m^2/s], c = concentration of the gas [mol/m^3], and x = thickness of the film [m]. After a certain build up time, a steady state is reached and gas will diffuse at constant rate through the film under constant pressure difference and constant diffusivity, and Equation 2.5 becomes

$$q = \frac{D(c_1 - c_2)}{l} \qquad 2.6$$

where l = thickness of the film [m], c_1 and c_2 = concentration of the gas on the surfaces of the film [mol/m^3]. When the penetrating gas is water vapor, the flux through pinholes is negligible compared to the diffusion through the film (Stannett 1973).

Henry's law (Castellan 1983) states that at a constant temperature, the amount of gas dissolved in a given volume of solvent (mole fraction) is directly proportional to the partial pressure of gas in equilibrium with the solvent. The permeation phenomenon is reasonably slow and Henry's law can be thus expected to apply on the surfaces. The concentrations can be expressed as partial pressure $c_i = Sp_i$, i=1,2, and Equation 2.6 becomes

$$q = \frac{DS(p_1 - p_2)}{l} = \frac{P(p_1 - p_2)}{l} \qquad 2.7$$

where p_1 and p_2 = partial pressure of the gas on the first and second surface of the film [Pa]. The solubility coefficient S expresses the amount of gas that penetrates the amount of polymer under constant temperature and unit pressure difference, and its SI unit is [m^3(STP)/m^3·Pa]. Chemical and morphological properties of the penetrant and the polymer affect both the diffusion and the solubility constant. The product DS is called permeability coefficient P. It refers to the amount of gas, by volume, which penetrates unit thickness and area of specimen per unit time, under constant temperature and unit pressure difference when permeation is stable [m^3(STP)·m/m^2·s·Pa]. In the literature, several other variants of this unit are often seen.

Permeability of polyethylene is a simpler phenomenon compared to paper materials, although some simplifications are usually made, for example the polymer is assumed non-porous. Permeability of PE is independent of the pressure gradient across the film, and the diffusion coefficient is independent of the concentration of water vapor at any point within the polymer film since the polymers swell negligibly by the absorbed water (Klute and Franklin 1958). As a consequence, the permeability plots against relative humidity are straight lines. For paper materials, water vapor permeability varies with partial pressure difference across the specimen, and concentration of the vapor (relative humidity) and thus moisture content (Yamauchi and Murakami 2002). The issue is further discussed in Chapter 2.2.2.

Several polymer and process related factors affect the permeability of polyethylene films. Polymeric films are interspersed with crystalline and amorphous regions. The gas molecules are assumed to be soluble only to the amorphous regions, and the solubility is roughly proportional to the amorphous content, which in turn is indicated by density (Li and Henley 1964). Close to squared relationships between permeability and the amorphous fraction have been reported for PE (Stannett 1973, Krohn and Jordy 1997). Follestad et al. (2006) present a modified permeability factor for PE films that include the amorphous fraction of the polymer. Based on the theory, permeability coefficient is a material constant and should not be dependent on the film thickness. However, lower permeability coefficients are reported for lower thicknesses than for higher thicknesses (Klute and Franklin 1958, Krohn and Jordy 1997). Also crystalline orientation of the polymer, molecular weight and molecular weight distribution affect the permeability (Krohn and Jordy 1997).

Temperature dependency of permeation through polyethylene

With very few exceptions the reaction rate increases with increasing temperature (Castellan 1983). The Arrhenius equation is an empirical relation that describes the temperature dependence of the rate constant of a reaction (Castellan 1983).

$$k = A e^{-E^*/(RT)} \qquad 2.8$$

where k = rate constant of the reaction, T = temperature [K] and R = gas constant [J/K·mol]. The constant A is the frequency factor (pre-exponential factor), E^* is the activation energy [J/mol]. The parameters A and E^* can be found from experiments by plotting $\log_{10}k$ against $1/T$ and recording the slope and intercept of the curve.

The diffusion coefficient and the solubility coefficient are temperature dependent, and the Arrhenius equation can be used to model the temperature dependence of these coefficients (Yamauchi and Murakami 2002)

$$S = S_0 \exp\left(\frac{-\Delta H}{RT}\right) \quad 2.9$$

$$D = D_0 \exp\left(-\frac{E_d}{RT}\right) \quad 2.10$$

where ΔH = heat of sorption [J/mol] and E_d = activation energy for the diffusion process [J/mol]. The sum of activation energy of diffusion and molar heat of sorption equals the activation energy of permeation E_p. Unlike gases like N_2, water vapor condenses inside the plastic film at the conditions of a typical measurement. For condensable gases, ΔH is negative and almost equal to the positive E_d. Thus the activation energy of permeation E_p is close to zero, and the permeation of water vapor through polyethylene is not strongly dependent on temperature as experimentally shown by, e.g., Piergiovanni et al. (1995), Lahtinen and Kuusipalo (2008). Klute and Franklin (1958) report activation energies of water vapor permeation in low-density polyethylene from several authors.

Water-vapor transmission rate (WVTR)
Permeability constants are often not intuitively understandable in practical applications. In addition, paper material is a non-homogeneous material and suffers from the ambiguity of thickness measurement. The water vapor permeability of paper materials is commonly expressed as the amount of water vapor in grams per square meter of material per 24 hours under given conditions of measurement. The constant is called water vapor transmission rate (WVTR). Typical measurement conditions used are 23°C/50% RH, 25°C/90% RH and tropic 38°C/90% RH (ISO 2528:1995).

WVTR is measured under steady-state conditions assuming no pinholes in the film. Equation 2.11 shows the measurement principle:

$$WVTR = \frac{1}{A}\frac{\Delta Q}{\Delta t} = P\left(\frac{p_1 - p_2}{l}\right) \quad 2.11$$

where A = exposed area [m^2], ΔQ = mass of water vapor passing through the film during the test [g], Δt = duration of the test [s], P = permeability, l = thickness of the layer, p_1 and p_2 = partial pressure of the gas on their surfaces of the film [Pa].

The methods to measure vapor permeability on paper materials can be divided into the following groups (Yamauchi and Murakami 2002):

- **Pressure gradient methods**. One variant of these methods is to measure the pressure change at the low-pressure side of the specimen during the test, and calculate the

amount of passing vapor from the measurement of pressure change at the low-pressure side. A prescribed pressure is maintained at the high-pressure side, which is far greater than the pressure on the other side of the specimen.

- **Gravimetric methods** involve measurement of vapor permeated through a constant area of a specimen under a constant humidity gradient under steady-state. The permeated vapor is measured as the weight change of the absorbent or the moisture source. This simple and widely used test is commonly known as the cup test, and it is used for the WVTR measurement.
- **Hygrometric methods** involve measurement of the change in concentration of water vapor at one side of the specimen while having constant concentration on the other side, and calculating the average WVTR from the concentration change as a function of the permeation time.

As Equation 2.11 shows, water vapor transmission rate is dependent on the thickness of the plastic layer. Figure 2.13 shows the permeation of PE coated paper as a function of coating weight.

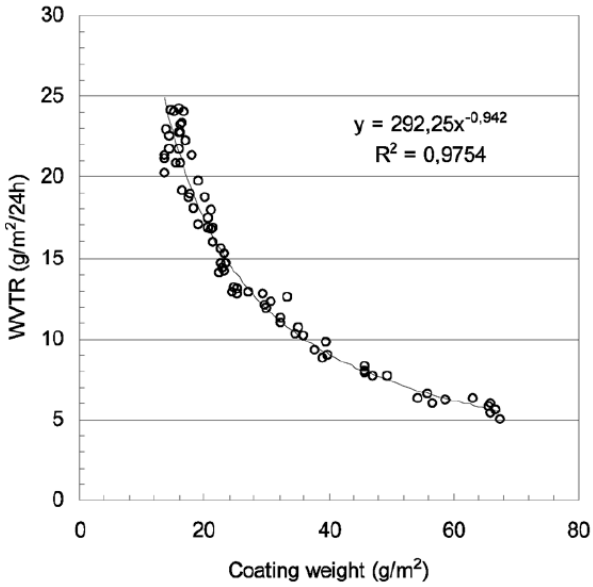

Figure 2.13: Water vapor transmission rate measurements of LDPE coated paper as a function of coating weight (38°C, 90% RH) (Kuusipalo and Lahtinen 2005).

Theoretically, a paper substrate that had perfectly even surface would have no effect on water vapor permeability constants of polyethylene coatings (Bhargava et al. 1957). Paper has very large permeability compared to PE, and the rate of permeation consequently is entirely governed by the polyethylene for normal thicknesses used in extrusion coating. In practice, the paper surface is rough, and two-sidedness of the vapor permeation on PE coated papers is seen in the experiments (Bhargava et al. 1957,

Stannett 1973). The permeability is higher when the paper side is exposed to high humidity instead of the PE side (see Figure 2.14). The cause lies in the fibers protruding from the paper surface acting as wicks between the polymer and the paper. The effect is slightly vapor pressure dependent due to the swelling of the wicks and their efficiency in transporting moisture. The effect disappears as the coating becomes thicker.

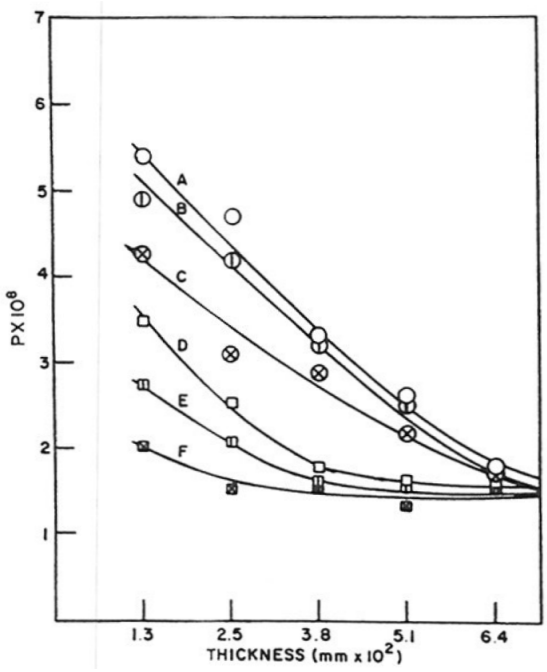

Figure 2.14: The effect of the coating thickness and the choice of the side facing the high humidity on the permeability of PE coated paper (30°C). Permeability [cm^3(STP)·cm/s·cmHg·cm^2] is calculated for PE thickness only. Kraft paper facing humidity: **A** 20 mmHg vapor pressure, **B** 15 mmHg vapor pressure (47% RH), **C** 10 mmHg vapor pressure, polyethylene facing humidity: **D** 20 mmHg vapor pressure, **E** 15 mmHg vapor pressure (47% RH), **F** 10 mmHg vapor pressure, (Stannett 1973).

Models predicting WVTR are normally based on regression or fitting data on pre-selected exponential models. Kuusipalo and Lahtinen (2005) present a simple model for the water vapor transmission through the LDPE coated paper which has the form $y(x) = Ax^{-1}$, where y = WVTR, x = coating weight, A = fitting parameter. The exponent was chosen to be -1 since the WVTR is inversely proportional to thickness and thus coating weight of the polymer. Kuusipalo and Lahtinen (2005) state that three data points with different coating weights are needed to regenerate the WVTR behavior of a certain polymer coating over a range of coating weights. It was found that increasing the mixing ratio (water mass per dry air mass) increases the rate of vapor permeation linearly in a PE coated paper. With regression modelling of WVTR for extrusion coated papers, Lahtinen and Kuusipalo (2008) compare the role of temperature and moisture content of the

surroundings of the experiment. Their second order regression models have temperature, layer structure, RH and mixing ratio as variables. It was found that mixing ratio is better suited for WVTR modelling than relative humidity, since RH does not define the absolute water concentration of the surroundings. Mixing ratio dominates over the effect of temperature as can be seen in Figure 2.15.

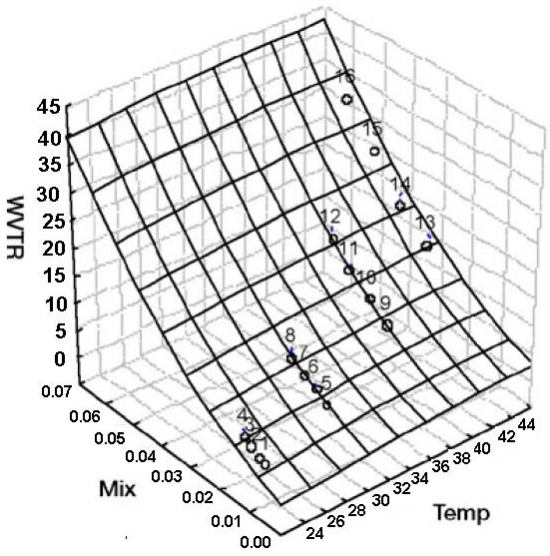

Figure 2.15: WVTR as a function of mixing ratio and temperature for 20 g/m2 LDPE coating, points 1-16 are measurements (Lahtinen and Kuusipalo 2008).

In the model of Piergiovanni et al. (1995), only one measurement data point is needed to calibrate the prediction model. The model in Equation 2.12 is based on Clausius-Clapeyron equation and permeability. The Clausius-Clapeyron equation relates temperature dependence of the vapor pressure of a liquid to the heat of evaporation (Castellan 1983). Permeability is a material constant at the reference and new climate. Piergiovanni et al. (1995) show results for several plastic films where WVTR increases linearly with increasing water vapor pressure. These results were obtained by varying both the temperature and the relative humidity, which motivated not to include temperature dependency of the diffusion of water molecules to the model.

$$WVTR_{new} = WVTR_{ref} \exp\left[-\left(5418,1K\left(\frac{1}{T_{new}} - \frac{1}{T_{ref}}\right)\right)\right]\left(\frac{\Delta RH_{new}}{\Delta RH_{ref}}\right) \qquad 2.12$$

where $WVTR_{\mathrm{ref}}$ and $WVTR_{\mathrm{new}}$ = water vapor transmission in reference and in new conditions, T_{ref} and T_{new} = temperature in reference and in new conditions [K], ΔRH_{ref} and ΔRH_{new} = difference in relative humidity across the permeable film under reference and new conditions [%].

Effects of polyethylene on tensile and tear of PE coated kraft paper

The polyethylene coating affects not only the moisture transport but also the mechanical properties of the kraft paper. Figure 2.16 shows the typical load-elongation curves for PE coated and non-coated kraft paper (Arnold 1956). Typical features include that the effect of coating takes place already from low force values. The coating elevates the tensile strength and elastic modulus is lower, but it doesn't affect the strain at break. The amount of polyethylene had only minor effect on the increase of the tensile strength.

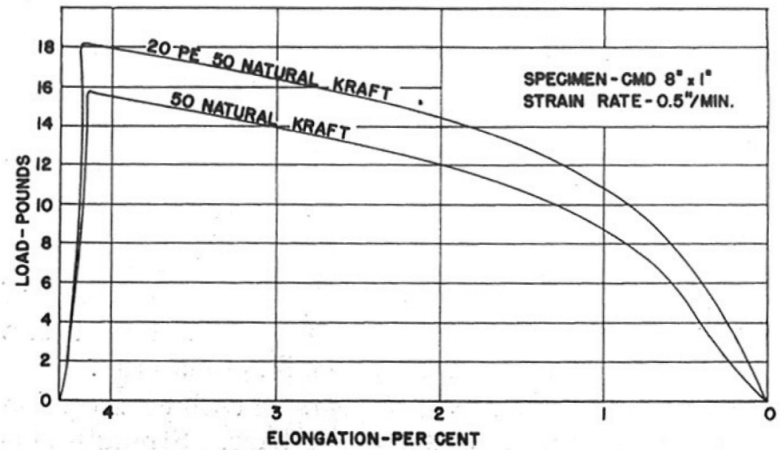

Figure 2.16: Load-elongation curve of PE coated and uncoated kraft paper; note that zero elongation is on the right side of the picture (Arnold 1956)

In certain packaging applications tear strength of the material is important. PE coating increases the tear strength linearly as a function of PE thickness, and the phenomenon is dependent on the degree of adhesion of the film onto the paper substrate (Arnold 1956). The adhesion between PE and paper substrate is affected by, e.g., process conditions during extrusion (temperature, nip pressure) (Guillotte and McLaughlin 1962), various parameters related to paper (density, surface smoothness) and the chemistry of its surface (surface tension, presence of resin acids) (Swanson and Becher 1966).

2.3.2 Solid fiberboard medium

The properties of solid fiberboard emerge mainly from the behavior of the solid fiberboard medium material since it comprises most of the grammage and thickness of the combined board (in this study 82% and 92%, respectively). The other components (polyethylene, kraft paper, glue) either amplify or dampen the effects. This chapter sheds light on how moisture and temperature affect selected paperboard properties.

Solid fiberboard medium is a one-layer paperboard fabricated from recycled fiber on the contrary to testliner, which is usually a multi-ply product (Laamanen and Lahti 2008). Old corrugated container (OCC) is the biggest recovered paper grade group with its 40%

share, and finds use in the production of packaging boards and papers (Göttsching and Pakarinen 2000). One large difference between papers made from recycled fibers and virgin fibers is that the former have lower strength due to losses in fiber-fiber bonding (Nazhad 1994). The loss of bond strength can be due to changes in fiber flexibility or surface conditions. These phenomena are very dependent on the recycling procedures and the yield of the pulp used (Nazhad 1994).

Elastic modulus

Due to the manufacturing process and the features of the wood fiber, paper behaves differently depending on the direction of measurement. Paper can be considered as a three-dimensional orthotropic material. Under moderate stress the response is elastic, and non-linear elastic-plastic at higher stress. Almost any mechanical study of the paperboard or paperboard boxes require the knowledge of at least the elastic constants: three elastic moduli (Young's modulus), three shear moduli, and six Poisson's ratios. Often it suffices to know the in-plane constants: elastic modulus in machine E_x and cross machine direction E_y, shear modulus G_{xy} and two Poisson's ratios ν_{xv} and ν_{yx}. The elastic properties of paper are greatly affected by the manufacturing process variables, e.g., fiber orientation in the sheet, degree and method of beating, wet pressing pressure (density of the sheet), and wet straining (Schulz 1961, Baum 1987).

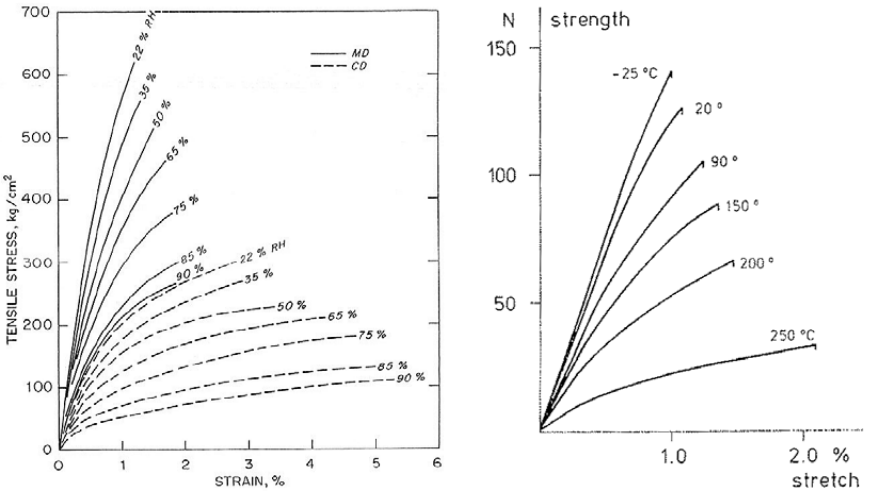

Figure 2.17: The effect of relative humidity and temperature on the stress-strain curve of paper. Left: Typical stress-strain curves in tension for various moisture levels, MD = machine direction, CD = cross-machine direction. The curves are based on generalized behavior of softwood unbleached kraft linerboard (Benson 1971). Right: Stress-strain diagram of dry fluting (112 g/m^2) in MD at strain rate $1.7 \cdot 10^{-3}$/s (Salmén and Back 1977).

It has been known long that moisture content and temperature affect mechanical properties of paper (Wink 1961, Niskanen 2008). Moisture and temperature have similar effects on the tensile behavior of paper as can be seen in Figure 2.17. At low moistures

and temperatures paper is brittle and stiff, and fail at low strain values. Elevation of both temperature and moisture content decreases the tensile strength and the elastic modulus (Figure 2.18), and increases the elongation at break.

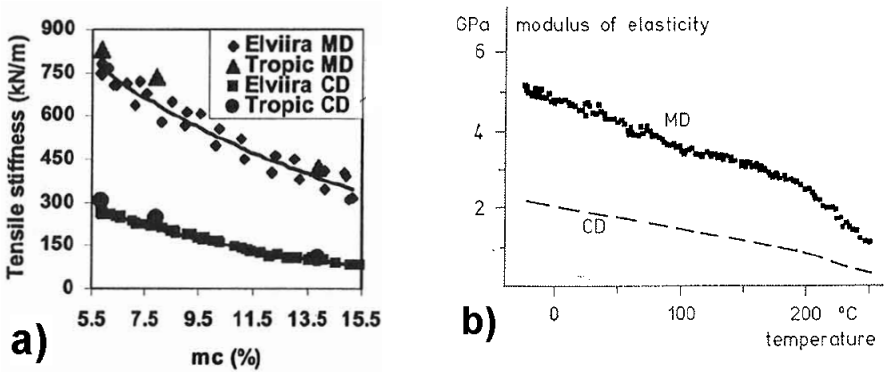

Figure 2.18: Effect of a) moisture content and b) temperature on elastic modulus of paper. Left: Fine paper in MD and CD measured with standard tensile test (Tropic) and a special measurement device (Elviira) (Lehti et al. 2003). Right: Dry fluting 112 g/m^2 in MD and CD (Salmén and Back 1977).

According to Lehti et al. (2003), the elastic modulus decays exponentially as the moisture content of paper is increased,

$$E = E_0 e^{-\gamma mc} \qquad 2.13$$

where E_0 = fitting parameter, mc = moisture content [%]. The curve fitting parameter γ gets values of 0.062-0.150 depending on the material direction and the type of paper (Lehti et al. 2003). Zausscher et al. (1996) use the theory of hydrogen-bonded solids to predict the decay of elastic modulus. The loss of elastic modulus is modeled as breakage of hydrogen bonds by water molecules. For the region where the moisture content is over a certain critical value, the same exponential relation as in Equation 2.13 is obtained. Zausscher et al. (1996) present the experimentally obtained C.I. (Cooperative index in H-bond theory) value of 6.7 which corresponds to γ value of 0.067. Some authors have presented linear relationships between moisture content and elastic modulus, especially on moisture contents from 4% to 13% (Benson 1971).

Temperature dependency of bone-dry paper is seen in Figure 2.18. The figure shows how elastic modulus decreases linearly until approximately 170°C. The sudden decrease in elastic modulus in MD after 200°C is due to the softening of the amorphous polymers (hemicellulose) in fibers (glass transition) (Salmén and Back 1977). In regular packaging applications such extreme temperatures are never reached. In addition, the combined effect of temperature and humidity on the properties of the material and the packaging is of interest instead of bone-dry paper behavior.

Figure 2.19 shows the combined effect of temperature and moisture content on the elastic modulus. Higher temperatures shift the softening region of the wood polymers to lower moisture contents. In practical packaging applications, the relative humidity affects mechanical properties of paperboard more than temperature. Elastic modulus is also known to vary non-linearly with moisture content in transient sorption conditions (mechanosorptive-effect) (Back et al. 1983). Thick and heavy papers that require long time to reach moisture equilibrium show long transient periods, and exact knowledge of elastic modulus after the change in relative humidity requires extensive testing which is often not practical.

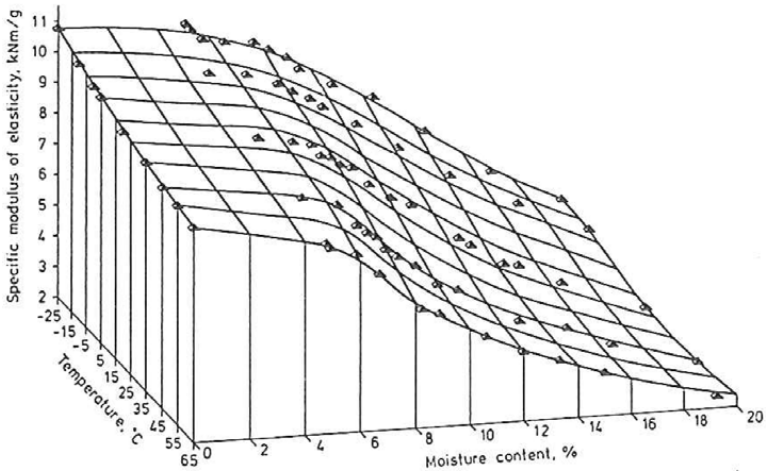

Figure 2.19: Specific elastic modulus of paper as a function of temperature and moisture content for a kraft sack paper (Salmén 1993)

The common interpretation is that the modulus of elasticity is the same in tension and in compression (Setterholm and Gertjejansen 1965). Chalmers (1998) presented contrary results based on studies of corrugated board components with vacuum compression apparatus both in tension and compression at relative humidities from 35 to 95%. He found that at higher relative humidities, the modulus of elasticity (tensile stiffness) is higher in compression than in tension both in MD and CD. The difference is more pronounced in CD than in MD. Chalmers (1998) anticipate that the reason lies in the anisotropically oriented wood fibers becoming tightly packed in increasing compressive loading.

The discussion in this chapter on elastic properties of paper materials have been purely phenomenological, i.e. describing the general tendencies on how moisture and temperature affect the elastic modulus of papers. Those interested in fundamental formulations of the orthotropic elastic constants of paper are referred to the following classical papers: Baum and Bornhoeft (1979), Baum et al. (1981), Baum (1987), Mann et al. (1980).

Deformation mechanisms of a sheet

Deformation of a paper sheet can arise either from deformation of individual fibers or changes in the interfiber bonds (Haslach 2000). Crystallinity and degree of polymerization affect the deformability of the fibers. Hydrogen bonding is the major source of cohesion between fibers. Most of the evidence favor deformation of the fibers as the main mechanism. Brezinski (1956) studied creep of hand sheets made of softwood pulp that was beaten to the desired level. He argues that the creep curves show such 'ideality' that no rate-controlling macroscopic mechanism, such as straightening or uncurling of the fibers, or major stress distribution between fibers and fiber-fiber bonds could occur during the test. He postulates that the only affecting mechanism should be operating on the molecular level in the fibers.

In the study of Schulz (1961) the effect of wet straining on properties of paper was studied. Straight after the wet pressing, the sheets were strained and held in constant elongation during drying. Through this procedure the formation of kinks and other compressions are avoided in the direction of straining. The effects of increasing degree of wet straining (DWS) are profound, e.g., tensile strength passes over a maximum, light-scattering coefficient increases. Increasing DWS decreases the creep deformation of the sheet. The bond strength measured as z-strength decreases continuously as DWS decreases. Schulz (1961) explains the findings by redistribution of stresses in the sheet when supporting a load.

Page and Tydeman (1962) introduced the concept of microcompressions of fibers that can be used to explain many of the effects of papermaking factors on mechanical properties of paper. By simply looking at the fiber network, the paper, through microscope it was noticed that free shrinkage of paper gives rise to small-scale compression in the fibers in the transverse direction at bonded crossings. The degree of straining during the drying of the sheet controls the formation of these compressions. Page and Tydeman (1962) showed that very few of the bonds break completely during tension and that there is only partial breaking of most bonds. The slow breaking of the bonds allow the micro compressed regions to be straightened resulting in greater extension. The bond strength partially controls the shape of the load-elongation curve, in particular the slope after the 'yield' stress. Seth and Page (1983) conclude that the modest role of bond breakage in the stress-strain curve is due to the reduction of how efficiently the strain is transferred from fibers to the sheet.

Compressive creep

During the transportation or the storage at warehouses, packages are stacked under certain atmospheric conditions. After a sufficiently long time a box may fail even if the load is far below the strength of the material seen in one-dimensional testing (Niskanen 2008). Both the box and the material experience compressive creep; slow time-dependent contractive deformation under constant loading. This section introduces how moisture affects the creep response of paper. A more detailed introduction to the creep behavior of paper can be found, e.g., in Coffin (2005) and Vorakunpinij (2003).

The creep response of polymer materials is customarily divided in three time sections: primary, secondary or steady state where the strain rate is constant, and tertiary creep

where the strain rate increases to the fracture (see Figure 2.20). The creep rate is the first time derivative of the curve. If the creep test is stopped before failure, some part of the creep strain is recovered instantaneously (elastic), a part after a recovery time (delayed-elastic), and a part is not recovered at all (permanent deformation). In creep of polymers, time and temperature can often be treated similarly (Coffin 2005). The creep behavior at one temperature can be related to behavior at another temperature by changing the time scale only. The result is a so called master curve. Creep can be measured either in tension or in compression, and different behavior is observed in these two cases (Vorakunpinij 2003, Coffin 2005).

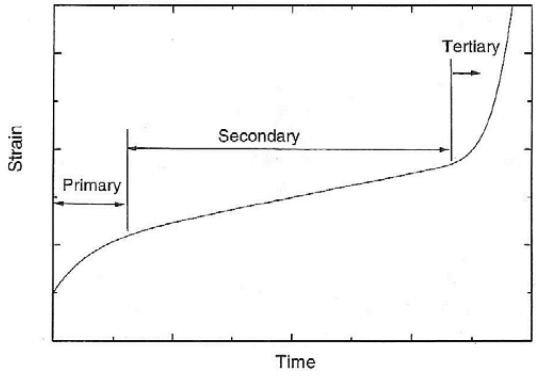

Figure 2.20: Creep response of a polymeric material (Coffin 2005).

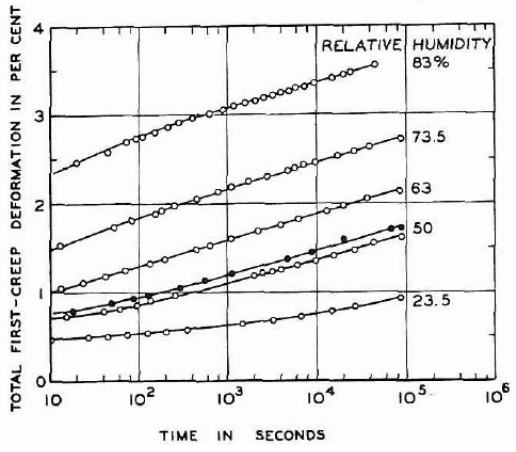

Figure 2.21: Creep strain of handsheets made from softwood at different relative humidity levels at constant load level of 3.75 kg/mm^2 (Brezinski 1956).

The creep rate is influenced by temperature and relative humidity (Niskanen 2008). Increasing constant relative humidity increases primary creep, the strain right after the

loading (Brezinski 1956). The (tensile) creep strain curves at higher moisture levels and at constant stress show larger deformation at same time instant (see Figure 2.21).

The creep rate on all paperboards becomes especially high if the relative humidity varies as can be seen in Figure 2.22. This is caused by the mechanosorptive effect. Fellers and Panek (2007) noticed that there is no low treshold in moisture ratio after which the accelerated creep effect emerges. Large strains before failure are reached in varying humidity compared to the constant RH case, and the failure occurs earlier. The difference between the creep strains in static and cyclic humidity becomes larger at larger stress levels (Byrd 1972).

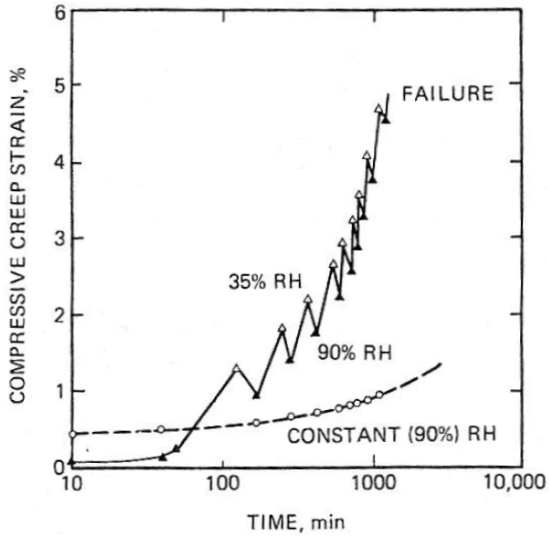

Figure 2.22: Creep response of paper at 57% of maximum compressive stress in constant relative humidity (90% RH) and in cyclic humidity (90-35% RH) (Byrd 1972).

The mechanosorptive effect arises from the interaction between the load, and repetitive moisture sorption and desorption into the material (Haslach 2000). Varying environmental conditions, also temperature, increases the rate of the creep rate from stable conditions. Moisture accelerated creep is a special case where the load is held constant but the ambient relative humidity is varying. Extensive research (for example Padanyi 1991, Söremark and Fellers 1995, Alfthan 2004, Panek et al. 2004, reviews: Haslach 2004, Coffin 2005) has been done on accelerated creep since the first presentation of the phenomenon on paper materials by Byrd 1972. The debate continues on the details of the causing mechanisms and also on proper quantification of the phenomenon.

Although mechanosorptive effects cannot be predicted from a single paper test (Söremark and Fellers 1995), hygroexpansive strain of papers is seen as a good predictor of creep rate at least for ranking materials. Considine et al. (1994) measured maximum

compressive creep rates of different corrugated media and linerboards at constant and cyclic humidities. They showed that even though hygroexpansion of the material does not predict the creep performance, the ranking of materials based on their hygroexpansive strain applies on the creep rates measured in different humidity cases. Kuskowski et al. (1994) observed a relationship between component hygroexpansion and combined board creep performance; as the material hygroexpansion increases, the creep rate of the combined board increases also. Chalmers (2001) found that their results from compressive accelerated creep experiments could be modelled as sum of cyclic hygroexpansive strain (sinus function) and static creep strain (exponential function).

Varying results have been presented on the effects of recycled fibers on the creep rate. In the case of accelerated creep, Byrd (1978) showed that the creep rate increased more in paperboards containing recycled or high yield fibers than in virgin fiber paperboards (see Figure 2.23).

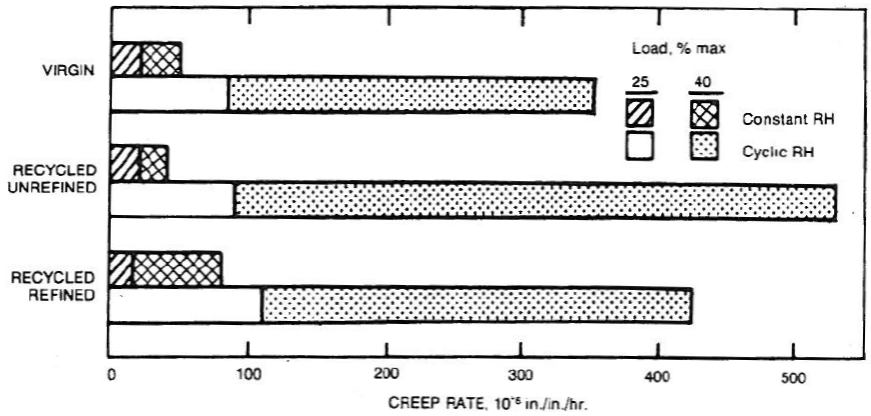

Figure 2.23: Edgewise compression creep rate in constant and cyclic humidity for corrugated fiberboard made from virgin and recycled pulps (Byrd 1978).

Considine et al. (1994) studied compressive creep of commercial paperboard corrugating components in the following conditions: (i) cyclic RH at high load, (ii) constant 96% RH, (iii) cyclic RH at low load, and (iv) constant 56% RH. Maximum creep rate was reported from the experiments. Unlike the results of Byrd (1978), the corrugating medium (127 g/m^2) from recycled fiber didn't show statistically any different maximum creep rates compared to the other corrugated medium types that were studied.

Coffin et al. (1999) studied the effect of recycled fibers on accelerated creep in tension by comparing handsheets made from never-dried and once-dried fibers. The effect of recycling was simulated by preparing handsheets from once-dried fibers. Equal tensile strength was obtained by additional refining. Results showed that papers from untreated once-dried fibers show higher degree of accelerated creep than never-dried sheets. Refining the fibers eliminates the excess accelerated creep. Söremark and Fellers (1995)

conclude that accelerated creep effects are larger for recycled fibers than for virgin fibers, and that the difference is enhanced at higher stress and strain levels (see Figure 2.24).

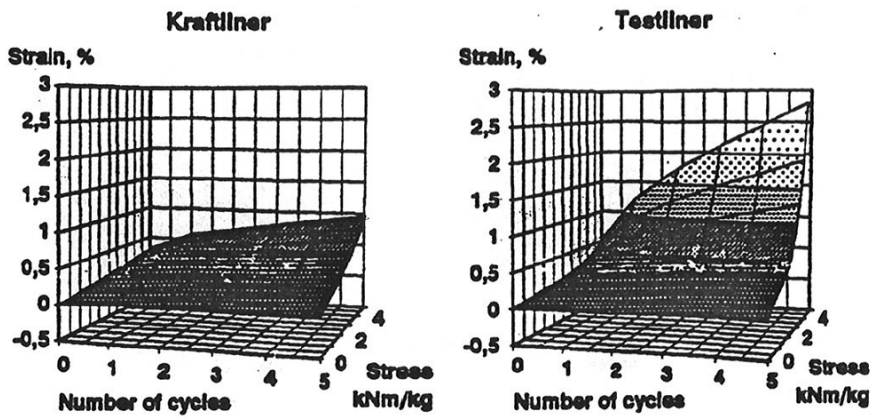

Figure 2.24: Tensile creep stiffness curves in CD as a function of moisture loading (50-90% RH) cycle number. The figures show how accelerated creep effect is larger at recycled fibers (testliner) at higher stress and strain levels (Söremark and Fellers 1995).

Byrd (1984) noticed that the combined corrugated fiberboard creeps 2-5 times faster than the individual components would indicate, and anticipates that the effect rises both from the material behavior and non-material factors like corrugated specimen support during the test and the relatively complicated geometry of corrugated board.

The mechano-sorptive factor (MSF) is loosely speaking the relation between accelerated creep and creep in constant humidity. More precisely the MSF is the relation between isocyclic creep stiffness index after three 7h moisture cycles and the creep rate at the low moisture content used in determining the isocyclic creep stiffness index after 21h (Fellers and Panek 2007). A higher MSF means that the material creeps less in a cyclic climate in relation to creep in the constant climate. Restrained drying has a similar effect on creep in cyclic and constant humidity (see Figure 2.25). The figure also shows that MSF of OCC material lies a little bit over the average among the other studied raw materials.

Tests of mechanical properties of paper are usually done at constant temperature. Varying the ambient temperature changes the moisture content of the sample, and the experimenter needs then to choose between constant relative humidity and constant moisture content which are both experimentally more complicated aims. The relative humidity depends on the saturation vapor pressure of water in air, which in turn depends on temperature. In order to hold relative humidity constant in increasing temperature, the absolute humidity in the test chamber must increase accordingly. The relation between moisture content and temperature in paper is not clearly understood (Haslach 2000). Skogman and Scheie (1969) showed that at high relative humidities (over 50% RH) the

moisture content of kraft paper increases from -20°C to approximately 5°C, and then decreases beyond that temperature. This maximum moisture content did not occur at the lowest relative humidity 30% RH that was studied. Benson (1971) report linearly decreasing moisture content of kraft linerboard as a function of temperature in the range of 15-50°C. Varying ambient temperature at constant relative humidity accelerates tensile creep, but the magnitude of the resulting creep strain is much smaller than when varying relative humidity (Haslach and Abdullahi 1995).

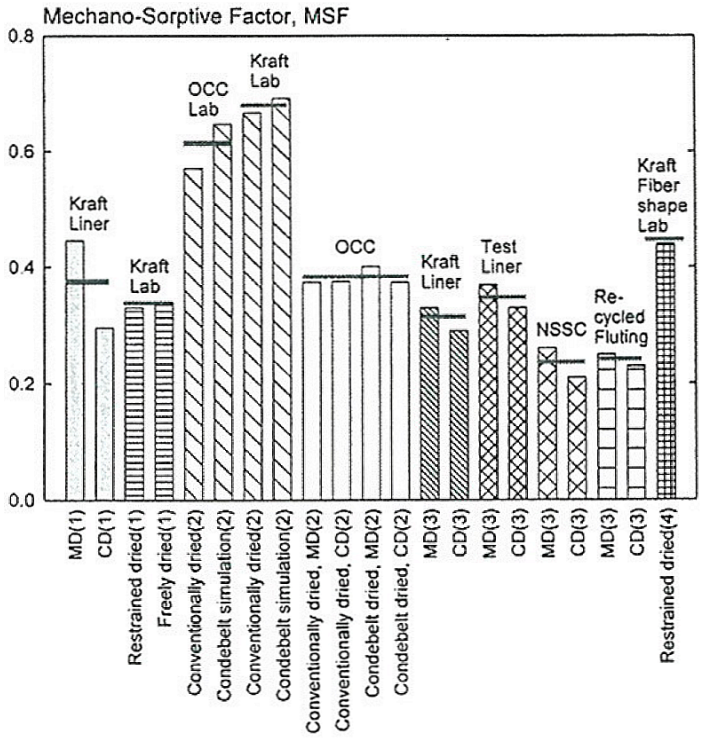

Figure 2.25: Mechano-soprtive factor of different board materials (Fellers and Panek 2007). The data is gathered from several authors.

Components of the total strain

In the above discussion, hygromechanical strain ε_{hygro}, elastic strain ε_E, and creep strain ε_{cr} have been introduced. The total strain of a material is expressed as a sum of these components (Equation 2.14). Other possible components include, e.g., plastic strain ε_E and thermal strain ε_T. Their relative share vary depending on the material and application in question, for example the thermal strain is usually left out when paper materials are studied.

$$\varepsilon_{tot} = \varepsilon_E + \varepsilon_P + \varepsilon_{hygro} + \varepsilon_{cr} + \varepsilon_T \qquad 2.14$$

2.3.3 Solid fiber boxes

Box properties emerge from the physical properties of the constituent materials and from the structural parameters of the box. Moisture affects the properties of board, glue, and coating layers that constitute the combined board, properties of the combined board itself and the service properties of boxes in end-use situation. Testing on all these levels is often needed, since the behavior at lower level of detail does not always predict the performance at the higher level due to complicated interactions.

This chapter discusses how the environment affects compression strength and creep of a box. The stacking of boxes is not covered, although it has been showed that the effect of misalignments in stacking is bigger than the effect of moisture content on compression strength of corrugated boxes (Singh 1999). Bending stiffness, which is an important property of paperboard in predicting the performance of boxes, is introduced.

Box compression strength

Box compression of single boxes has since long been used to simulate the performance of the box in the end-use situation, even though the box cannot sustain the stacking load obtained in a compression test (Kellicutt and Landt 1952, Kellicutt 1960). The box compression test (BCT) shows a large standard deviation in the results due to, e.g., variation in raw material, imperfections in the box geometry produced by the manufacturing process, and environmental conditions during the testing. The variation easily masks the effects of the studied variables. In a controlled test environment, the 2-sigma variation of BCT results of individual factory made boxes of same quality over time is normally ±14%, even as high as ±20% (Carlson 2002). Still the same conditions that change the top-to-bottom compressive strength in laboratory, change also the duration that the box can support dead loads when stacked during transportation or in storage (Kellicutt 1963).

In the box compression test (BCT), sometimes called the top-to-bottom test (TTB), a box is loaded from top to bottom between two platens, and the force is recorded as a function of vertical displacement (BCT curve). The test is carried out according to standards, e.g., ISO 12048-2:1994. In the test, a box is loaded from top to bottom between two platens, and the force is recorded as a function of vertical displacement. Figure 2.26 shows a typical BCT curve.

Typical phases of a force-elongation curve are as follows (Steadman 2002):

A. Any unevenness of the box is leveled out as the platens compress the box. The top scorelines start to roll as the box begins to take load. The slope is affected by the quality of the scores.

B. The vertical edges of the box start to take load. This part of the BCT curve has the steepest slope, since the corners of the box are the stiffest elements in the structure. The vertical edges of regular slotted containers (RSC) are reported to carry 40-64% of the total force during compression (Maltenfort 1980, Meng et al. 2007).

C. The peak is caused by the small scale yielding of the fold scorelines.

D. The long panels start to buckle outward, and the load is taken up by the short panels.

E. At the maximum force (BCT value) the box corners compress and the short panels begin to buckle. The box moves into general failure.

F. A localized stability caused by the buckled structure temporarily assuming more stable configuration. Such stabilities are not always observed.

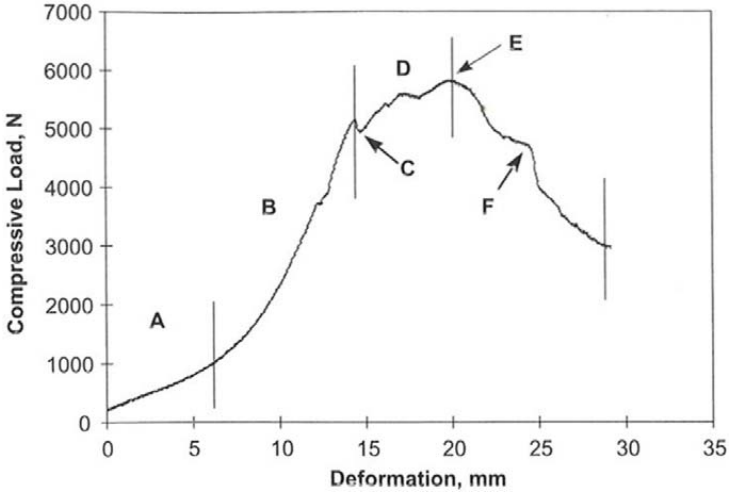

Figure 2.26: Schematic load-deformation curve from box compression test (BCT curve) (Steadman 2002).

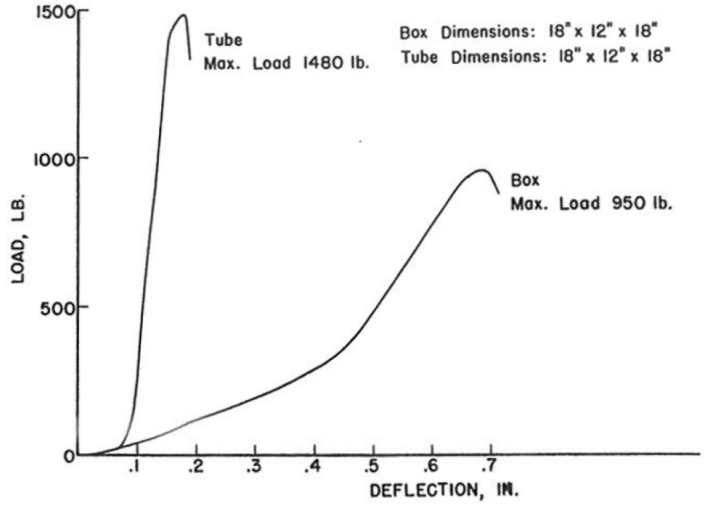

Figure 2.27: Compression load vs. deformation curve for box and tube (McKee and Gander 1957).

Flaps and flap scorelines have a large effect on the compression characteristics of the box. The sensitivity of BCT test offers a means to optimize the scoring process. Compressive properties of panels (Biancolini and Brutti 2003, Hansson 2008), tubes (Peterson and Schimmelpfenning 1982), panel scoreline sections (McKee and Gander 1957), hand holes (Han and Park 2006), and even the glue used in corrugated board (Leake Wojcik 1989) have been studied to locate the effects of loading on different structural parts of the box. Figure 2.27 shows how the middle section of the box has higher stiffness than the top and bottom sections, where the behavior of the creases affect the compression stiffness. The compression strength of a box is approximately 70% of that of a tube.

The moisture content affects the mechanical properties of paperboard materials, and thus the boxes made of paperboard (Kellicutt and Landt 1952). Kellicutt (1960) found a negative exponential relationship between compression strength Y of corrugated board boxes and their moisture content m:

$$Y = b10^{-mx} \qquad 2.15$$

where b = compressive strength of box at zero moisture [N], m = average slope of the curve where logarithm of compressive strength is plotted against moisture, and x = dry-based moisture content (ratio between the weight of water in the board and the oven-dry weight of the fiberboard). Kellicutt (1960) observed that the boxes made of different corrugated materials (non-coated) responded essentially the same way to the increase in moisture content, and the parameter m was found to have the value of 3.01. Figure 2.28 shows the compressive strength against moisture content for different corrugated materials.

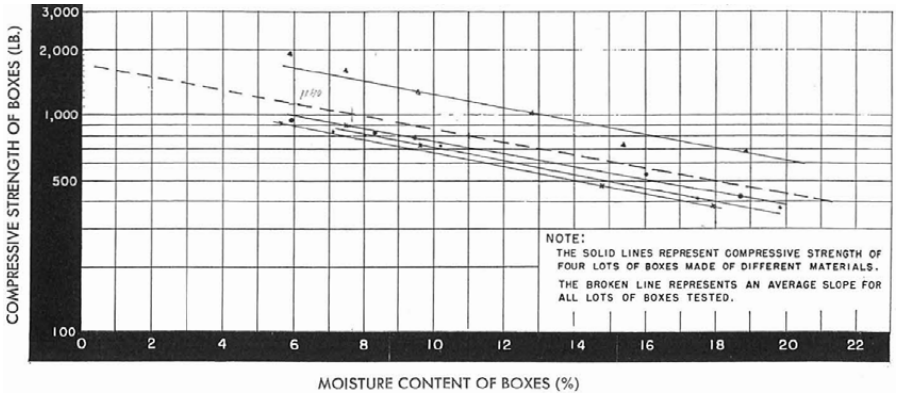

Figure 2.28: Influence of moisture content of corrugated fiberboard on compressive strength of boxes (Kellicutt 1960).

Corrugated boxes loose 50%-60% of the BCT when RH is increased from 50% to 90% (Whitsitt and McKee 1972). Sonneveld (1986) reports that at 96% RH/9°C the

compression strength of boxes made of solid fiberboard without polyethylene coating was 77% of the values of the test conditions 90% RH/20°C.

The strain at BCT and the strain at compression strength of panels are often unaffected by certain variables of the test. The in-plane deformation of panels at collapse has been found to be independent of deformation rate, relative humidity and the magnitude of dead-load (Hansson 2008). Hansson (2008) derived the conclusion by studying corrugated panels under compression, which was considered as a more controllable test set-up than compression of whole boxes. If extended to boxes, this would mean that the vertical displacement at compression strength is independent on moisture content of the box, and that the box failure criterion could be expressed as a critical strain limit. Haraldsson et al. (1997) studied the accelerated creep of corrugated boxes, and noticed interestingly that the failure of boxes occurred always at certain deformation (0.5%) no matter if one or more cycles were completed. They suggest also that the overall functionality of the box is related to the strain or buckling of the box panels instead of relating it to stress (BCT value).

Predicting box compression strength

When a container is subjected to a compressive force, the vertical panels buckle outward, and from a certain force the vertical box corners carry most of the load. This behavior can be modeled with an equation describing the behavior of a plate in compressive loading (Engman et al. 1978). The strength of a multi-ply or laminated paperboard panel depends on the edgewise compression strength and bending stiffness of the material as described by Equation 2.16 (Engman et al. 1978):

$$P_c = k\sqrt{F_c S_{b,geom}} = k\sqrt{F_c\sqrt{S_{bx}S_{by}}} \qquad 2.16$$

where P_c = panel compression resistance [N], F_c = edgewise compression strength of the material in the loading direction of the box [N/m], S_{bx} and S_{by} = bending stiffness in MD and CD direction [Nm], $S_{b,geom}$ = geometric mean of bending stiffness in MD and CD [Nm]. k is an experimentally defined parameter which theoretical value is 2π. The value depends on the dimensions and arrangement of the flaps of the box.

Increasing bending stiffness and compression strength of paperboad increases box compression strength. In practise, it's far easier to influence the bending stiffness than compression strength by modifying the layer structure (Niskanen 2008). For corrugated fiberboard a similar equation to Equation 2.16 is known as the McKee equation. The McKee equation gives an empirical relation between the box circumference, material parameters and compression strength of the box.

Bending stiffness

The bending stiffness of a structure is defined as the relationship between the applied bending moment and the resulting curvature of the structure. It combines the effect of the

material properties and the geometry of the structure. For a homogeneous structure with a constant elastic modulus, the calculation formula is simply:

$$S_b = E\frac{h^3}{12} \qquad 2.17$$

where S_b = bending stiffness (per unit width) [Nm], h = thickness of the beam [m] and E = elastic modulus [N/m^2]. Bending stiffness typically is measured with 2-, 3-, or 4-point methods (Steadman 2002), which measure the bending moment and the corresponding deformation. For thick boards the only possibility is the 4-point method. Comparisons of these methods can be found in Koran and Kamden (1989) and Fellers (1997). The highly beneficial structure and low grammage give corrugated fiberboard a bending stiffness index, which is significantly higher than that of multi-ply paperboards, 119 MNm^7/kg^3 vs. 1.35 MNm^7/kg^3 (Niskanen 2008). Bending stiffness index is used to compare boards that have different grammage. It is defined by dividing the bending stiffness by the cube of grammage.

The elastic properties of multi-ply boards, either laminated or stratified, vary in the thickness direction. The multi-layer structure of a stratified sheet is created in the forming section of paper machine. The bending stiffness of the combined board is obtained in analogy to Equation 2.17 by summing the contribution of each layer i:

$$S_{b,i} = E_i\left[\frac{d_i^3}{12} + d_i(h_i - z_0)^2\right] \qquad 2.18$$

where z_0 = coordinate of the mid-plane of the structure [m]. Parameters for the layer i: $S_{b,i}$ = bending stiffness contribution [Nm], E_i = elastic modulus [N/m^2], d_i = thickness [m], h_i = coordinate of the mid-plane of the layer i [m].

The optimal organization of the layers in the laminate structure can be understood based on Equation 2.18. The outermost layers of a multi-layer structure play an important role due to the effect of geometry. The high elastic modulus of these layers comes into effective use as they lie far from the neutral axis and thus possess a high area moment of inertia. Bulky, low density boards are suited as middle layers since the basic function of the intermediate layers is to keep the outermost layers separated.

Hamelink (1963) and Luey (1963) were the first authors to point out these geometrical facts for paper materials. Newer research on optimizing the bending stiffness of multi-ply paper include the work of Häggblom-Ahnger (1999) who optimized the bending stiffness of 3-ply copy paper and the consumption of pulps by locating various sulfate pulps in middle and surface layers. Navaee-Ardeh and Nazhad (2008) built a model that maximizes the bending stiffness of a symmetric 3-ply board by varying the basis weight of the middle-layer. Good agreement was achieved with the experiments. Deng et al. (2001) optimized experimentally the bending stiffness of multi-ply folding boxboard by varying elastic modulus of surface plies and the proportional share of basis weight

among the plies. The amount of refining and the softwood pulp content in the surface plies were found to be the critical control variables in improving the bending stiffness while keeping selected quality variables unaffected.

Old corrugated containers (OCC) is a raw material type that gives good panel compression index as Figure 2.29 shows. Usage of fillers reduces the panel compression strength. Intrinsic properties of the pulp, papermaking process, and handling of the paperboard in converting, for example given as an angle of wrap (arch of contact) when guiding the paperboard web, affect the bending stiffness (Edholm 1998).

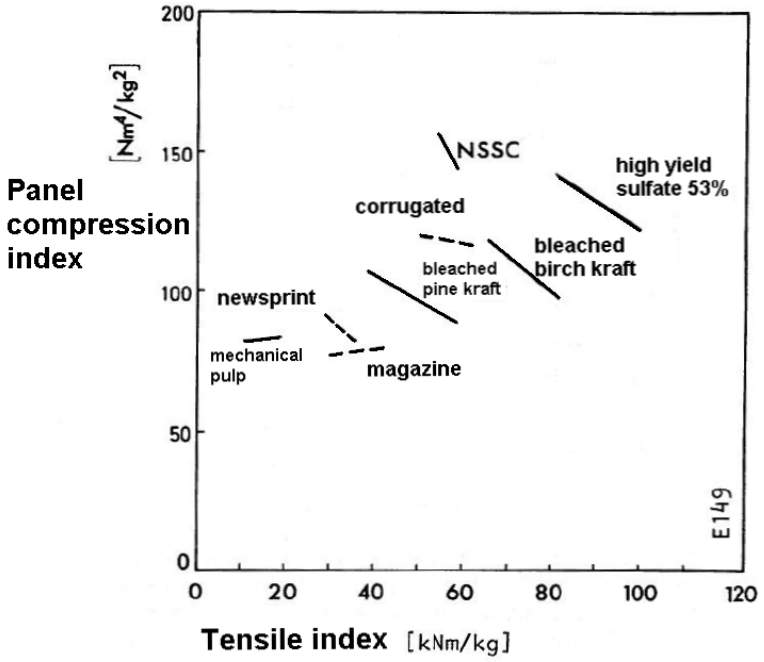

Figure 2.29: Panel compression potential of different recycled pulps. Dashed lines - recycled fiber pulps, solid lines - virgin pulp, NSSC = neutral sulphite semi-chemical (Engman et al. 1978).

Creep of boxes

In addition to BCT, another typical way to characterize the performance of boxes is to measure the lifetime of the box in a creep test. The box is loaded at a fraction of the compression strength, and the time to failure at constant or varying RH is measured. Creep behavior of containers is a combination of the following factors (Bronkhorst 1997). The same list applies to the compression behavior during BCT test.

- Material behavior: Elastic and creep behavior of the paperboard, moisture transfer properties, mechano-sorptive behavior.
- Small-scale structural behavior: Mechanical coupling between layers, moisture content variation through the combined board.

- Large-scale structural behavior: Design and geometry of the box, buckling response of the vertical panels, moisture content variations throughout the box.
- Pallet structural behavior: Box placement within the pallet, stacking misalignments, damages caused by transport.

Time to failure in constant environment decreases logarithmically as the dead load approaches the compression strength of a single box (Bronkhorst 1997). There is no standard apparatus or climate for creep testing of boxes, but it is generally advised that the creep test of boxes should be carried out at service conditions (Steadman 2002). The shape and phases of the deformation-time curve of a box are essentially the same as those for the material creep test as seen in Figure 2.20. Haraldsson et al. (1997) suggest that creep testing of a material is used to predict the lifetime of the box.

One of the major factors affecting the creep behavior of boxes is the moisture content. Leake and Wojcik (1993) studied the moisture content of corrugated boxes in varying environmental conditions (relative humidity and temperature), and noticed that the moisture content responds quickly to the changes in ambient humidity. In moisture barrier coated board materials, the moisture must first transport through the coating which causes a delay and slows down the rate of moisture penetration.

Figure 2.30 demonstrates the effect of humidity cycling on the lifespan of boxes, i.e. time to failure in creep test, compared to constant humidity. Boxes that were equilibrated at 32°C/90% RH had the moisture content of approximately 20% and the moisture change was 0% during the test. Even at this high but static moisture content the box lifetime was considerably longer than at any of the studied cyclic conditions. Environmental cycling reduces the time to failure by at least 70% from 90 days to 15 days (two cycles/day). The slower the cycling, the lower the lifespan. In cyclic conditions the moisture varied between 10.3% and 13.7% (two cycles/day). The study of Leake and Wojcik (1993) also shows that the change in height of boxes is different in each of the three studied moisture cycling rate cases.

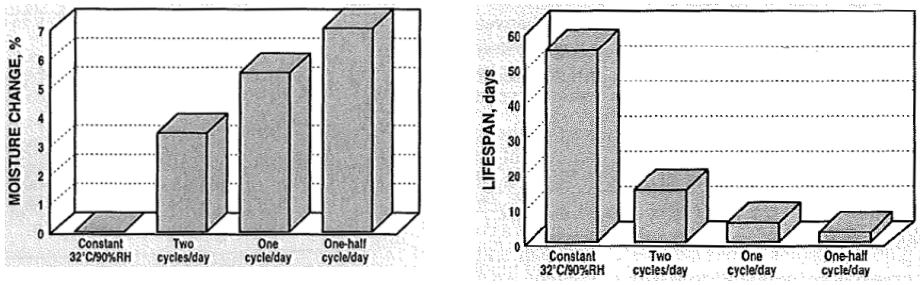

Figure 2.30: Left: Change in moisture content of corrugated boxes in constant and cyclic environmental (both moisture and temperature) conditions. Right: Lifespan of corrugated boxes in creep test with 90.7 kg dead load at constant and cyclic moisture conditions (Leake and Wojcik 1993).

Polyethylene coating reduces the creep of boxes in cyclic relative humidity and temperature conditions (Kirkpatrick and Ganzenmuller 1997). Figure 2.31 shows how the deflection of the PE coated boxes after the test period is 30% of the non-PE coated boxes made of recycled fibers. The moisture content of the PE coated boxes increases very slowly, which has a major contribution on the slow creep rate, small buckling of the side panels and small top-to-down deflection during the test.

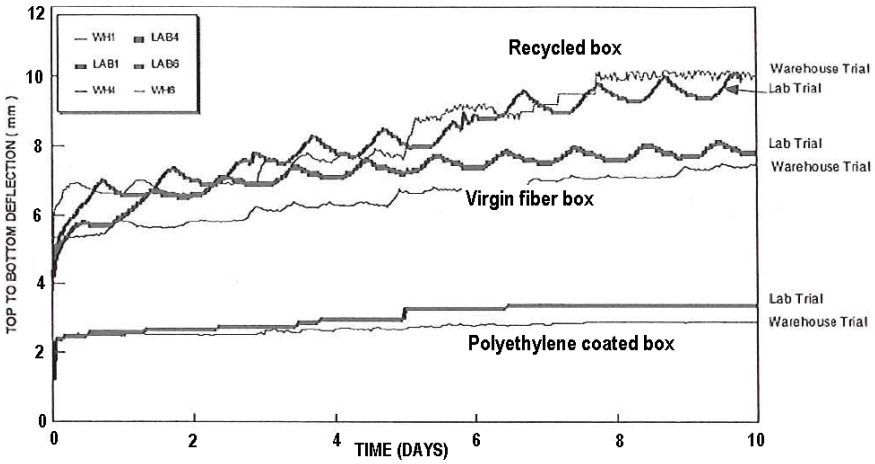

Figure 2.31: Creep data of stacks of corrugated boxes in cyclic humidity and temperature. Types of corrugated boards: virgin fiber, recycled fiber, and polyethylene coated. Humidities: random 25-85% RH in warehouse trials, controlled 58-90% RH in laboratory trials (Kirkpatrick and Ganzenmuller 1997).

Chapter 3

MATERIALS AND METHODS

3.1 Solid fiberboard lamination and structure

There are numerous methods of lamination depending on the substrates and the glue used. The lamination process specific to the solid paperboard used in this study is presented in the following section (Stylo and Levang 2009). The glue is water-based dispersed emulsion of polyvinyl acetate (PVA), clay as filler and several additives. PVA is a typical fast binding adhesive for porous materials. Additives are used, e.g., for controlling the rheology, adhesion, and odor properties of the glue emulsion.

The lamination process starts with dispersing the dry glue in water to form a mixture that has 24% solid content. The liquid glue is heated to 70°C, and pumped to a glue bath (50°C) where glue attaches to a rotating applicator roll. The excess of glue is scraped off to the desired dose. The amount of glue used is 5 g/m^2 (dry matter) per adhesion layer. From the roll the glue is transferred on the paper web (Figure 3.1). Depending on the surface structure of the paper, more or less glue is applied. The glued paper webs proceed to the pressing and cutting unit, which applies a pressure of 3-5 bar for the glue to adhere to the surfaces, and cuts the web sheets to desired size (1180 mm × 990 mm). The speed of the laminator is 170 m/min. (2.9 sheet/s). The sheets are stored in stacks of 20 pieces waiting for converting. The boxes arrive at the customer three days after the lamination.

Figure 3.1: Glue applicator roll.

During the lamination, approximately 80 g/m^2 water from the liquid glue (15.8 g/m^2 water/glue layer) absorbs in the paper and paperboard layers and elevates their moisture content. The water gets practically trapped inside the material due to the plastic coatings.

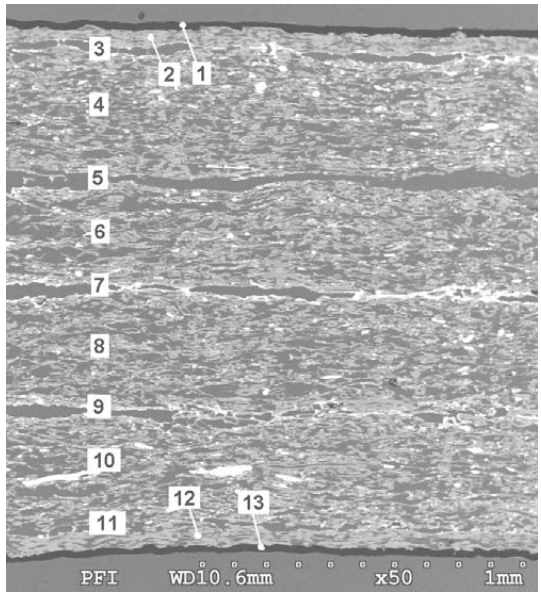

Figure 3.2: A SEM picture of the cross-section of the solid fiberboard.

The solid fiberboard grade studied in this work consist of four paperboard layers (layers 4, 6, 8 and 10 in Figure 3.2), two kraft paper layers (layers 2 and 12) that have double extruded polyethylene coating (layers 1 and 13), and five adhesion layers (layers 3, 5, 7, 9 and 11). The middle layers are made of recycled fibers (OCC), and they are heavily rosin sized. No wet strength chemicals are used.

Table 3–1: Grammage and thickness of the layers in the solid fiberboard.

Layer name	Layer No. in Figure 3.2	Grammage [g/m^2]	Thickness [mm]
PE coating	1, 13	20	0.02
Kraft paper	2, 12	60	0.07
Paperboard	4, 6, 8, 10	250	0.39
Adhesion	3, 5, 7, 9, 11	10	--

The approximate grammages and thicknesses of the layers of the laminate are given in Table 3–1. The grammage of the combined solid fiberboard is 1220 g/m^2 and the thickness 1.73 mm. The lamination process compresses the constituent layers 11%. The thicknesses in Table 3–1 are calculated based on thickness measurement of the

constituent layers before lamination and assuming even compression in the thickness direction. No thickness is given to the heterogeneous adhesion layer due to the difficulty in deciding the correct way to express the thickness as can be seen in Figure 3.2.

Samples of solid fiberboard and the constituting layers were retrieved from the production line in September 2008. They were cut to A4 size samples for storing in standard climate (50% RH, 23°C) inside a corrugated box. These same samples were used in all the material tests reported in the Papers.

The A4 size samples of all the materials were cut using a knife and an A4 size precision plate. For tensile testing of paper and paperboard, a punch was used to cut the 15 mm wide test strips. All specimens of the solid fiberboard were first measured with a caliper or ruler, and then cut with the knife due to the extensive thickness of the material. The accuracy and precision of this method was tested. The target width of the test piece was 38.00 mm. The width of 18 test pieces (38 mm × 70 mm) was measured with a caliper on both ends of each test piece. The mean and the standard variation of the 36 width readings was 37.9mm ± 0.3mm. The paralleleness of the long sides of the test pieces (wedge shape) was 0.10° ± 0.07° for 18 test pieces.

3.2 Transport box design

The outer measures of the transport box studied in Paper C are 790 mm × 380 mm × 138 mm. The erected box is shown in Figure 3.3.

The design of the transport box is more complex than the commonly used regular slotted container (RSC) or similar boxes. The box has double-panel long walls, and the sleeves of the inner panels of long walls are glued on the bottom panel at the mill. Single panels construct the short walls. The small flaps seen inside the box along the short sides hide a corner structure (webbed corner) that prevent leakages of the contents and also penetration of liquid water into the material. Moisture can penetrate through the open material edges of the flaps and approach the vertical edges and corners that are critical to load bearing ability of the box. The webbed corner allows the vertical edges and short panels to buckle outwards when the box is vertically loaded. Four small flaps hold the box structure together when glued onto the outer long wall panels.

Boxes were sent to Innventia, Sweden to testing from the mill in Trondheim. The boxes were delivered flat with the inner long wall panel glued on the bottom panel. The pallet of flat boxes was covered with a plastic film at the mill to preserve the original moisture

content. The storing occurred in room conditions at Innventia. Before the tests the boxes were erected and glued manually without a gluing rig.

Figure 3.3: Transport box studied in paper B.

3.3 Material tests

The mechanical tests were conducted in two equilibrium moisture contents: standard (50% RH, 23°C) and in high moisture content (90% RH, 27°C). The temperature 27°C is due to the usage of climate chamber that has no temperature control. Both the temperature and the humidity have an effect on the measured mechanical properties of paper materials (Wink 1961). The effects of temperature are not studied in this work.

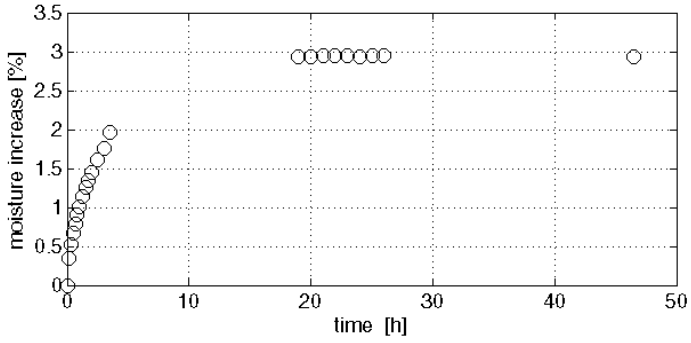

Figure 3.4: Stabilization of moisture content of a solid board strip (210 mm × 15 mm) after a step change in relative humidity (from 50 to 90% RH).

The properties of paper materials are measured when the material is at equilibrium with the environment. Moisture transport into solid fiberboard is exceptionally slow, and thus sorption tests on the solid fiberboard samples of different sizes were done to ensure long enough exposure times in high humidity climate. Figure 3.4 shows the stabilization of

moisture content on a 210mm × 15mm size sample after a step change in relative humidity. Based on the curve it is seen that 20 hours is enough to reach the equilibrium moisture content.

Bending stiffness of the solid fiberboard was measured with a Lorentzen&Wettre 4-point bending tester according to SCAN (P 65:91), with 150 mm free span. The 45 mm wide samples were allowed to stabilize 480 h (20 days) at 90% RH/27°C prior to testing. The samples that were tested at 50% RH were cut from A4 size samples that had been stored in standard climate for several months prior to testing.

Hygroexpansion of the solid fiberboard was measured with a Lorentzen&Wettre micrometer system (type 3-2), which is based on measuring the length change of 15mm × 200mm test pieces. The results are presented in Report A.

Moisture penetration into solid fiberboard was determined by using various standard and non-standard techniques. Water permeability of the PE coated paper was tested with Cobb (ISO 535:1991). Edge wicking of the combined board was determined with a modification of the Klemm test (ISO 8787:1986). Water vapor penetration was measured with the cup test (T 448 om-97). Determination of in-plane diffusivity is based on weight measurement after a step change in relative humidity when the vapor penetration is restricted to in-plane direction. Paper A presents the moisture penetration methods used in detail.

Moisture content of the combined board and its constituents was measured by gravimetric measurements. The drying time of the solid board samples that had the approximate size of 20mm × 20mm was 72 hours in 103°C. At higher temperatures the PE started to soften considerably.

Tensile properties of the combined board and its constituents before the lamination were determined by recording stress strain curves in tension with a Zwick tensile testing apparatus according to ISO 1924-2:1994. The speed of the tensile testing of paper samples was 25%/min. The elastic modulus was determined from the curves as the maximum slope. The method is described in Paper B, and the results were used for calculating bending stiffness of the combined board.

Thickness of the solid fiberboard and its constituting paperboard layers before lamination were measured as standard thicknesses (ISO 534:1988), integrated mean thicknesses (STFI thickness), and by measuring from SEM images with the help of an image analysis program. The thickness measurement methods are described in detail in Paper B. The thicknesses found by different techniques were used in calculating the bending stiffness of the combined board.

3.4 Box tests

The boxes were exposed to the climate that normally prevails during fish transport (90% RH and 4°C). Some of the boxes had water inside to simulate the effect of fish and ice. Some boxes were pre-dried before the climate treatment to introduce a larger initial

moisture content range. Moisture content, buckling displacement of panels, and box compression strength was measured during the experiment. The results are presented in Paper C.

Moisture penetration into the boxes was measured by cutting samples from selected positions of the box (gravimetric moisture content measurement) and by weighing the whole box. The drying time of the solid board samples was 72 hours in 103°C.

Box compression tests (BCT) were done using an Alwetron CT100 (Lorentzen&Wettre) compression tester according to ISO 12048-2:1994. The compression strength and corresponding displacement were read from the load-displacement curves of single boxes. Tests with cyclically increasing loading and deloading were also run.

Buckling measurement: The outward buckling of the long outer panel during the box compression test was measured with three linear displacement transducers (RDP Electronics LTD, type DCT1000A) that were mounted on a rack. The transducers were placed vertically in the middle of the long side of the box. The distance between the sensors and box edges was one quarter of the height of the box. The transducers were connected via Contrec AQ-Box to a PC, and Contrec Winlog 2000 program was used for collecting data (sampling frequency 50 Hz per channel).

Creep test of the boxes were carried out by loading a stack of three boxes with a dead-weight of 244 kg at 4°C/90% RH. After eight days of exposure the boxes were compression tested in room (non-standard) conditions. The creep load selected (244 kg) is close to the 260 kg dead-weight that the lowest transport box in a stack should endure in the end-use situation.

Chapter 4

SUMMARY OF APPENDED PAPERS

4.1 Paper A: Moisture content of polyethylene coated solid fiberboard after industrial lamination

The aim of this paper was to identify and quantify main external moisture sources affecting the material moisture content during 8 days in different locations of a sheet. Knowledge of the development of the moisture content provides insight in understanding the dynamics of strength reduction of the boxes.

The original moisture content was measured gravimetrically from a newly laminated sheet (Figure 4.1). In the middle of the sheet, the moisture content is close the

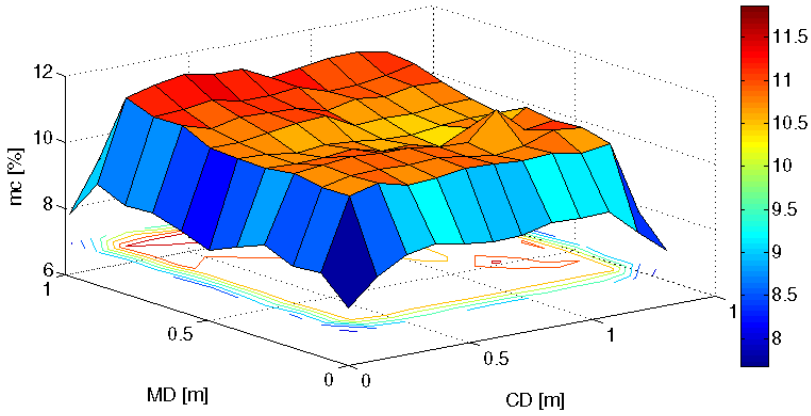

Figure 4.1: Moisture content of a solid fiberboard sheet two days after the lamination.

equilibrium moisture at 90% RH (11%), while a maximum 100 mm wide band around the sheet edges has lower moisture content. The polyethylene layer was confirmed to be practically impermeable for liquid water. In the horizontal edge wicking test, the penetration length of liquid water was found to be 40-50 mm during eight days of exposure.

Diffusivities were measured to be able to compare the water vapor penetration through the planes and the edges of the solid fiberboard sheet. The polyethylene coating restricts the lateral diffusion, and thus the main moisture transport is in the in-plane direction.

Based on an integrated unsteady state moisture transport equation and moisture sorption measurements, the in-plane moisture diffusivity ($5.87 \cdot 10^{-10}$ m^2/s, 50/90% RH, 27°C) was found to be nine times larger than the transverse diffusivity of the polyethylene. The in-plane diffusion process was found to be Fickian due to the large internal mass transfer resistance compared to the external mass transfer resistances.

The calculated diffusivity value is strongly affected by the equilibrium moisture contents at boundaries. In addition, the method doesn't address the dependency of the diffusivity on the moisture content. To define the moisture content dependency, sorption and desorption isotherms should be established first. Then diffusivity is determined at several step-wise changes in RH level for the whole range of moisture contents.

Table 4–1: Transverse diffusivity of solid fiberboard surface layer (polyethylene coated kraft paper) and in-plane diffusivity of the solid fiberboard based on measurements at the given climates. WVTR values are measured with the cup test. (*) The estimated values are based on measurements at a different climate.

	0/50% RH/ 23°C	**0/90% RH/ 27°C**	**50/90% RH/ 27°C**
Polyethylene coated kraft paper			
WVTR [g/m^2/24 h]	2.8	8.2	3.2 (*)
Transverse diffusivity [m^2/s]	$6.3 \cdot 10^{-11}$	$7.3 \cdot 10^{-11}$	$6.5 \cdot 10^{-11}$(*)
Solid fiberboard			
In-plane diffusivity [m^2/s]	--	--	$5.9 \cdot 10^{-10}$
Solid fiberboard medium			
WVTR [g/m^2/24 h]	$1.7 \cdot 10^{2}$	$1.1 \cdot 10^{3}$	--
Transverse diffusivity [m^2/s]	$8.4 \cdot 10^{-8}$	$2.1 \cdot 10^{-7}$	--

The results show that the original moisture content changes only little during the eight days transport, approximately 0.3 percentage points based on the calculations assuming a constant 10% RH driving force (the difference between ambient 90%-100% RH and 80%-90% RH inside the material) at 4°C. The moisture content of the sheet is controllable with reasonable efforts during the manufacturing. From the producer's point of view, even a slight reduction in the amount of water in the glue used for laminating the board creates stronger transport boxes. The moisture transport through the solid fiberboard edges creates locally stronger and weaker areas, the effect of liquid water reaching 30-40 mm from the open edge. The Equation 4.1 (Bird 1960) gives penetration thickness due to diffusion in a semi-infinite slab,

$$\delta_M = 4\sqrt{\alpha t} \qquad 4.1$$

where δ_M [m] = penetration thickness of moisture, α [m^2/s] = diffusivity, t [s] = time. Based on Equation 4.1, the penetration thickness of the solid fiberboard is 80 mm in eight days. That is, for distances $y > \delta_T$, the moisture content changes less than 1 per cent of the difference between equilibrium moistures in 50% RH and 90% RH. Joint effects of liquid water and water vapor were not studied.

4.2 Paper B: Modeled and measured bending stiffness of polyethylene coated solid fiberboard

In this paper, the role of the adhesion layers to bending stiffness of solid fiberboard was studied using classical laminate theory, where each layer was modeled as a homogeneous elastic medium having certain E modulus and thickness. The solid fiberboard studied has six paper and paperboard layers with different properties which can be measured before the lamination. The glue layers can either be discarded from the model as insignificant, or included in the model as having parameter sets based on measured values.

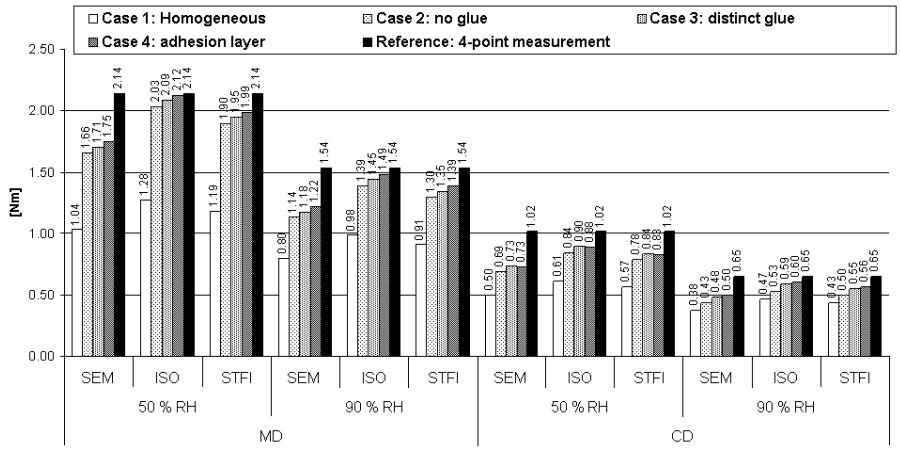

Figure 4.2: Measured and modeled bending stiffness [Nm] of solid fiberboard in two moisture contents together with 4-point measurement as reference. Three different thickness measurement methods are used

The thickness measurement of paper materials is a problematic task since the thickness of paper is not well defined. Thickness determination still has a crucial role in the bending stiffness calculation. The suitability of the following thickness measurement techniques to the modelling task was studied: (i) ISO method (hard-platen technique), (ii) structural thickness method (spherical platen technique) and (iii) from SEM pictures of the cross-section of the combined board. The best agreement of measured and predicted bending stiffness values was reached when thickness values obtained by the ISO method were used in the prediction model (Figure 4.2, columns with the label ISO). Probably the ISO technique that measures the thickness with hard platens best imitates the contact of two rough paperboard surfaces.

Best agreement with the measured bending stiffness values was obtained by a 11-layer model with ISO thicknesses, where the adhesion layers joining the paperboard sheets are seen as reinforcement to the surrounding paperboard structure (see Figure 4.2, Case 4). The PE and kraft paper are combined. This model gives 0.9% (MD) and 13.7% (CD) smaller values in 50% RH, and 3.2% (MD) and 7.7% (CD) smaller values in 90% RH compared to the reference. Tensile tests of glued 2-layer paperboard sandwiches verify that the adhesion layer has an effect on the tensile stiffness. Omitting the adhesion layers gives 5.1% (MD) and 17.6% (CD) smaller values in 50% RH, and 9.7% (MD) and 18.5% (CD) smaller values in 90% RH compared to the reference measurement.

In the model, the effect of moisture was introduced as a reduced elastic modulus of the layers. Hygroexpansion of the material was not addressed. At high humidity levels the ZD hygroexpansion increases the thickness of the combined board. The models are based on the thicknesses measured at standard conditions. For the layered structure with adhesion layers and ISO method as thickness determination method (Figure 4.2, Case 4), the reduction is 32% in MD and 37% in CD. from 50% RH to 90% RH. The high humidity treatment reduces the measured (4-point) bending stiffness approximately 28% in MD and 36% in CD compared to the standard conditioned samples.

4.3 Paper C: The effect of moisture content on compression strength of boxes made of solid fiberboard with polyethylene coating - An experimental study

The aim of this paper was to study the effect of moisture on the strength of boxes that have non-standard geometry and material type. The boxes were exposed to the environment and duration of the transport (4°C/90% RH, 8 days). BCT tests with constantly increasing force and cyclic force were measured during and after the climate treatment. BCT tests were accompanied by gravimetric and overall moisture content measurements. Also creep was measured during the climate treatment.

The main result is that the box failure can be expressed as a critical vertical displacement value that is not dependent on the moisture content of the box. In Figure 4.3, the displacement at the compressive failure of the box is constant (approximately 10 mm) throughout the moisture content range. Similar results have earlier been shown on panels or RSC boxes. The same displacement based failure criterion can be extended to this special box type with double-walls and webbed corners and PE coating.

Buckling of the outer long panel of the box and moisture content are negatively correlated (see Figure 4.3). It was found that the boxes mainly deform plastically, and that the share of the plastic deformation increased as the material got moister. As moisture content increased, the increased share of plastic deformation can accommodate more of the total deformation and as a consequence the panels show less outward

buckling. The share of (secondary) creep deformation from the total deformation of the boxes was found to be approximately 2%.

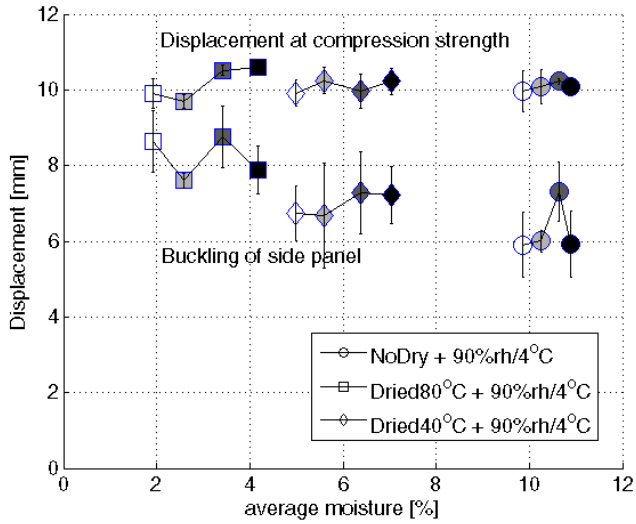

Figure 4.3: Displacement at compressive failure [mm] and outward buckling of the long vertical panel [mm] against the average moisture content [%].

The decrease of BCT values was almost linear with respect to the moisture content, as also reported by Kellicutt (1960). The compression strength decreases 380N per moisture content percent. The polyethylene coated solid fiberboard boxes lost 15% (from 5500N to 4700N) of their compressive strength by being exposed to high humidity in eight days. During that time, the moisture content increased by 1 percentage point. Data presented by Kellicutt (1960) shows that an increase in moisture content from 6% to 7% decreases the compression strength of uncoated corrugated boxes by 9%. An increase from 6% to 18% in moisture content would result in 56% reduction in compression strength. The decrease of 15% in compression strength for PE coated boxes is in line with the results by Kellicutt (1960), keeping in mind the moisture barrier role of the polyethylene. The results seem to hold even for the non-standard box design studied.

The moisture content of the boxes didn't stabilize in eight days after a step change in the relative humidity. The polyethylene coating slows down the moisture transport. After eight days of exposure, the moisture content close to the open edges is higher than in the middle of the board sheet. The effect is seen up to 100 mm from the edges. This local variation in moisture pick-up makes the usage of average moisture content doubtful. The independence of displacement from moisture in Figure 4.3 may be partly be explained by relatively stable moisture content in the load-bearing parts of the box.

4.4 Report A: Effect of polyethylene coating on in-plane hygroexpansion of solid fiberboard

The aim of the study was to investigate the effect of the polyethylene coating and its substrate paper on the hygroexpansion of the combined solid fiberboard. The hygroexpansion study here is done to understand and comment on how sorbed moisture affects boxes in end-use situations. The effect was studied in one sorption-desorption cycle (from 50% to 90% and back to 50% RH) instead of several cycles that is normal in hygroexpansion studies.

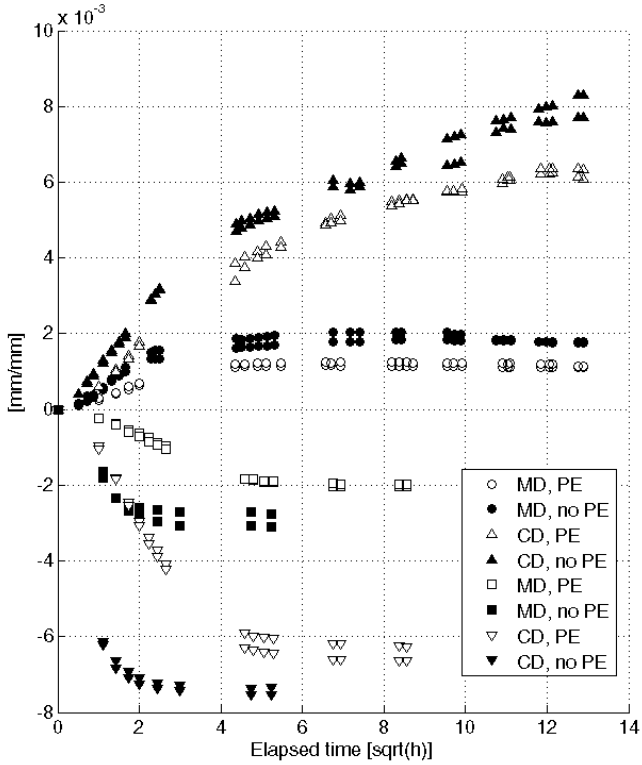

Figure 4.4: Hygroexpansion of the solid fiberboard with and without polyethylene coated kraft paper (the outer coated paper layers) in CD and MD in sorption phase (the curves above the zero displacement) and in desorption phase (the curves below the zero displacement line).

Figure 4.4 shows the relative change in length of the samples after the step change from 50 to 90% RH (curves above zero relative displacement). The desorption phase of the same samples after the step change from 90 to 50% RH is presented below the zero line.

Open symbols represent samples with the PE coated kraft paper, filled symbols represent samples without the coated paper layer.

The main findings are as follows:

- For PE coated samples in sorption, the MD strain stabilizes in pace with the moisture content, but CD strains needed ten times more time to reach the full strain.
- Without PE layers in desorption, the equilibrium contraction is reached in one third of the time required with PE layer. No difference in time to equilibrium expansion was observed in desorption between MD and CD.
- Hygroexpansion coefficients measured were: 0.0023%/% RH (MD, with PE), 0.0036%/% RH (MD, without PE).
- The polyethylene layer restricts the solid board approximately 13% in CD contraction, (insufficient data on expansion), and 34% in MD contraction and expansion.
- The tests without PE coating show that the phenomena at the board/surrounding air surface are masked out with other features arising from the bulk structure of the combined board. The same results was obtained in Paper A.

The topic and the results are interesting since there are no published results available on hygroexpansion of this specialty packaging board grade. The dimensions of paperboard boxes change due to moisture transport and subsequent swelling and contraction of the fibers. In the box, two of the vertical panels are oriented in CD and two in MD direction. The hygroexpansion properties of the material in machine and cross-machine directions affect the stability of the stacked boxes when they experience varying environments during storage and transportation. If the transport box is to be understood and modelled in detail, the magnitude and rate of the hygroexpansion is one of the phenomena to be considered.

The results reported show a clear trend, but the experiments should still be repeated to increase the reliability of the conclusions. In the data reported, the variation in the sorption data of the CD samples is substantial. The early phases of sorption and desorption are of interest, and more data points should be recorded from those phases. The control of the humidity conditions during the experiment should be ensured. In this work the PE coated kraft paper was peeled of. For studying only the effect of the PE, the role of the kraft paper should be identified.

Chapter 5

SUMMARY AND FUTURE WORK

This work has studied moisture penetration to a paperboard material, effects of moisture on selected mechanical properties of this paperboard grade, and on the strength of transport packages made from this material. The issues studied followed the logical chain of tasks when developing a new transport package. The development starts with identifying and gathering the requirements of the transport package. It is to be quantified in what climate the transport box will be used and what kind of loadings it will be exposed to. The material will be engineered to sustain the climate conditions, and the box is designed to withstand the static and dynamic forces during the intended lifetime of the transport box.

Scientific relevance

Scientifically the work contributes to the knowledge on moisture effects on a special, plastic coated paperboard grade and boxes. The main findings are related to the overall moisture penetration characteristics into the material and the boxes, the role of the glue layer in the bending stiffness of the paperboard, and the failure criterion of the boxes.

Moisture penetration into solid fiberboard is a slow phenomenon. The polyethylene coating substantially slows down the transverse moisture transfer, and the combined board itself has high grammage and glue layers that restrict the moisture transfer. The in-plane diffusivity ($5.9 \cdot 10^{-10}$ m^2/s) was found to be nine times higher than the transverse diffusivity thorough the PE. The consequence is that the time to equilibrium moisture content is very long, which affects the material testing. Larger structures like boxes do not reach equilibrium with environment within practical time limits, at least not during the intended life time of eight days. Due to the uneven moisture penetration into the boxes, the average moisture of a box is a questionable measure of moisture pick-up. Instead one should consider the moisture content of the load bearing parts. On the other hand, the overall moisture pickup is a very easy measurement. By applying it, the decrease of BCT was 380N per moisture percent which equals around 4.8% of the highest measured BCT values (8000N). The PE coated box loses only 15% of its BCT during eight days in 90% RH/4°C.

Best agreement with the measured bending stiffness values was obtained by an 11-layer model, where the properties of the adhesion layers are taken from the sandwich tests (paper-glue-paper). The PE and kraft paper are combined in the model. With this model, the calculated results are close to the measured reference at 50% RH (difference 1% for MD and 14% for CD). Neglecting the adhesion layers gives 5% smaller values in MD and 18% in CD compared to the reference measurement. The larger errors in 90% RH

are probably due to too low thickness values. The thickness measurements were carried out only in 50% RH. Adhesion layers affect the mechanical properties of the combined board and need to be addressed in laminate models.

The problematic nature of the thickness measurement became clear when the different thickness measurements methods were used to gather input data for the bending stiffness model. In this application, the ISO technique provided thickness measurements that brought the calculated bending stiffnesses closest to the reference. The other thickness measurement techniques were structural thickness method and direct measurement from SEM pictures of the cross-section of the combined board. SEM pictures reveal that there are large voids in-between the paperboard layers. Probably the ISO technique that measures the thickness with hard platens, best imitates the contact of two rough paperboard surfaces. The effect of the voids seen in SEM picture is twofold. The holes reduce the bending stiffness of the solid fiberboard. On the other hand, the holes are strengthened with a hard glue film that makes the structure more resistant to bending.

In this work, it was found that top-to-bottom failure criterion of a box can be expressed as a critical vertical displacement that is independent of moisture content. Earlier researchers have discovered similar indications when studying corrugated board panels (Hansson 2008) or the creep failure of boxes in cyclic humidity (Haraldsson et al. 1997). Failure occurs at a certain strain. This research shows that the strain dependent failure criterion apply also on more complex structures like the boxes in question that have double long walls and webbed corners. Earlier results were from studying either panels or simpler RSC boxes.

Fluctuations in raw material quality and process conditions cause variation in paper properties, which affect the repeatability of the presented results. For example the original moisture content of the solid fiberboard sheets is used in the considerations presented in this work, but the actual moisture content value varies according to the process conditions. The same material samples were used throughout this study. Since there is some change in paper properties during storage, the reported properties might not be exactly the same as straight after production. General trends and levels should be reliable within normal paper variance levels. The results found in this work are representative for laminated paperboard materials that have OCC as main raw material type, internally sized medium layers, and LDPE coating on both sides.

Relevance to the packaging producer

The results of this work help the paperboard producer and the box converter to better meet the specifications for a transport box. Water from the environment during the transport affects only 40-50 mm of the solid fiberboard sheet edges. Based on the in-plane diffusivity coefficient, water vapor can theoretically affect 80 mm from the board edge. These figures are applicable for the case when the relative humidity changes from 50% to 90% RH. They can be understood as maximum values, since the driving forces to moisture transport are much smaller in the real end-use situation. The box design should ensure that the open material edges are at least 80 mm away from the load bearing sections of the box. The 15% loss of BCT value during 8 days indicates that the present box design and material meet reasonably well the end use requirements. Impact tests and

tests with vibration loading should be executed to provide a complete idea of the box performance.

In the middle of the sheet the moisture content increases moderately, approximately 0.3 percentage points during the transport. The original moisture content, i.e. the solids content of the glue and the moisture content of the paperboards before lamination, has a large effect on the strength of the transport box. Even a small reduction in the original moisture content increases the strength of the box. In practice the moisture content cannot be optimized based on strength properties only. Too low a material moisture content will make the material more brittle and may cause cracking during converting operations, for example the creasing.

Future work

The papers presented in this work have brought information on how fast moisture penetrates a particular solid fiberboard grade, how the moisture affects certain mechanical properties of the material and one unusual box type. The next logical step would be to build a model of the transport box. The information produced in this work could serve as starting values to modeling work. The model could be used to test different design configurations, e.g., the effect of hand holes or ventilation holes on the compression strength of the box, and to optimize the material choices and usage when the size of the box varies, e.g., what would be the thinnest material that survived the compression strength requirements. Box modeling considerably reduces the need for expensive testing although it does not completely eliminate the need. With the model the most plausible designs can be screened, and the designs that would certainly fail can be rejected in an early phase.

Based on the results, the material model used in the box model would be based on elastic-plastic theory, since the share of the viscoelastic (creep) behavior of the solid fiberboard was observed to be relatively small compared to plastic behavior. The solid fiberboard expands when it comes to contact with water, but only a very extensive material model would include that behavior. Other effects, like the moisture effect on elastic properties, are more important. Based also on the results, the failure of the whole box can be expressed as critical top-to-bottom displacement. The plastic deformation of the boxes was mainly due to the plastic (permanent) crushing of the creases.

Solid fiberboard with its many material types and layers, and laminated thick paperboard materials are not very typical subjects for studies. More work could be put on relating the properties of the constituents and the behavior of the combined board. The role of the adhesion layers and the polyethylene on mechanical properties of the combined board and on the moisture transport inside the combined board could for example be more thoroughly investigated. However, the presented work covers a large field of properties and the produced information can be utilized when aiming at new transport package solutions from solid fiberboard.

Chapter 6

REFERENCES

Arnold, K. A. (1956): Physical properties of paper coated with polyethylene by extrusion. Tappi, 39(5), 324-329.

Alfthan, J. (2004): Micro-mechanically based modeling of mechano-sorptive creep in paper. Doctoral Thesis. KTH, Solid Mechanics, Stockholm, Sweden.

Back, E., Salmén, L., & Richardson, G. (1983): Transient effects on mechanical properties of paper during sorption of moisture, Tappi International Paper Physics Conference 1983 - Seminar proceedings (p. 173-179). Wychmere Harbor Club, Harwichport, MA: Tappi Press.

Baum, G. A. (1987): The elastic properties of paper : a review. In Kolseth, P., Fellers, C., Samlmén, L. & Rigdahl, M. (Eds.), Design criteria for paper performance, STFI Meddelande A969, 1984 Seminar on Progress in Paper Physics (p. 1-27). Stockholm, Sweden: STFI.

Baum, G. A., & Bornhoeft, L. R. (1979): Estimating poisson ratios in paper using ultrasonic techniques. Tappi, 62(5), 87-90.

Baum, G. A., Brennan, D. C., & Habeger, C. C. (1981): Orthotropic elastic constants of paper. Tappi, 64(8), 97-101.

Benson, R. E. (1971): Effects of relative humidity and temperature on tensile stress-strain properties of kraft liner. Tappi, 54(5), 699-703.

Bhargava, R., Rogers, C. E., Stannett, V., & Szwarc, M. (1957): Studies in the gas and vapor permeability of plastic films and coated papers - Part III. Effect of paper substrate. Tappi, 40(7), 564-716.

Biancolini, M. E., & Brutti, C. (2003): Numerical and experimental investigation of the strength of corrugated board packages. Packaging Technology and Science, 16(2), 47-60.

Bird, R. B., Stewart, W. E., & Lightfoot, E. N. (1960): Transport phenomena. New York: Wiley, XXI, 780 pp.

Brezinski, J. P. (1956): The creep response of paper. Tappi, 39(2), 116-128.

Bristow, J. A. (1968): The Absorption of Water by Sized Papers. Svensk papperstidning, 71(2), 33-39.

Bristow, J. A., & Kolseth, O. (Eds.). (1986): Paper - Structure and properties (Vol. 8, In: International Fiber Science and Technology). New York, Basel: Marcel Dekker Inc, 390 pp.

Bronkhorst, C. A. (1997): Towards a more mechanistic understanding of corrugated container creep deformatino behaviour. Journal of Pulp and Paper Science, 23(4), J174-J181.

Buck, A. L. (1981): New equations for computing vapor pressure and enhancement factor - Notes. Journal of Applied Meteorology, 20(12), 1527-1532.

Byrd, V. L. (1972): Effect of relative humidity changes on compressive creep response of paper. Tappi, 55(11), 1612-1613.

Byrd, V. L. (1984): Edgewise compression creep of fiberboard components in a cyclic-relative-humidity environments. Tappi, 67(7), 86-90.

Byrd, V. L., & Koning, J. W. (1978): Edgewise compression creep in cyclic relative humidity environments. Tappi, 61(6), 35-37.

Carlson, D. A. (2002): Box compression variation. Corrugating Int, 4(2), 7-9.

Castellan, G. W. (1983): Physical chemistry, 3rd Edition, 943 pp, California, USA: The Benjamin/Cummings Publishing Company, Inc.

Chalmers, I. R. (1998): The effect of humidity on packaging grade paper elastic modulus. Appita Journal, 51(1), 25-28.

Chalmers, I. R. (2001): A comparison between static and cyclic humidity compression creep performance of linerboard. Appita Journal, 54(5), 435-438.

Coffin, D. W. (2005): The creep response of paper: review. In I'Anson, S. J. (Ed.), Advances in Paper Science and Technology: 13th fundamental research symposium, Cambridge, 11-16 Sept. 2005, [Pulp and Paper Fundamental Research Society, 2005, 3 vols (ISBN 0954527232)] (Vol. 2, p. 651-747).

Coffin, D. W., Habeger, C. J., & Waterhouse, J. F. (1999): Effect of recycling fibers on accelerated creep. Atlanta, Georgia: IPST Technical paper series, number 829, Institute of paper science and Technology. http://hdl.handle.net/1853/1884

Considine, J. M., & Laufenberg, T. L. (1992): Literature Review of Cyclic Humidity Effects on Paperboard Packaging. In Laufenberg, T. L. & Leake, C. H. (Eds.), Cyclic Humidity Effects on Paperboard Packaging (pp. 1-10). Madison, Wisconsin, USA: TAPPI, USDA.

Considine, J. M., Stoker, D. L., Laufenbacher, T. L., & Evans, J. W. (1994): Compressive creep behaviour of corrugating components affected by humid environment. Tappi Journal, 77(1), 87-95.

Cramm, R. H. (1990): Polymers. In Kouris, M. (Ed.), Pulp and paper manufacture - Coating, Converting, and specialty processes (3rd ed., Vol. 8, 386 pp.). Canada: The joint textbook committee of the paper industry, Tappi, CPPA.

Deng, C., Retulainen, E., Palokangas, A., & Nazhad, M. (2001): Improving the bending stiffness of folding boxboard, 55th Appita Annual General Conference (Vol. 1, p. 251-258). Hobart, TAS, Australia: Appita Inc.

Edholm, B. (1998): Bending stiffness loss of paperboard at conversion-predicting the bending ability of paperboard. Packaging Technology and Science, 11(3), 131-140.

Eklund, D. (1969): Dimensional stability of paper from different types of pulp. Paperi ja puu - Paper and timber, 51(2), 153-161.

Engman, C., Fellers, C., Thun, M., Lundberg, R., & Ruvo, A. (1978): Kartong - Grundläggande samband mellan råvaror och mekaniska egenskaper hos skiktade ark, Serie D nr 50. Stockholm: Svenska Träforskningsinstitutet, 193 pp.

EU (1994): European Parliament and Council Directive 94/62/EC of 20 December 1994 on packaging and packaging waste. from http://eur-lex.europa.eu/LexUriServ/LexUriServ.do?uri=CELEX:31994L0062:EN:NOT, accessed May 18, 2010.

Fellers, C. (1997): Bending stiffness of paper and paperboard - a round robin study. Nordic Pulp and Paper Research Journal, 12(1), 42-44.

Fellers, C., & Panek, J. (2007): Effect of relative humidity cycle start point and amplitude on the mechano-sorptive creep of containerboard, 61st Appita annual conference and exhibition. Gold Coast, Australia, 6-9 May 2007.

Follestad, A., Nilsen, J., & Helland, I. (2006): Barrier properties of liner polyethylene films, ANTEC 2006 Plastics: Annual Technical Conference Proceedings (p. 1042-1046). North Carolina, USA: Society of Plastics Engineers.

George, H. O. (1958): Methods of affecting the dimensional stability of paper. Tappi, 41(1), 31-33.

Guillotte, J. E., & McLaughlin, T. F. (1962): Calculating the adhesion of polyethylene coatings on kraft paper. Tappi, 45(3), 200-208.

Gunderson, D. E., Considine, J. M., & Scott, C. T. (1988): The compressive load-strain curve of paperboard: rate of load and humidity effects. Journal of Pulp and Paper Science, 14(2), J37-J41.

Göttsching, L., & Pakarinen, H. (2000): Recycled fiber and deinking (Vol. 7). Helsinki, Finland: Finnish paper engineers' association and TAPPI, 649 pp.

Hamelink, J. (1963): The Effect of Fiber Distribution upon Stiffness of Paperboard. Tappi, 46(10), 151A - 153A.

Han, J., & Park, J. M. (2006): Finite Element Analysis of Vent/Hand Hole Designs for Corrugated Fibreboard Boxes. Packaging Technology and Science, 20(1), 39-47.

Hansson, T. (2008): Deformation based failure criterion for corrugated board panels. KTH, Solid Mechanics, Stockholm, 31 pp.

Haraldsson, T., Fellers, C., & Söremark, C. (1997): Creep Properties of Paper - Principles of Evaluation. In Chalmers, I. R. (Ed.), 3d International Symposium, Moisture and Creep Effects on Paper, Board and Containers (p. 237-246). Rotorua, New Zealand, 20-21 February 1997.

Hashemi, S. J., Gomes, V. G., Crotogino, R. H., & Douglas, W. J. M. (1997): In-plane diffusivity of moisture in paper. Drying Technology, 15(2), 265-294.

Haslach, H. W. (2000): The Moisture and Rate-Dependent Mechanical Properties of Paper: A Review. Mechanics of Time-Dependent Materials, 4(3), 169-210.

Haslach, H. W. (2002): Moisture-accelerated creep. In Mark, R. E., Habeger, C. C., Borch, J. & Lyne, M. B. (Eds.), Handbook of Physical Testing of Paper (Vol. 1, p. 173-232). New York Basel: Marcel Dekker Inc.

Haslach, H. W., & Abdullahi, Z. (1995): Thermally cycled creep of paper. In Perkins, R. (Ed.), Mechanics of cellulosic materials ASME 1995 (Vol. AMD-vol. 209/MD-vol. 60, p. 13-22). Los Angeles CS, June 28-30 1995.

Häggblom-Ahnger, U. (1999): Optimum location of softwood sulfate pulp in three-ply office paper. Tappi, 82(6), 181-187.

ISO, Packaging — Complete, filled transport packages — Compression and stacking tests using a compression tester (ISO 12048-2:1994).

ISO, Paper and board — Determination of capillary rise — Klemm method. (ISO 8787:1986).

ISO, Paper and board — Determination of resistance to bending (ISO 2493:1992).

ISO, Paper and board — Determination of thickness and apparent bulk density or apparent sheet density. (ISO 534:1988).

ISO, Paper and board — Determination of tensile properties — Part 2: Constant rate of elongation method (ISO 1924-2:1994).

ISO, Paper and board — Determination of water absorptiveness — Cobb method (ISO 535:1991).

ISO, Sheet materials - Determination of water vapor transmission rate - Gravitmetric method (ISO 2528:1995).

Kajanto, I. M., & Niskanen, K. J. (1996): Optical measurment of dimensional stability, 1996 Progress in paper physics - A seminar proceedings (p. 75-77). Stockholm, Sweden.

Kellicutt, K. Q. (1960): Structural notes for corrugated containers. Note no 13: Compressive strength of boxes - Part III. Package Engineering, 5(2), 94-96.

Kellicutt, K. Q. (1963): Effect of contents and load bearing surface on compressive strength and stacking life of corrugated containers. Tappi, 46(1), 151A-154A.

Kellicutt, K. Q., & Landt, E. F. (1952): Development of design data for corrugated fiberboard shipping containers. Tappi, 35(9), 398-402.

Kirkpatrick, J., & Ganzenmuller, G. (1997): Engineering Corrugated Packages to Survive Cyclic Humidity Environments - A Case Study. In Chalmers, I. R. (Ed.), 3d International Symposium, Moisture and Creep Effects on Paper, Board and Containers (p. 257-264). Rotorua, New Zealand, 20-21 February 1997.

Kirwan, M. J. (2005): Solid fiberboard packaging. In Kirwan, M. J. (Ed.), Paper and paperboard packaging technology (p. 373-385). Oxford, UK: Blackwell Publishing Ltd.

Klute, C. H., & Franklin, P. J. (1958): The permeation of water vapor through polyethylene. Journal of Polymer Science, 32(126), 161-176.

Koran, Z., & Kamden, D. P. (1989): Bending stiffness of paperboard. Tappi, 72(6), 175-179.

Kouris, M. (Ed.). (1996): Dictionary of Paper, 5th Ed. Atlanta, Georgia, USA: TAPPI Press, 347 pp.

Krohn, J. V., & Jordy, D. W. (1997): A Comparison of the oil, oxygen and water vapor permation rates of various polyethylene blown films. Tappi Journal, 80(3), 151-156.

Kuskowski, S. J., Considine, J. M., & Lee, S. K. (1994): Corrugating components and their relationship to combined board performance. In Fellers, C. & Laufenbacher, T. L. (Eds.), Moisture-Induced Creep Behaviour of Paper and Board (p. 223-228). Stockholm, Sweden: STFI and USDA Forest Service, Forest Products Laboartory.

Kuusipalo, J., & Lahtinen, K. (2005): Influence of Temperature and Mixing Ratio on Water Vapor Barrier Properties of Extrusion-Coated Paper. International Journal of Polymer Analysis and Characterization, 10(1), 71-83.

Kuusipalo, J., Savolainen, A., Laiho, E., & Penttinen, T. (2008): Extrusion coating and products. In Kuusipalo, J. (Ed.), Papermaking science and Technology, Book 12: Paper and paperboard converting (p. 108-166). Helsinki, Finland: Finnish Paper Engineers' Association.

Laamanen, M., & Lahti, J. (2008): Fibre-based packaging materials. In Kuusipalo, J. (Ed.), Papermaking science and Technology, Book 12: Paper and paperboard converting (p. 209-242). Helsinki, Finland: Finnish Paper Engineers' Association.

Lahti, J., Hatanpää, I., & Lahtinen, K. (2008): Converting of fibre-based packaging materials. In Kuusipalo, J. (Ed.), Papermaking science and Technology, Book 12: Paper and paperboard converting (p. 244-283). Helsinki, Finland: Finnish Paper Engineers' Association.

Lahtinen, K., & Kuusipalo, J. (2008): Statistical prediction model for water vapor barrier of extrusion-coated paper. Tappi, 7(9), 8-15.

Leake, C. H., & Wojcik, R. (1989): Influence of the combining adhesive on box performance. Tappi, 72(8), 61-65.

Leake, C. H., & Wojcik, R. (1993): Humidity cycling rates: how they influence container life spans. Tappi, 76(10), 26-30.

Lehti, S. T., Ketoja, J. A., & Niskanen, K. J. (2003): Measurement of paper rheology at varied moisture contents, 2003 International Paper Physics Conference (p. 57-60). Victoria, BC, Canada.

Li, N. N., & Henley, E. J. (1964): Permeation of gases through polyethylnee films at elevated pressures. A.I.Ch.E Journal, 10(4), 666-670.

Luey, A. T. (1963): Stiffness of Multi-Ply Boxboard. Tappi, 46(11), 159A - 161A.

Lyne, A. L., Fellers, C., & Kolseth, P. (1996): The effect of filler on hygroexpansivity. Nordic Pulp & Paper Research Journal, 11(3), 152-152.

Maltenfort, G. G. (1980): Compression load distribution on corrugated boxes. Paperboard Packaging, 65(9), 71-72,74,76-78,80.

Mann, R. W., Baum, G. A., & Habeger, C. C. (1980): Determination of all nine orthotropic elastic constants for machine-made paper. Tappi, 63(2), 163-166.

Marmur, A., & Cohen, R. D. (1997): Characterization of Porous Media by the Kinetics of Liquid Penetration: The Vertical Capillaries Model. Journal of Colloid and Interface Science, 189(2), 299-304.

Massoquete, A., Lavrykov, S. A., Ramarao, B. V., Goel, A., & Ramaswamy, S. (2005): The effect of pulp refining on lateral and transverse moisture diffusion in paper. Tappi, 4(12), 3-8.

Matthews, G. P. (2000): Computer modelling of fluid permeation in porous coatings and paper – an overview Nordic Pulp and Paper Research Journal, 15(5), 475-485.

McKee, R. C., & Gander, J. W. (1957): Top-Load Compression. Tappi, 40(1), 57-64.

Meng, G., Trost, T., & Östlund, S. (2007): Stacking misalignment of corrugated boxes - a preliminary study, 23rd IAPRI Symposium on Packaging, 3-5 September 2007,. Windsor UK.

Mies, W., Potter, J., Miller, D., & Kenney, J. (Eds.). (2006): Global Pulp & Paper Fact & Price Book 2006. Bedford, MA, USA: RISI, 391 pp.

Nanri, Y., & Uesaka, T. (1993): Dimensional stability of mechanical pulps - drying shrinkage and hygroexpansivity. Tappi, 76(6), 62-66.

Navaee-Ardeh, S., & Nazhad, M. M. (2008): A new model for maximizing the bending stiffness of a symmetric three-ply paper or board. Tappi, 7(10), 28-32.

Nazhad, M. M. (1994): Fundamentals of strength loss in recycled paper. Dissertation, The University of British Columbia, Faculty of forestry, Vancouver, Canada.

Nilsson, L., Wilhelmsson, B., & Stenström, S. (1993): The diffusion of water vapor through pulp and paper. Drying Technology, 11(6), 1205-1225.

Niskanen, K. (2008): Paper physics (Vol. 16/19). Helsinki Finland: Finnish Paper Engineers' Association/Paperi ja Puu Oy, 360 pp.

Nordman, L. S. (1958): Laboratory investigations of dimensional stability of paper. Tappi, 41(1), 23-30.

Norwegian Seafood Export Council, Report: Statistical Overview 2008.

Padanyi, Z. V. (1991): Mechano-sorptive effects and accelerated creep in paper, 1991 International Paper Physics conference (p. 397-411).

Page, D. H., & Tydeman, P. A. (1962): A new theory of the shrinkage, structure and properties of paper. In Bolam, F. (Ed.), Transactions of the Fundamental Research

Symposium, Oxford (Vol. 1, Formation and structure of paper, p. 397-421): Technical Section of the British Paper and Board Makers' Association, London, UK.

Panek, J., Fellers, C., & Haraldsson, T. (2004): Principles of evaluation for the creep of paperboard in constant and cyclic humidity. Nordic Pulp & Paper Research Journal, 19(2), 155-163.

Peterson, W. S., & Schimmelpfenning, W. J. (1982): Panel edge boundary conditions and compressive strengths of tubes and boxes. Tappi, 65(8), 108-110.

Piergiovanni, L., Fava, P., & Siciliano, A. (1995): Mathematical model for the prediction of water vapour transmission rate at different temperature and relative humidity combinations. Packaging Technology and Science, 8(2), 73-83.

Radhakrishnan, H., Chatterjee, S. G., & Ramarao, B. V. (2000): Steady-state moisture transport in a bleached kraft paperboard stack. Journal of Pulp and Paper Science, 26(4), 140-144.

Ramarao, B. V., Massoquete, A., Lavrykov, S., & Ramaswamy, S. (2003): Moisture diffusion inside paper materials in the hygroscopic range and characteristics of diffusivity parameters. Drying Technology, 21(10), 2007-2056.

Roberts, R. J. (2004): Liquid penetration into paper. Thesis (Doctor of Philosophy), The Australian National University, 348 pp.

Rogers, C., Meyer, J. A., Stannett, V., & Szwarc, M. (1957): Studies in the gas and vapor permeability of plastic films and coated papers - Part III. Some factors affecting the permeability constant. Tappi, 40(3), 142-146.

Salame, M., & Steingiser, S. (1977): Barrier polymers. Polymer - Plastics Technology and Engineering, 8(2), 155-175.

Salmén, L. (1993): Responses of paper properties to changes in moisture content and temperature, Tenth fundamental research symposium at Oxford, Vol.1 (p. 369-430). Surrey, UK: Pira International.

Salmén, N. L., & Back, E. L. (1977): Simple stress-strain measurement on dry papers from -25 °C to 250 °C. Svensk papperstidning, 80(6), 178-183.

Salminen, P. (1988): Studies of water transport in paper during short contact times. Laboratory of Paper Chemistry, Department of Chemical Engineering, Åbo Akademi 1988.Åbo, 94 pp.

SCAN, Böjstyvhet Fyrpunktsmetoden - Wellpapp, papp och kartong (SCAN P 65:91).

Schulz, J. M. (1961): The effect of straining during drying on the mechanical and viscoelastic behaviour of paper. Tappi, 44(10), 736-744.

Seafish Industry Authority, UK, Fish Technology department, Data sheet no: 1996/03/ FT Fresh fish wholesale packaging (www.seafish.org).

Seth, R. S., & Page, D. H. (1983): The stress strain curve of paper. In Brander, J. B. (Ed.), The Role of Fundamental Research in Papermaking (Vol. 1, p. 421–452): Mechanical Engineering Publications Ltd, London, UK.

Setterholm, V. C., & Gertjejansen, R. O. (1965): Method for measuring the edgewise compressive porperties of paper. Tappi, 48(5), 308-313.

Singh, S. P. (1999): Stability of Stacked Pallet Loads and Loss of Strength in Stacked Boxes Due to Misalignment. In Serra-Tosio, J.-M. & Vullierme, I. (Eds.), 4th International symposium - Moisture and Creep Effects on Paper, Board and Containers (p. 16-25). Grenoble, France, 18-19 March, 1999: E.F.P.G.

Skogman, R. T., & Scheie, C. E. (1969): The effect of temperature on the moisture adsoprtion of kraft paper. Tappi, 52(3), 489-490.

Smook, G. A. (1990): Handbook of pulp & paper terminology - A guide to industrial and technological usage. Vancouver, Canada: Agnus Wilde Publications, 447 pp.

Sonneveld, C. (1986): Suitability of solid fibreboard boxes in cooled distribution of fresh produce. Verpack.-Rundsch, 37(19), 63-65 (Suppl.)

Soroka, W. (2009): Packaging functions (Ch. 2). In Emblem, A. & Emblem, H. (Eds.), Fundamentals of packaging technology (p. 19-36). Leichestershire, UK: The Institute of Packaging, First published 1995 by IOPP, USA.

Stannett, V. T. (1973): Fundamentals of barrier properties, Fundamental Properties of Paper Relating to Its Uses, Symposium Transactions (Vol. 2, p. 412-427).

Statistics Norway, 10.05 Fishing and fish farming, Table: Aquaculture. Final figures, 2008.

Steadman, R. (2002): Corrugated board. In Borch, J., Lyne, M. B., Mark, R. E. & Habeger, C. C. (Eds.), Handbook of physical testing of paper (2nd ed., Vol. 1/2, p. 563-660). New York: Marcel Dekker.

Stylo, T. & Levang, G. H. (2009), Communications with Tom Stylo, Borregård, and Gunvor Haga Levang, Peterson Emballage

Swanson, J. W., & Becher, J. J. (1966): The adhesion of polyethylene on paper. Tappi, 49(5), 198-202.

Söremark, C., & Fellers, C. (1995): Assessing cyclic creep behaviour of different paper grades. In Fellers, C. & Laufenberg, T. L. (Eds.), Moisture-Induced Creep Behaviour of Paper and Board (p. 275-285). Stockholm, Sweden, Dec 5-7, 1994: STFI and USDA Forest Service, Forest Products Laboratory.

Tappi, Water vapor transmission rate og paper and paperboard at 23 oC and 50% RH (Tappi T 448 om-97).

Uesaka, T. (1991): Dimensional stability of paper: upgrading paper performance in end use. Journal of Pulp and Paper Science, 17(2), 39-46.

Vorakunpinij, A. (2003): The effect of paper structure on the deviation between tensile and compressive creep responses. Institute of Paper Science and TechnologyAtlanta, Georgia, 151 pp.

Vähälä, M., & Grootel, J. (2001): Polyethylene technology in extrusion coating, 2001 European PLC Conference Proceedings: Tappi.

Washburn, E. W. (1921): The dynamics of capillary flow. Physical review, 12(3), 273-283.

Whitsitt, W. J., & McKee, R. C. (1972): Effect of relative humidity and temperature on stacking performance. Project 2695-9, report one : a summary report to Technical Division Fourdrinier Kraft Board Institute, Inc.: Georgia Institute of Technology, Appleton, Wisconsin, 51 pp., http://hdl.handle.net/1853/953.

Wink, W. A. (1961): The effect of relative humidity and temperature on paper properties. Tappi, 44(6), 171-179A.

Yamauchi, T., & Murakami, K. (2002): Porosity and gas permeability. In Borch, J., Lyne, M. B., Mark, R. E. & Habeger, C. C. (Eds.), Handbook of Physical Testing of Paper (Vol. 2, p. 267-302). New York - Basel: Marcel Dekker, Inc.

Zauscher, S., Caulfield, D. F., & Nissan, A. H. (1996): The influence of water on the elastic modulus of paper. Tappi Journal, 79(12), 178-182.

COLLECTION OF PAPERS

Paper I

Moisture content of polyethylene coated solid fiberboard after industrial lamination

Abstract

Solid fiberboard is used mainly in highly demanding packaging applications. One solid fiberboard quality having six paper and paperboard layers, a thickness of 1.7 mm, and polyethylene coating was studied. Several material tests on liquid water and water vapor penetration were done to assess the environmental moisture sources that change the material moisture content after the lamination process. The in-plane diffusion coefficient of the combined board was determined based on an integrated unsteady state moisture transport equation and moisture sorption measurements. The transverse diffusion coefficient of the polyethylene coated kraft paper and the solid fiberboard medium were based on WVTR measurements. The original moisture content of the solid fiberboard sheet was measured gravimetrically two days after the lamination at the mill. The results show that high relative humidity conditions during the transportation (4 °C/90% RH) change the moisture content of the transportation box made from a solid fiberboard sheet very little in eight days. Local moister (or drier) areas are created near the sheet edges due to in-plane moisture transport through open material edges. The in-plane diffusivity for the solid fiberboard grade in question was $5.87*10^{-10}$ m^2/s.

Authors: Sara Paunonen[1] (*) (sara.paunonen@chemeng.ntnu.no, tel. +47 73 55 03 97, fax: +47 73 55 09 99), Marianne Lenes[2] (marianne.lenes@pfi.no, tel. +47 73 55 09 00, fax: +47 73 55 09 99), Øyvind Gregersen[1] (oyvind.gregersen@chemeng.ntnu.no, tel. +47 73 59 40 29), [1]Norwegian University of Science and Technology, Department of Chemical Engineering, Høgskoleringen 6B (PFI building), NO-7491 Trondheim, [2]PFI, Høgskoleringen 6b, NO-7491 Trondheim, Norway, and Norway, (*) Corresponding author

Keywords: moisture content, moisture tests, diffusion constant, paper laminates, container boards

1. Introduction

Containerboard is the largest grade group by volume in the paper industry, accounting for 31% (117 million tons) of the world's total paper and board production [1]. Corrugated containers make the majority of packaging production. Solid fiberboard is a multi-layer paper-based packaging material often based on recycled fibers. The material can be finished with a variety of lining papers and optionally polyethylene coating.

Most grades are glued together in an off-line laminator. Solid fiberboard boxes account for 0.5% of U.S. total industry corrugated shipments [1]. Solid fiberboard is mainly used in demanding packaging applications where the product is wet, frozen or greasy. The difference in consumption is reflected in the extent of research done on these materials.

Several paperboard layers are glued together in a lamination process to form a solid fiberboard sheet. The glue contains water. The lamination process together with the moisture content of the sheets determines the original moisture content of the laminated paperboard. As a transport box, the sheet is exposed both to liquid water and water vapor. The exposure takes place through the edges and planes of the sheet. Mechanical properties of paper-based materials depend strongly on the moisture content of the material [2]. The strength of the container box is thus dependent on the initial moisture content after production, and how the material resists additional moisture penetration into the material.

This work aims at evaluating the effect of different moisture sources in the environment on the moisture content of the sheet when it is used as a transport box. This topic is justified from a practical point of view, since the mechanical properties of the transport box folded from a solid fiberboard sheet depend on the evolvement of the material moisture content during transportation.

In the present work, the original moisture content of a newly fabricated solid fiberboard sheet was measured. Several material tests were carried out to evaluate the sensitivity of the sheet to ambient moisture changes. Exposure both to liquid water and water vapor was investigated. In-plane diffusivity of the solid fiberboard and the transverse diffusivity of the polyethylene coated kraft paper, which makes the outermost layers of the solid fiberboard, were determined to judge the relative importance of moisture penetration through the sheet edges and planes.

2. Moisture transport

Capillarity

Moisture transport into and inside paper materials is a complicated phenomenon comprising many moisture transport mechanisms. One of the mechanisms is meniscus flow of the liquid water in thin capillaries in between fibers and inside fibers. Roberts [**3**] showed that a major fluid transport mechanism is the advancing of the wetting fluid along the channels formed by fiber overlaps, not the intuitive gradual filling of the pores. The basis of the capillary approach is the Lucas-Washburn equation. The equation states that the time for rise in a capillary of certain length is proportional to the second power of that length and to the viscosity of the liquid, and inversely proportional to the radius of the capillary, surface tension of the liquid, and contact angle between liquid and the capillary wall. In early works, only single capillary models were used to describe the liquid imbibition. In later research, equivalent cases are sought for the porous materials and sets of cylindrical capillaries [**4**]. The capillary penetration approach is challenged by the complexity of the paper void system. Modeling of the three-dimensional structure is challenging, but there are attempts. The water penetration to paper can be

simulated by first building a network representing the void system in paper with simplified elements, e.g., cubic pores and cylindrical throats, and then calculating how water enters the system of capillaries [**5**]. An additional challenge posed on modeling is the concurrent swelling of fibers caused by liquid water. Capillary penetration models also neglect totally the amount of liquid that is transported by other processes, for example by diffusion.

One-dimensional flow of liquid into paper under capillary suction forces is similar to the flow observed in diffusion [**6**]. In both cases, the distance moved by a point of certain concentration is proportional to the square root of the time elapsed. Thus in any homogeneous porous material where Darcy's law (relation between discharge rate through a porous medium, the viscosity of the fluid and the pressure drop over a given distance) and continuity equation (conservation of mass) are obeyed, no assumption needs to be made about the structure of the pore and the capillary system [**6**]. The penetration of liquids can be treated either as capillary based or diffusion based.

Diffusion

The other, simultaneously occurring moisture transport mechanism is diffusion. Moisture transport is normally represented with diffusion models when liquid water is not present as a boundary condition [**7**]. The driving force of diffusion is the gradient in the moisture concentration in the fibers or in the partial pressure of water vapor in the pores. The phenomenon is described by Fick's first law (Equation 1). The diffusive flux J [g/m^{2}s] equals the concentration gradient $\partial c / \partial x$ [g/m^3/m] times a diffusion coefficient (moisture diffusivity) D [m^2/s].

$$J = -D\frac{\partial c}{\partial x} \tag{1}$$

The diffusion inside paper is partly an unknown process. Types of diffusion can be listed in many ways, e.g. as follows: water vapor diffusion in the intra-fiber and inter-fiber pores, surface diffusion from one hydrophilic spot to another along the fiber surfaces, and bulk water (condensed water) diffusion within the cellulosic material [**3**]. A different set of diffusion types is normally given for sorption and desorption. The exact order of occurrence of these phenomena is not known, but the rate determining mechanism will be the fastest one. If the aim is to model moisture transport in more detailed a fashion than as diffusion in a homogeneous material [**8**], the typical choice is to assume vapor transport in the void volume and condensed (bound) water transport in the fiber volume, and local interchange between these two fluxes, e.g., in [**9, 10, 11**].

From a practical point of view, diffusion in paper materials takes place from high vapor pressure (relative humidity) or water concentration to lower, and thus the overall or effective diffusivity resulting from all the diffusion processes in a fibrous pore system are considered. The effective moisture diffusivity is strongly affected by moisture content [**12**] and ambient temperature [**13**]. The vapor diffusivity measured for kraft paperboard sheets is approximately constant up to relative humidity 60%, but increases sharply after this value [**14, 10**]. In drier sheets, the diffusion of water vapor in pores dominates, and operations that increase the tortuosity or reduce the pore volume, e.g.,

refining or wet pressing, tend to decrease the diffusivity. As the relative humidity increases, the moisture content dependent transport of condensed water becomes more important [**10**]. Depending on the paper grade in question, the magnitude of the underlying diffusion phenomena vary, and the resulting overall dependency on relative humidity may deviate from this general trend [**12**]. An extensive review on steady and unsteady state diffusion models assuming paper as a homogeneous material or a composite of fibers and voids is given in [**12**].

The middle layers of the solid fiberboard studied here are strongly internally sized. For liquid water penetration into sized papers, it has been noticed that at short absorption times the water enters first the cavities on the surface before absorption to the pore system commences [**15**]. Further, the only mechanism of moisture transport is the diffusion flow within the fibers, no bulk or film fluid flow in inter-fiber or intra-fiber pores or lumen is observed [**3**]. The result was proved with cryo 2-photon confocal laser scanning microscopy (CLSM) techniques. The same result was anticipated earlier [**13**]. Sizing with hydrophobic agents (AKD) does not significantly affect the water vapor diffusivity and sorption [**8**].

In-plane diffusion of moisture

For moisture barrier coated products, the in-plane diffusion dominates the moisture transport. In-plane (lateral) diffusivity of paper materials is generally larger than transverse (through thickness) diffusivity [**10, 16**]. Massoquete [**10, 16**] measured the lateral diffusivity of handsheets of refined bleached kraft pulp by using circular samples that were glued together with poly-isopropylene. Moisture was fed through an eccentric hole in the stack, and it evaporated out from the outer edge of the stack. Steady state flux was calculated based in steady state weight loss. Two resistances for diffusion were considered: vapor layer inside the reservoir, and the paper stack itself. The effect of the external air boundary layer was considered negligible. Depending on the density of the sheets and the difference in relative humidity, the in-plane diffusivity was reported to be 1-6 times higher than the transverse diffusivity. In-plane diffusivities decrease less as a function of density than transverse diffusivities [**16**].

Hashemi et al. [**7**] equilibrated kraft handsheets to a desired moisture content, fastened them to a rig with a moisture sink along the perimeter of the round samples, and measured the moisture content in desorption on several locations along the sample radius with IR sensors. Hashemi et al. [**7**] report logarithmically increasing in-plane diffusivities ~0 – $0.25 \cdot 10^{-8}$ – $0.15 \cdot 10^{-5}$ m^2/s in the moisture content range 0.1 – 0.2 –1.3 kg water/kg fiber (moisture content 9 – 17 – 56%). Over the fiber saturation point (~ 0.8 kg/kg), the liquid water is present as a boundary condition at the fiber surfaces. Hashemi et al. [**7**] compare their in-plane results to the transverse diffusivities found in the literature, and state that the ratio of in-plane and transverse diffusivities is as high as 10^6 when moisture content is 0.2 kg/kg. Amiri et al. [**17**] studied moisture diffusion of newsprint rolls that had either the ends or the surface of the rolls sealed, and report diffusivities in axial direction to be 2.4-4.5 times the diffusivity in radial direction of the roll.

Fiber orientation has a profound effect on most paper properties, but there are indications that the lateral moisture diffusivity is isotropic with respect to the sample machine and cross-machine direction [**18**]. This result was obtained by exposing round test pieces to a step change in relative humidity, and observing the forced convection drying with magnetic resonance imaging (MRI). One of the studied materials was polyethylene coated paperboard. Hojjatie et al. [**19**] showed that measuring surface temperatures by infrared tomography is a suitable method for determining in-plane diffusivities. Infrared tomography detects not only liquid-phase molecules, but also gas-phase molecules of water in low concentrations.

Methods for determining diffusivity

The moisture sorption and desorption is a simultaneous and complicated process of heat, mass, and momentum transfer. Therefore the experimental methods for determining apparent diffusivities have a central role. A useful review of methods for experimental determination of moisture diffusivity in solids, not concentrating on paper materials, is given in [**20**]. The methods can be divided to permeation and sorption kinetic types. In permeation methods, the diffusant is allowed to penetrate through a thin material sheet or film until steady state is reached. In permeation methods, the sheet is placed in between two constant concentrations of the diffusant and either the time to reach the steady state (time lag method) or the flux at steady state (steady state method) is measured. In sorption kinetic methods a sample with known initial concentration is placed in a constant concentration source. The weight of the sorpted diffusant is measured. Both these methods will be used in this work. The reported diffusivities of paper vary considerably in magnitude due to the dependency on driving force, the material in question, and moisture. Hashemi et al. [**7**] suggest that the technique and the conditions for determining the diffusivity should be as close as possible to the intended exploitation of the determined parameter.

In the present work, in-plane diffusivity is estimated using an analogy between the diffusion of heat and moisture in the test piece. Equation (2) describes the heat transfer in one-dimensional case (T = temperature, t = time, y = position). Fick's second law that predicts how diffusion causes the concentration field to change with time, has the same form if the temperature T is replaced by concentration c, and the thermal diffusivity α by diffusivity D. A test piece occupies the space between $y = -b$ [m] and $y = b$ and has an initial even moisture concentration c_o (see Figure 1).

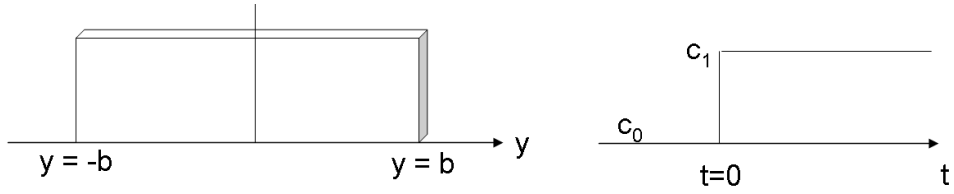

Figure 1. One-dimensional moisture transfer in a sheet.

$$\frac{\partial T}{\partial t} = \alpha \frac{\partial^2 T}{\partial y^2} \qquad (2)$$

Equation (3) gives the solution to how the moisture concentration c [g/m^3] in a test piece evolves in time after the surfaces at y = b and y = -b are suddenly exposed to constant concentration c_1 at time t=0. D is the in-plane diffusivity of moisture in the sheet [m^2/s]. The development of the solution can be read from [**21**].

$$\frac{c_1 - c}{c_1 - c_0} = 2\sum_{n=0}^{\infty} \frac{(-1)^n}{(n+½)\pi} e^{-(n+½)^2 \pi^2 Dt/b^2} \cos\left[(n+½)\frac{\pi y}{b}\right] \quad (3)$$

By integrating Equation (3) over the length y, the average moisture content c in the test piece is obtained as a function of time. The in-plane diffusivity can then be obtained by selecting the coefficient D so that it gives corresponding results to the measured values from the sorption test. This straight-forward approach doesn't pay attention to the structural details of wet fiber network or cell walls (porosity, tortuosity, pores size distribution). In this model, the driving force of diffusion is only the moisture content gradient and the diffusivity is independent of moisture and position. The edges of the test piece are assumed to be in equilibrium with the static environmental conditions.

3. Experimental

Materials

The paperboard studied in this work is a unidirectionally stacked solid fiberboard. The four middle layers are made of 100% recycled fiber and are strongly internally sized. The outer layers on both sides are made of bleached machine finished kraft paper. The kraft paper has a double extrusion coated low-density polyethylene layer. The six paper and paperboard layers are glued together in an industrial lamination process. The glue used in lamination contains poly-vinyl alcohol (PVA) as an active agent, clay, additives and water. The solids content of the liquid glue used in lamination is 24.6%.

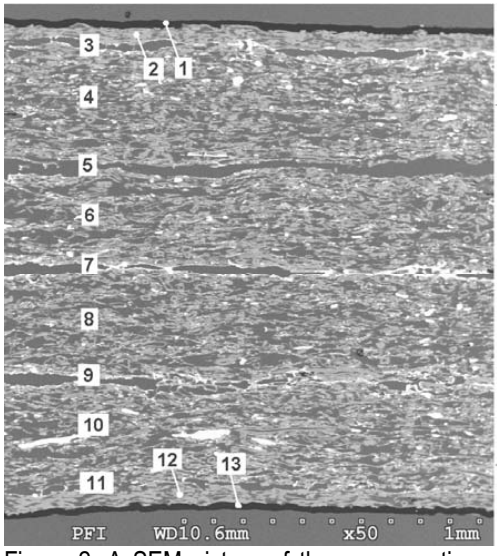

	Name of the layer	Grammage [g/m^2]	Thickness(*) [mm]
1	Polyethylene coating	20	0.02
2	Kraft paper 1	60	0.07
3	Adhesion layer 1	10	
4	Middle layer 1	250	0.39
5	Adhesion layer 2	10	
6	Middle layer 2	250	0.39
7	Adhesion layer 3	10	
8	Middle layer 3	250	0.39
9	Adhesion layer 4	10	
10	Middle layer 4	250	0.39
11	Adhesion layer 5	10	
12	Kraft paper 2	60	0.07
13	Polyethylene coating	20	0.02
	Solid fiberboard	1220	1.73

Figure 2. A SEM picture of the cross section of solid fiberboard together with grammage and thickness and the layers. (*) Indicative thicknesses based on thickness measurements of the

layers before the lamination. The layers 1 and 2, and the layers 12 and 13 are practically inseparable, and treated as single layer in the experiments.

Figure 2 shows a SEM picture of the cross section of the combined board. The figure shows also grammages and the thicknesses of the layers. The thicknesses are based on thickness measurements of the layers before the lamination taking into account that the lamination process compresses the layers 11%. No thickness is assigned for the non-homogeneous adhesion layers.

The original moisture content of the solid fiberboard sheet was recorded gravimetrically. The sheet was received from the mill two days after the lamination. The environmental conditions during that time are not known. The measurements formed a grid; twelve readings were taken in CD direction and eleven in MD direction (grid spacing 100 mm × 100 mm). Each moisture content reading is an average of two samples with the average size of 20 mm × 20 mm. The samples were dried 72 h in 103 °C, and weighed after 24 h cooling time in a dessicator. The tolerance of the maximum permissible error of the scale is ±0.0002g in the range of the test piece weights. The scale is calibrated annually. Both the scales used were calibrated according to these criteria.

To predict the development of the sheet moisture content after the production process, different standard and non-standard liquid water and water vapor penetration tests were carried out. Figure 3 lists the tests.

Moisture penetration through PE coated kraft paper
a) Liquid water
- Cobb (ISO 535)

b) Water vapor
- Water vapor transmission rate WVTR (Tappi 488)
- WVTR at 90% RH/ 27°C

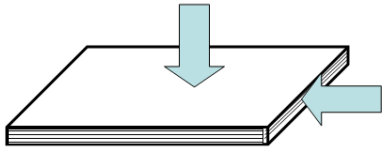

Moisture penetration through solid fiberboard edges
a) Liquid water
- Gravimetric edge wicking test

b) Water vapor
- Weight gain after change in RH (50%→90% RH, 27°C)

Figure 3. The measurements of water penetration into the solid fiberboard.

Liquid water and water vapor penetration through the plane
Moisture penetration tests through the planes were done only on the PE coated kraft paper. The Cobb test was used to confirm water tightness of the polyethylene coating, and the PE layer was thus facing the water. The testing was done according to ISO 535:1991 [**22**] in standard climate. The exposure times were extended up to 22 hours. During the longest exposure times the sealing ring of the Cobb device would easily leak water, and the leaked water would reach the untreated sample edges. If the penetration through the edges was suspected, the samples were discarded.

Water vapor penetration through the polyethylene coated kraft paper was measured as water vapor transmission rate (WVTR) according to T 448 om-97 [**23**] (the cup test). The polyethylene layer was facing towards the higher humidity in both tests. The cups were sealed with silicone before closing to force the water vapor transport through the polyethylene layer. WVTR was measured also in high humidity conditions. The cups were held in a climate chamber that had the atmosphere 90% RH/27 °C. The weighing occurred in standard climate. The cups were taken from the climate chamber, and put into a plastic bag, and taken to the scale. The cups were taken out of from the bag one-by-one and weighed. WVTR values for the solid fiberboard middle layer in standard and in high humidity (90% RH/27°C) were measured in the same fashion.

Liquid water and water vapor penetration through the edge

The testing of the moisture penetration through the edge of the solid fiberboard was based on the determination of the height of capillary rise, known also as Klemm test, ISO 8787:1986 [**24**]. The aim is to find how far the water penetrates through the open edge in a vertically positioned wide sample. The Klemm test measures the height of rise, but here the moisture content as a function of the penetration length was measured. Instead of the 15 mm strips used in the Klemm test, 250 mm × 110 mm size board samples were tested both in CD and MD. In this modified test, the de-ionized water was colored with a bromophenol blue indicator solution to observe qualitatively the rise of the water in to the sheet. The lower ends of the test pieces were immersed to a depth of 6-7 mm. Water was added to hold the water level unchanged. After eight days of exposure four 15 mm × 110 mm vertical strips were cut with knife from the middle of the test piece in standard climate. The strips were cut further to 15 mm × 5 mm pieces with a guillotine cutter, and weighed in standard climate as quickly as possible. The four pieces at the same distance from the edge were cut and measured together. Moisture content was determined gravimetrically (drying 103°C/ 24h). Figure 4 shows the Klemm test setup.

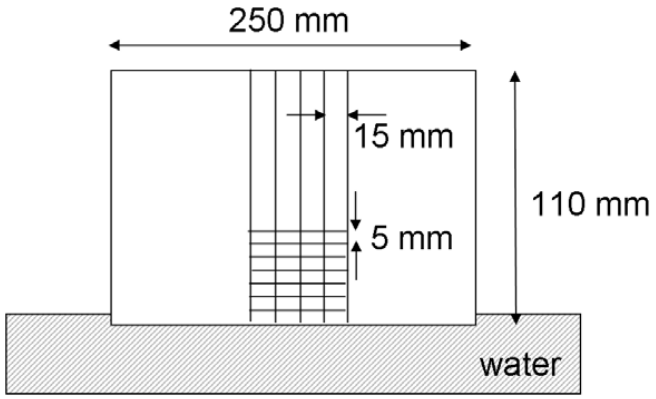

Figure 4. Test setup for the Klemm test.

Water vapor sorption was studied by exposing different size test pieces to a step change in humidity (from 50% to 90% RH) and recording the weight change as a function of

time. The test piece sizes were: 400 mm × 100 mm, 300 mm × 75 mm and 200 mm × 50 mm. Six test pieces were studied; one each size and main material direction. The samples were in equilibrium with standard climate before exposing them to high humidity (90% RH/ 27°C). The samples were weighed inside the climate chamber. An exponential polynomial of the form $y = a \cdot e^{-(t/b)^c}$ (y = weight increase, t = time, a, b, and c = parameters) was fitted to the measurement data. As time increases, the fitted curve approaches zero. The weight increase and thus the moisture content were considered stable when the fitted curve reached 0.01%.

In-plane diffusivity of the solid fiberboard

Four 180 mm long test pieces were prepared. The widths were 30 mm and 46 mm (MD samples) and 30 mm and 55 mm (CD samples). To control the water penetration through only two open opposite edges, a plastic film was melted onto two edges and the planes. A 250 μm thick polyethylene film was laminated on the planes with an office laminator (heating temperature 140°C). A 120 μm film was melted on the edges of the test piece with an iron. The test pieces that were in equilibrium with standard climate were exposed to a step change in relative humidity (from 50% to 90% RH, 27°C) by putting them to a climate chamber. The amount of penetrated water [g/m^3] was measured. At selected times, the samples were taken out of the climate chamber, put in a plastic bag, and taken one by one out of the bag for weighing in standard climate. With each weighing round, the samples were 9 minutes out of the of the climate chamber.

4. Results

The moisture content distribution in the plane of a solid fiberboard sheet (1180 mm × 990 mm) measured two days after the lamination process is shown in Figure 5.

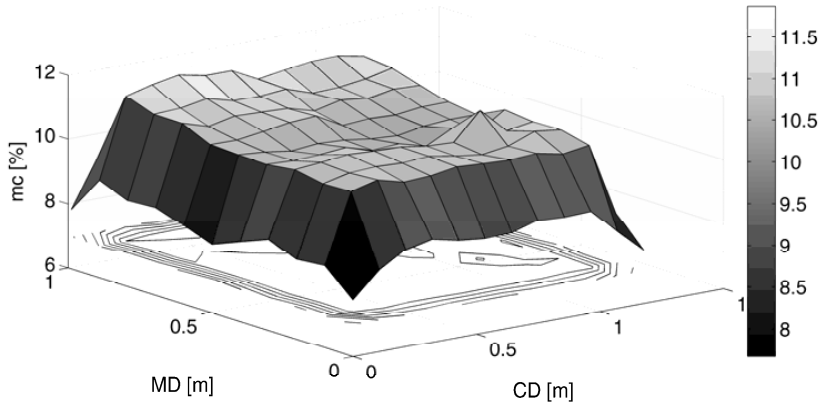

Figure 5. Moisture content of a solid fiberboard sheet two days after the lamination.

Moisture penetration through the plane

The Cobb test was used to study how much liquid water penetrates through a polyethylene coated kraft paper that is the outermost layer of the solid fiberboard studied. Figure 6 shows the Cobb test results after exposure times 0 min, 5 min, 30 min, 1 h, 6 h, 16 h, 22 h. Water can adhere on polyethylene surface without penetrating through it. The amount of water adhering on the surface of polyethylene was measured by the waiting time 0 min.

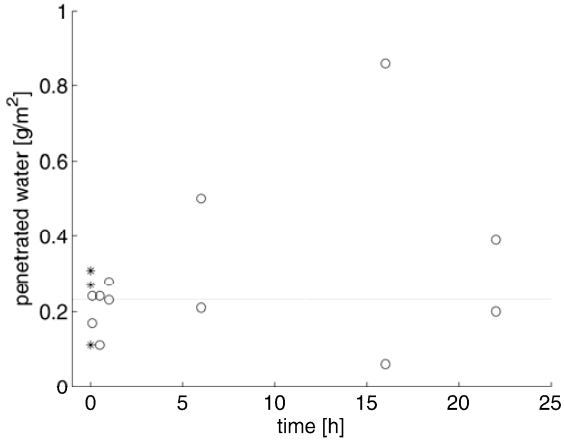

Figure 6. Liquid water penetration through a polyethylene coated kraft paper. (o) Cobb measurements after 5 min, 30 min, 1 h, 6 h, 16 h, 22 h, (*) Cobb measurements at time 0 min. The horizontal line gives the amount of water adhering on the PE surface (mean value of Cobb results for 0 min).

Water vapor transport values were measured with the cup tests. The WVTR value for the polyethylene coated kraft paper for standard climate was 2.8 g/m^2/day and for the high humidity climate (90% RH/ 27°C) 8.2 g/m^2/day. For the solid fiberboard middle layer, the values were 170 g/m^2/day and 1100 g/m^2/day for the corresponding climates.

Moisture penetration through the edge

Figure 7 shows the moisture content of solid fiberboard as a function of distance from the solid fiberboard edge. The horizontal line shows the equilibrium moisture content of the material in standard climate. The results should be considered indicative because the moisture evaporated quickly from the small size samples. Figure 8 shows the sorption test results, where the time to reach stable moisture is given against the half of the sample width. The moisture was considered stable when the fitted moisture increase curve and thus moisture content reached 0.01%.

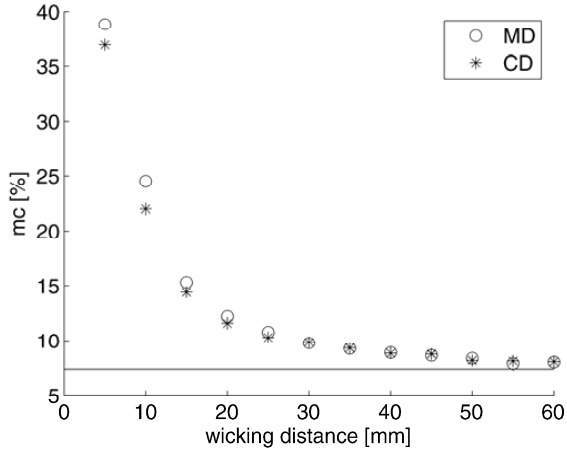

Figure 7. Moisture content of vertical solid fiberboard as a function of wicking distance after eight days of exposure. Average of 4 samples.

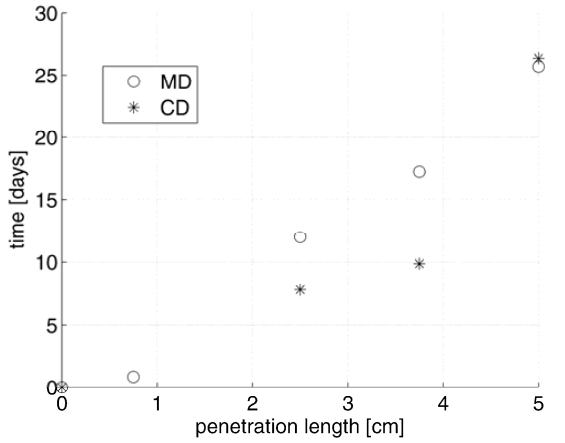

Figure 8. The time to reach stable moisture as a function of penetration length (half of the sample width). The moisture is considered stable when the moisture increase of the test piece reached 0.01%. The data set doesn't include CD sample at 1 day.

Diffusivities

The weighing of the samples occurred in standard climate, which considerably disturbed the sorption process and causes error in the calculated diffusivity value. The moisture sorption to and desorption from the solid fiberboard in question are slow processes compared to other paper materials. Figure 9 shows how a test piece (size 15 mm × 210 mm) looses moisture when it is exposed to a step change from 90% to 50% RH. In nine minutes it looses 0.3% of its weight, in one minute the weight loss is 0.05%. Actual test pieces for diffusivity determination had smaller edge area to volume ratio, which indicates that the rate of moisture loss is smaller than for the smaller test pieces, and is considered negligible. In the following figures and calculations, the times that the

samples are out of the climate chamber but most of the time in a plastic bag, are subtracted from the total sorption time (9 min per each measurement at specific time).

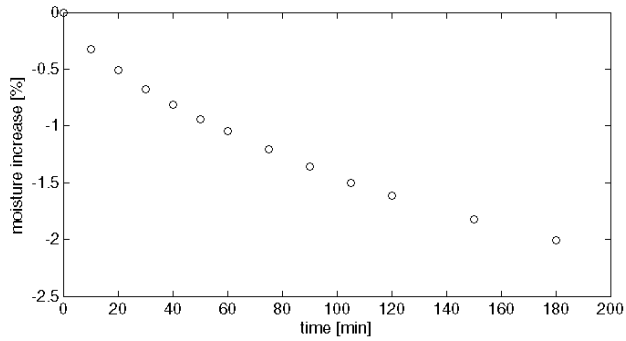

Figure 9. Moisture loss of a test piece after a step change in relative humidity from 90% to 50%.

Figure 10 shows the weight of the sorbed moisture into the four solid fiberboard test pieces through the two opposite open edges. There were no significant difference in the behavior in MD and CD, and thus a mean value over the densities of the CD and MD samples was calculated for further analysis. The decision is supported by Leisen et al. [**18**], who report that diffusion of moisture in the plane of the sheet is isotropic.

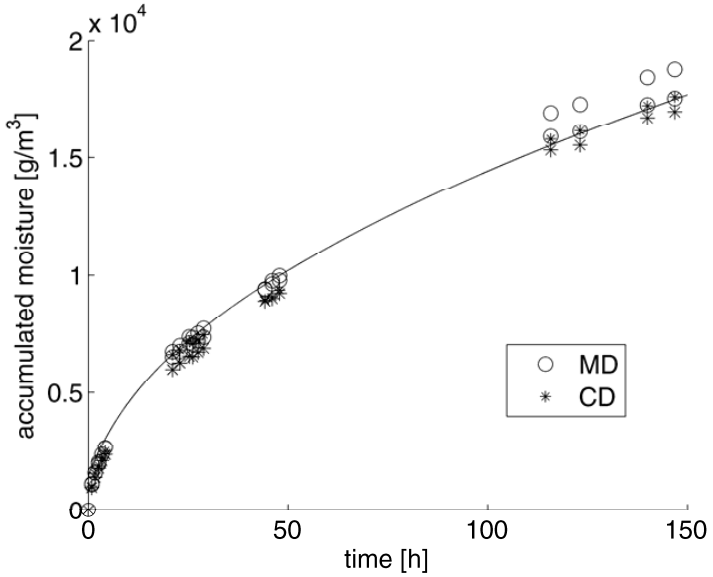

Figure 10. Measured (o), (*) and calculated (–) average amount of sorbed moisture into solid fiberboard test pieces through two open edges.

After the integration of Equation 3, the following values were used for calculating the average moisture content in the test pieces: original moisture content at standard climate $c_o = 5.011*10^4$ g/m^3 (7.04%), equilibrium moisture content in 90% RH $c_1 = 8.968*10^4$ g/m^3 (12.61%), half length of the test pieces b = 0.090 m, number of terms in the series n = 10. By minimizing the sum of squared errors with a gradient based optimization

algorithm, the in-plane diffusivity for the solid fiberboard becomes $5.87*10^{-10}$ m^2/s. The moisture sorption with this diffusivity value is shown in Figure 10 together with the measurements.

The transverse diffusivities of the polyethylene and solid fiberboard medium for the temperature and driving forces in question can be calculated by taking the WVTR values as the flux in Fick's law. The transverse diffusivities in the driving force 0%/90% RH and temperature 27°C are shown in Table 1.

Piergiovanni et al. [**25**] present a model for estimating the water vapor transmission rate values in certain ambient temperature and humidity based on measurements in other climates (Equation 4). The model is based on the Claysius-Clapeyron's relationship between water vapor pressure and temperature and a constant permeance (WVTR's relation to vapor pressure) of the material. The model is well applicable to 23 μm thick LDPE film [**25**], which corresponds to the PE layer studied here (20 μm).

$$WVTR_{new} = WVTR_{old} \exp\left[-5418.6\left(\frac{1}{T_n}-\frac{1}{T_o}\right)\right]\left(\frac{\Delta RH_n}{\Delta RH_o}\right) \quad (4)$$

where T_n = temperature in the new [K] and T_o = old conditions [K], the change in relative humidity in the new ΔRH_n and the old conditions ΔRH_o

By using Equation 4, the transverse diffusivities of polyethylene can be estimated in the same climate where in-plane diffusivity of solid fiberboard was measured (50%/90% RH, 27 °C). The same estimation cannot be done on the solid fiberboard medium. The results are given in Table 1. Equation 4 can also be used to estimate the elevation of the moisture content of a solid fiberboard sheet. Figure 11 shows how much the water vapor penetration solely through the polyethylene layer elevates the moisture content during eight days of exposure. It is assumed that the driving force of diffusion is constant. The calculation is based on following parameters: WVTR 8.2 $g/m^2/day$, 27 °C, 50% RH driving force, weight of the sheet 1146 g.

	Driving force/temperature		
	0%/50% RH/ 23°C	**0%/90% RH/ 27°C**	**50%/90% RH/ 27°C**
Polyethylene coated kraft paper (80 g/m²)			
WVTR [g/m²/day]	2.8	8.2	3.2 (*)
Transverse diffusivity [m²/s]	6.3E-11	7.3E-11	6.5E-11
Solid board (1220 g/m²)			
In-plane diffusivity [m²/s]	--	--	5.9E-10
Solid board medium (430 g/m²)			
WVTR [g/m²/day]	1.7E+02	1.1E+03	--
Transverse diffusivity [m²/s]	8.4E-08	2.1E-07	--

Table 1. Transverse diffusivity of solid fiberboard surface layer (polyethylene coated krat paper) and in-plane diffusivity of the solid fiberboard. WVTR values are measured with cup test. (*) Estimated by the model from [**25**].

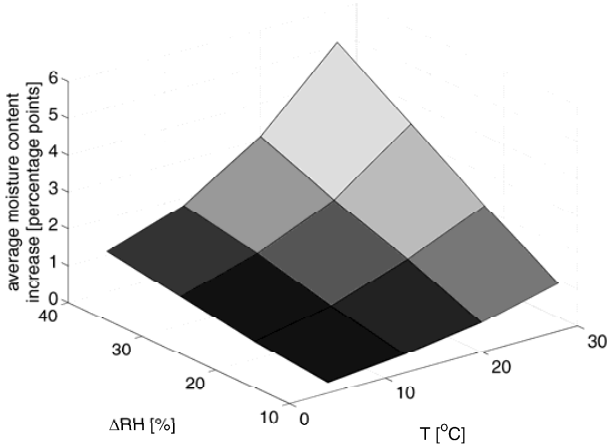

Figure 11. An average rise of the moisture content of a solid fiberboard sheet (1180 mm × 990 mm) after 8 days of exposure to a certain temperature and relative humidity.

5. Discussion

The aim of the work was to describe how the moisture content of the solid fiberboard sheet will evolve after lamination. Sheets are converted to transport boxes that are used in wet (ice and liquids inside) and humid conditions to transport fish. The transportation takes up to 8 days, and the climate inside the truck is 100% RH/ 4°C.

The starting point of the evaluation is the moisture content of the newly produced sheet. Figure 5 shows that the sheet has high moisture in the middle, approximately 11% (equilibrium moisture in 90% RH is 11-12%). After two days in mill environment, the moisture has diffused out from the sheet through the edges and the moisture content has dropped to 8% at the edges.

The main use of the determined moisture diffusivites was to compare water vapor penetration through sheet edges and planes. The in-plane diffusivity of the solid fiberboard ($5.87*10^{-10}$ m^2/s) is nine times higher than the transverse diffusivity of the polyethylene ($6.5*10^{-11}$ m^2/s). On the other hand, the area of the sheet planes (1.9 m^2) is much higher than the area of the edges ($3.3*10^{-3}$ m^2). Moisture transport through edges creates drier and moister areas, but the effect is quite local and the penetration is a slow process. In the vapor penetration test (Figure 8), the planes were not sealed and moisture is thus transported through the PE layer in addition to edges. After 8 days from a step change in relative humidity, only 20-30 mm distance from the sheet edge is in equilibrium with the ambient relative humidity.

The in-plane diffusivity coefficients reported in the literature vary greatly. Ramarao et al. [**12**] give a summary of moisture diffusivities found in the literature. Here are some examples of in-plane diffusivities for different materials [**12**]: waxed board $6.4 \cdot 10^{-13}$ m^2/s, newsprint $9.5 \cdot 10^{-10}$ m^2/s, corrugated $1.6 \cdot 10^{-11}$ m^2/s. Westerlind et al. [**8**] measured

effective diffusivities $1.5 \cdot 10^{-11}$ m^2/s for AKD sized linerboards (140 g/m^2) made of various recycled fibers. The coefficients were independent of the dose of AKD. The recent results by Massoquete [**10**] are in the lower end of the reported in-plane diffusivity range: $4*10^{-6}$ m^2/s for kraft handsheets. The results are affected by the experimental and theoretical technique of determination of the coefficient, the assumed underlying moisture transport model, experimental conditions, and properties like tortuosity, pore volume, density of the paper sheet, and chemical characteristics of the fibers. The glue layers of the solid fiberboard may also have an effect.

Observed non-Fickian behavior would mean that diffusivities based on Fick's law assuming the material to be homogeneous would lack physical validity. Resent results show that transverse moisture diffusion in paper materials tend to be intrinsically non-Fickian due to relaxation processes and local moisture variations in the sheet, even if the external factors causing departure for Fickian sorption are eliminated [**26**]. The external resistive surface boundary layer causes the humidity on the sample-air interface to deviate from the bulk humidity, resulting in non-Fickian behavior. Also if the ramp time of the external humidity change is slow compared to the diffusion time, the sorption process tends to be non-Fickian [**26**]. The presence of resistive layers can be seen as a sigmoidal shape in sorption curves plotted against $\xi = t^{1/2}L$ (t = elapsed time, L = half-length of the sample). In the present case no such sigmoid was observed (Figure 12). The curve seems reasonably linear. In addition, in the in-plane case the external mass transfer resistances are negligible compared to the internal resistance of the test pieces of this study (the sorption length 90 mm).

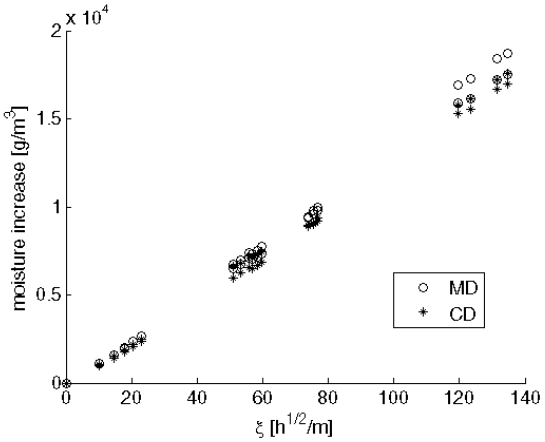

Figure 12. Moisture content increase as a function of $\xi = t^{1/2}L$.

This technique of determining diffusivity is sensitive to the selection of boundary conditions. Slightly different equilibrium moisture contents can easily be obtained for the same paperboard quality. By changing the moisture concentrations, the calculated diffusivity changes considerably, e.g. for equilibrium moisture contents 8.02% (50% RH) and 11.40% (90% RH), the diffusivity value is $8.99 \cdot 10^{-10}$ m^2/s. In addition the technique doesn't address the moisture dependence of diffusivity. In spite of these

weaknesses, the method offers a means for evaluating the in-plane moisture transport into the material.

The transportation box never experiences very high driving forces for moisture transport during transportation. The ambient RH is constantly close to 100%, and the moisture content after the lamination corresponds to 80%-90% RH. The converted sheets will be used as fish boxes at approximately 20 degrees lower temperature than used in the testing. Figure 11 shows the moisture content of the sheet rises approximately 0.3% due to water vapor penetration through polyethylene when it is used as a transportation box. The material tests on moisture penetration provide additional basis for evaluations. The polyethylene coating on the solid fiberboard is practically water tight. The large variation of Cobb test results especially at 16 hours (Figure 6) indicates that there might be sporadic pin holes in the polyethylene coating. The occurrence of pinholes in PE is unwanted since they increase the permeability of the coating to water. The overall level of Cobb test results show that the liquid water penetration values through PE is practically negligible compared grammage of the solid fiberboard (1220 g/m^2). One can conclude that moisture penetration through the planes is small.

Figure 7 shows that after eight days of exposure, only 60-80 mm of the material in from the edge of the liquid water penetration has higher moisture content than the equilibrium moisture content in 50% RH. The first 20 mm has higher moisture content than the equilibrium moisture in 90% RH. Based on the presented in-plane coefficient, water vapor can theoretically affect 80 mm from the board edge. The box designer should thus ensure that the open material edges are at least 80 mm away from the load bearing sections of the box.

The original moisture content has a major effect on the strength of the transport box. It is controllable with reasonable efforts during the manufacturing. The moisture transport through the solid fiberboard edges creates local stronger and weaker areas depending on the geometry of the box, normally close to box walls. From the producer's point of view, even a slight reduction in the amount of water in the glue used for laminating the board creates stronger transport boxes.

6. Conclusion

The moisture content of a newly laminated solid fiberboard sheet was measured gravimetrically. In-plane water vapor diffusivity of solid fiberboard was determined by transient vapor transfer experiment. The in-plane diffusivity was found to be $5.87*10^{-10}$ m^2/s (50%/90% RH, 27 ^oC). The in-plane moisture sorption was observed to follow Fickian behaviour, but the technique is very sensivite to boundary conditions. The transverse water vapor diffusivity of the polyethylene coated kraft paper was determined based on WVTR values, and was found to be $6.5*10^{-11}$ m^2/s (50%/90% RH/ 27^oC). The diffusivities were used together with additional material tests on moisture penetration to estimate the moisture transport rates affecting the moisture content of the transport box converted from the sheets. The results show that the moisture content of solid fiberboard sheet after industrial lamination changes only approximately 0.3 percentage points in climate 4 ^oC/100% RH during eight days transportation due to

vapor penetration through polyethylene coating. During that time, the moisture transport through the edges creates drier or moister areas. Maximum penetration length for liquid water is 40 mm from the open sheet edges, and 80 mm for water vapor.

7. Acknowledgements

The Research Council of Norway, Peterson AS, Eka Chemicals AB, and the Foundation of Paper and Fiber Reserch Institute in Trondheim, Norway (PFI) are greatfully acknowledged for the financial support. Dr. Jan-Erik Gustafsson and Dr. Johan Alfthan at the Swedish Pulp and Paper Institute (Innventia) are acknowledged for the discussions concerning mathematics of diffusion.

References

1. W. Mies, J. Potter, D. Miller and J. Kenney (Editors), *Global pulp & paper fact & price book 2006*, RISI, Bedford, MA, USA, 2006.
2. K. Niskanen, *Paper physics*, vol. 16, Finnish Paper Engineer's Association/Paperi ja Puu Oy, 2008.
3. R. J. Roberts, "Liquid penetration into paper," *The Australian National University*, vol. Thesis (Doctor of Philosophy) 2004, p. 348.
4. A. Marmur and R. D. Cohen, *Characterization of porous media by the kinetics of liquid penetration: The vertical capillaries model*, Journal of Colloid and Interface Science **189** (1997), no. 2, 299-304.
5. G. P. Matthews, *Computer modelling of fluid permeation in porous coatings and paper – an overview* Nordic Pulp and Paper Research Journal **15** (2000), no. 5, 475-485.
6. M. J. Denton, *The capillary absorption of liquids in paper and other porous materials*, Journal of Choromatography **18** (1965), 615-616.
7. S. J. Hashemi, V. G. Gomes, R. H. Crotogino and W. J. M. Douglas, *In-plane diffusivity of moisture in paper*, Drying Technology **15** (1997), no. 2, 265-294.
8. B. S. Westerlind, A. Gustafsson and L. A. Carlsson, "Diffusion of water vapor in paper," *1996 Progress in paper physics - A seminar proceedings*, Stockholm, Sweden, 1996, pp. 71-74.
9. J. R. t. Donkelaar and C. R. Jaeger, "Transport and sorption of water vapour in corrugated board," *4th International symposium on moisture and creep effects on paper, board and containers*, Ecole Francaise de Papeterie et des Industries Graphiques, Grenoble, France, 18-19 Mar 1999, 1999, pp. 245-255.
10. A. Massoquete, S. A. Lavrykov, B. V. Ramarao, A. Goel and S. Ramaswamy, *The effect of pulp refining on lateral and transverse moisture diffusion in paper*, Tappi **4** (2005), no. 12, 3-8.
11. H. Gupta and S. G. Chatterjee, "Facets of moisture diffusion in paper under steady-state conditions," *2002 Progress in paper physics seminar*, D. S. Keller and B. V. Ramarao (Editors), Syracuse, NY, USA, 8-13 Sept. 2002, 2002, pp. 254-258.
12. B. V. Ramarao, A. Massoquete, S. Lavrykov and S. Ramaswamy, *Moisture diffusion inside paper materials in the hygroscopic range and characteristics of diffusivity parameters*, Drying Technology **21** (2003), no. 10, 2007-2056.

13. P. Salminen, "Studies of water transport in paper during short contact times," Laboratory of Paper Chemistry, Department of Chemical Engineering, Åbo Akademi 1988., Åbo, 1988, p. 94.
14. H. Radhakrishnan, S. G. Chatterjee and B. V. Ramarao, *Steady-state moisture transport in a bleached kraft paperboard stack*, J. Pulp Pap. Sci. **26** (2000), no. 4, 140-144.
15. J. A. Bristow, *The absorption of water by sized papers*, Svensk papperstidning **71** (1968), no. 2, 33-39.
16. A. Massoquete, S. Lavrykov, B. V. Ramarao, A. Goel and S. Ramaswamy, "Anisotropic moisture diffusion study on refined paper," International Paper Physics Conference, Proceedings, Technical Assoc. of the Pulp and Paper Industry Press, Victoria, BC, Canada, 2003, pp. 253-257.
17. R. Amiri, J. Hamel and J. D. McDonald, *Moisture distribution in paper rolls: The effect of wrapping materials*, J. Pulp Pap. Sci. **28** (2002), no. 5, 143-150.
18. J. Leisen, B. Hojjatie, D. W. Coffin and H. W. Beckham, *In-plane moisture transport in paper detected by magnetic resonance imaging*, Drying Technology **19** (2001), no. 1, 199-206.
19. B. Hojjatie, J. Abedi and D. W. Coffin, *Quantitatieve determination of in-plane moisture distribution in paper by infrared thermography*, Tappi **84** (2001), no. 5, pp. 11.
20. N. P. Zogzas, Z. B. Maroulis and D. Marinos-Kouris, *Moisture diffusivity methods of experimental determination - a review*, Drying Technology **12** (1994), no. 3, 483-515.
21. R. B. Bird, W. E. Stewart and E. N. Lightfoot, *Transport phenomena*, Wiley, New York, 1960.
22. "Paper and board — determination of water absorptiveness — cobb method," ISO 535:1991.
23. Tappi, "Water vapor transmission rate og paper and paperboard at 23 oc and 50% rh," T 448 om-97.
24. "Paper and board — determination of capillary rise — klemm method.," ISO 8787:1986.
25. L. Piergiovanni, P. Fava and A. Siciliano, *Mathematical model for the prediction of water vapour transmission rate at different temperature and relative humidity combinations*, Packaging Technology and Science **8** (1995), no. 2, 73-83.
26. A. Massoquete, S. Lavrykov and B. V. Ramarao, *Non-fickian behaviour of moisture diffusion in paper*, J. Pulp Pap. Sci. **31** (2005), no. 3, 121-127.

Paper II

Is not included due to copyright

Paper III

The effect of moisture content on compression strength of boxes made of solid fiberboard with polyethylene coating – An experimental study

Sara Paunonen(*) (sara.paunonen@chemeng.ntnu.no, tel. +47 73 55 03 97, fax: +47 73 55 09 99), **Øyvind Gregersen** (oyvind.gregersen@chemeng.ntnu.no, tel. +47 73 59 40 29), Norwegian University of Science and Technology NTNU, Department of Chemical Engineering, Høgskoleringen 6B (PFI building), NO-7491 Trondheim, Norway, (*)Corresponding author.

Abstract
Factory-made transport boxes made from polyethylene coated solid fiberboard were studied. The boxes had double panel walls. Compression strength, vertical deformation, and buckling of long panels during top-to-bottom compression were studied for different moisture contents. The boxes were exposed to high humidity for eight days (90% RH; 4°C), and both standard BCT tests and cyclic load BCT tests were executed. During the BCT tests, buckling of the longest side was measured with linear transducers. The compression strength was observed to decrease linearly by 380 N per one percent change in moisture content. During eight days of exposure to a high humidity environment, the boxes lost 15% of their compression strength and gained 1 percent moisture content. The decrease of the BCT value relative to change in moisture is comparable to earlier results for uncoated corrugated boxes. The polyethylene coated boxes take longer to reach the moisture content change. Box failure can be expressed as a critical vertical displacement value that does not depend on the moisture content of the box. The boxes deformed mainly permanently during compression. The permanent deformation increased as a function of moisture content, and as a consequence the outward buckling of the vertical box decreased as the moisture content increased. Because of the polyethylene coating, the moisture was unevenly distributed in the boxes.

Keywords: box compression, moisture, buckling, laminated board, shipping containers

INTRODUCTION

The main purpose of the transport box is to resist mechanical and to some extent environmental loadings so that the contents reach the final destination intact. The mechanical loadings include mechanical dynamic loading (e.g., accelerations from transport vehicle), static loading (dead weight of the stack) and hydrostatic loading (contents). The boxes undergo irreversible changes to their shape under the applied forces. During long term transportation and storage, the container also experiences time dependent phenomena typical for paper-based materials, e.g., creep. The ambient relative humidity and temperature affect the mechanical properties of boxes [1]. The usual and simplest way of quantifying a box's performance is to measure the maximum force applied in a box compression test (BCT) at standard conditions.

This work studies the effects of moisture on the performance of transport boxes that are made from polyethylene coated solid fiberboard. Boxes have an unusual, more complicated design compared to well-known regular slotted containers. The box testing is done at conditions close to the actual transport conditions of fresh round fish (constant 4°C and 90% RH). Creep of the boxes at constant RH is studied, but creep in varying humidity is left out since the conditions do not change during transport. The transport duration (eight days) is taken as the time frame of the experiments.

The objectives of the study are to
(i) Quantify the moisture content and determine its impact on box compression strength,
(ii) Examine the deformation of boxes, and
(iii) Examine the outward buckling of the outer panel of a double-paneled box wall

BACKGROUND

Box compression test (BCT)

Single box compression has been used to simulate box performance in the end-use situation for a long time, even though a box cannot sustain the same stacking load obtained in a compression test [2],[3]. BCT tests have a large standard deviation in the results due to, variation in raw material, imperfections in the box geometry from the manufacturing process, and environmental conditions during the testing. The large standard deviation easily masks the effect of the variables studied. In a controlled test environment, the 2-sigma variation of BCT results of individual factory made boxes (same quality) over time is normally ±14 %, even as high as ±20 % [4]. The same conditions that change the top-to-bottom compressive strength in the laboratory, also change the amount of time that a box can support dead loads when stacked during transportation or in storage [5].

Compression strength of a container depends on the material properties of the paperboard layers, their geometric arrangement in the built-up board, the manufacturing process of the box (e.g., depth of scoring) [6], the geometry of the box, and the test environment. For corrugated fiberboard, the key parameter contributing to the box performance is the compressive strength of the liner [7]. For solid fiberboard, no such clear results exist. One can anticipate that the compression strength of all layers is of importance.

The box compression test measures how different structural parts of the box; panels, edge creases, possible flaps and flap creases, resist the total top-to-bottom compressive load. The geometry of the box, the allocation and position of board materials all affect the distribution of compressive stress in transport boxes [8]. The vertical edges of regular slotted containers (RSC) are reported to carry 40%-64% [8, 9] of the total load during compression. The remaining load is carried by the panels. Meng et al. [9] used a pressure sensitive film to detect the load distribution along the box perimeter. Different parts of the package contribute to the stiffness of the whole box. The stiffness of the middle section of a box is higher than of the top and bottom sections, where the behavior of the creases affect the compression stiffness [10, 11].

In a compression test, a box is loaded from top to bottom between two plates, and the force is recorded as a function of vertical displacement (BCT curve). Due to the irregular shape and the lack of precision in dimensions of the box during converting, the plates of the box compression tester don't contact the perimeter of the box evenly at the beginning of the test. The effect is seen as a flat slope in the BCT curve. In BCT test standards, e.g., [12], the effect of this gradual build-up of the load is handled with a preload that is a function of the expected strength of the box. The measurement of deformation is considered to start from this point. As the compression proceeds, the horizontal scoreline regions start to take the load by both crushing and rotation [13]. The sidewall tube bears the same load, but since the stiffness of the sidewalls is greater than the stiffness of the scoreline areas, the deformation occurs mainly in the scoreline areas. The end of the scoreline crushing phase shows up as a change in slope in the BCT curve. For corrugated boxes, 90 % of the total deformation at maximum load (measured from zero load) occurs in the creased areas [13].

Since the edges of the box experience the most stress, failure starts at the box corners (regions where the length, width and depth meet) and progresses into the panels [8, 13, 14]. Visible lines appear at the corners, and they grow towards the centre of the panel, and ultimately cause the panels to buckle. For corrugated fiberboard, McKee and Gander [13] suspect that the failure is due to compressive failure of the fluted medium. The failure is seen as a rapid decrease in the BCT curve. For corrugated boxes, the failure mechanism can be attributed to the loss of transverse shear rigidity of the corrugated board [15]. Other possible mechanisms include local buckling of the liner or global buckling of the panel depending on the slenderness ratio of the panel [16]. No results are available on the failure mechanism of solid fiberboard materials in transport packages.

Marcondes [17] studied the effect of loading history on the compression strength of corrugated boxes. He loaded the boxes to 60% and 80 % of the compression strength 1 to 20 times before loading to failure. He found out that preloading do not significantly alter the compression strength of corrugated boxes.

Moisture effects on BCT

The moisture content affects the mechanical properties of paperboard materials [1] and thus the boxes made of paperboard [2]. Kellicut [18] found a negative exponential relationship between compression strength Y of corrugated boxes and their moisture content m,

$$Y = b \cdot 10^{-mx} \tag{1}$$

where b = compressive strength of a box at zero moisture content, m = average slope of the curve where moisture is plotted against the logarithm of compressive strength, and x = dry-based moisture content (ratio between the weight of water in the board and oven-dry weight of the fiberboard). Kellicut [18] observed that the boxes made of different corrugated materials responded in a similar way to increases in moisture content, and thus the parameter m was found to have a value of 3.01.

The in-plane deformation of panels at collapse is independent of deformation rate, relative humidity and the magnitude of dead-load [19]. Hansson [19] derived this conclusion by studying corrugated panels under compression, which was considered to be a more controllable test set-up than compression of whole boxes. If extended to boxes, the vertical displacement at compression strength would be independent of moisture content of the box. The box failure criterion could be expressed as

$$u \geq u_c \tag{2}$$

where u = vertical displacement of the box, and u_c = critical vertical displacement independent of material moisture content.

Often the moisture content is considered as a global variable of the box. One reading can be taken as an average of a samples of several boxes [20]. Sometimes the relative humidity on both sides of the box wall are recorded [21]. The rate of the moisture penetration into the boxes or the local variation in the moisture content is usually not studied.

Creep

Compression tests are performed relatively quickly, and no attention is paid to the time-dependent characteristics of the material. In reality, box failure occurs slowly. Compressive creep failure is the main reason for the transport boxes to fail in service [22]. The creep effect is accelerated both in paperboard and corrugated boxes in environments where the humidity changes. This causes earlier failure than at constant humidity [23]. Even though mechano-sorptive effects occur with small moisture content changes [24], mechano-sorptive creep is left out of the study since both the temperature and the relative humidity are stable during the transport in an air-conditioned truck. In addition, the high grammage and the PE coating of solid fiberboard slow down the moisture transport, the hygroexpansion and creep response, and make measurements challenging. The environment during transportation is a constant 90%-100% RH/4°C. Coffin [25] gives a comprehensive survey on creep behavior of paper at constant and varying humidity.

EXPERIMENTAL

Materials

The paperboard studied is a uni-directionally stacked solid fiberboard; see Table 1 for material properties. The four middle layers are made of 100% recycled fiber (OCC) and are heavily internally sized. The outer layers on both sides are made of bleached machine finished kraft paper. The kraft paper has a double extrusion coated low-density polyethylene layer. The six paper and board layers are glued together in an industrial lamination process that compresses the material. The glue used in lamination contains poly-vinyl alcohol (PVA) as an active agent, clay, additives, and water. The solids content of the liquid glue is 24%.

Table 1. Grammage and thickness of the solid fiberboard and its layers.

	Name of the layer	Grammage [g/m^2]	Thickness(*) [mm]
1	Polyethylene coating	20	0.02
2	Kraft paper 1	60	0.07
3	Adhesion layer 1	10	
4	Middle layer 1	250	0.39
5	Adhesion layer 2	10	
6	Middle layer 2	250	0.39
7	Adhesion layer 3	10	
8	Middle layer 3	250	0.39
9	Adhesion layer 4	10	
10	Middle layer 4	250	0.39
11	Adhesion layer 5	10	
12	Kraft paper 2	60	0.07
13	Polyethylene coating	20	0.02
	Solid fiberboard	1220	1.73

The design of the transport box is more complex than the commonly used regular slotted container (RSC) or similar boxes. The box has long walls that are made of two panels. The long inner panels are glued to the bottom panel. The short walls are made of single panels. The webbed corners prevent leakages and allow the vertical edges and short panels to buckle outwards when vertically loaded. Four small flaps hold the box structure together when glued onto the outer long wall panels. The outer dimensions of the transport boxes are 790 mm × 380 mm × 138 mm. The erected transport box is shown in Figure 1.

Figure 1: The transport box design used in the study.

Box compression tests

Boxes with different moisture contents were exposed to a humid environment (90% RH, 4^{o}C) for eight days. Before the trial, the boxes were stored at the test site at room (non-standard) temperature and relative humidity. Table 2 summarizes the different treatments. For Case B and C, boxes were pre-dried. The 3 liter water content was used to simulate the water present in the boxes during the transport.

Table 2. The five test cases for studying liquid water and water vapor penetration into fiberboard boxes.

Test	Pretreatment		Box content	Environmental conditions	
	T [°C]	Time [d]		Climate [% RH/°C]	Time [d]
A	--	--	--	90/4	8
B	40	4	--	90/4	8
C	80	2	--	90/4	8
D	--	--	water (3 l)	90/4	8
E	--	--	water (3 l)	~ 50/23	8
Ref	--	--	--	--	--
RefB	40	4	--	--	--
RefC	80	2	--	--	--

After 24 hours (1 day), 96 hours (4 days) and 192 hours (8 days) three boxes from each case were taken from the climate room and box compression tested (BCT) at non-standard conditions (21°C-23°C, 28%-41% RH) with Alwetron CT100 (Lorentzen&Wettre) compression tester and Test&Motion (ICS) software according to the ISO standard 12048-2:1994 [12]. Throughout the work, empty boxes were tested, and the loose small flaps inside the box were taped onto the short panels. The rate of loading was 10 mm/min. The sampling frequency of the force-displacement data was 50 Hz. In the BCT test data analysis, the deformation is considered to start after a threshold value of 250 N. Table 2 also shows the reference cases (Ref, RefB, RefC) without the climate treatment.

Moisture content was measured at locations shown in Figure 2 by cutting two samples and drying them at 103°C for 3 days. Moisture content was also measured as weight increase in a whole box.

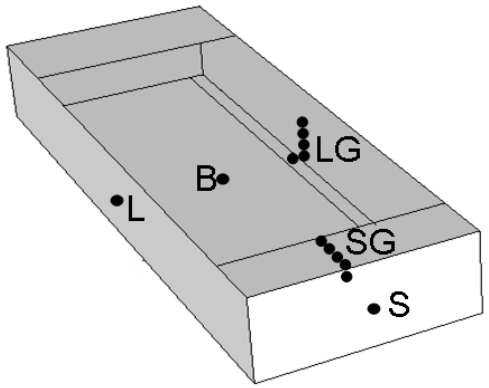

Figure 2: The locations for cutting material moisture samples: short panel (S), long panel (L), bottom panel (B), gradient measurement (five 20 mm long samples) from the short edge (SG), gradient measurement from the long sheet edge (LG). The length of the gradient measurement is 100mm. The size of the material samples was approximately 20 mm × 20 mm.

Deformation of boxes

To study the deformation of the boxes more closely, a simplified version of the above mentioned test was executed. The treatments A and B shown in Table 2 were selected. Moisture and cyclic box compression were tested after 8 days of climate treatment. Reference boxes Ref and RefB were tested without the climate treatment. Six parallel boxes were compression tested cyclically with increasing loads (1000 N, 2000 N, 3000 N, …). The box was loaded to the first load level, the load was removed and the compression plates were brought to the original position. Then the load was increased to the next force level, etc. Data from the unloading phase was not recorded.

In the creep test, a stack of three empty boxes was kept for eight days in a humid environment (90% RH, 4°C). The stack was loaded with a dead weight of 244 kg, which corresponds to 40% of the BCT value. The transport box at the bottom of the stack stack should be able to endure a dead-load of 260 kg. After eight days of exposure the creep tested boxes were BCT tested at room temperature.

Buckling of the panels

The outward buckling of the long outer panel during the box compression test was measured with three linear displacement transducers (RDP Electronics LTD, type DCT1000A) that were mounted on a rack. The transducers were placed vertically in the middle of the long side of the box. The distance between the sensors and box edges was one quarter of the height of the box as seen in Figure 3. The transducers were connected via Contrec AQ-Box to a PC, and Contrec Winlog 2000 program was used for data acquisition at a sampling frequency of 50 Hz.

Figure 3. Three displacement transducers measuring the outward buckling of the long wall before the start of a BCT test.

RESULTS AND DISCUSSION

Moisture content of boxes

Figure 4 shows the change in moisture content over 8 days when the boxes were pre-dried in 40°C before they were exposed to 90% RH and 4°C (test Case C). Moisture penetrates through the material edges and the moisture content increases gradually further and further away from the edges. The penetration through box side panels is

relatively low. After eight days, only the first 100mm from the sheet edge is affected by moisture penetration. The overall moisture uptake of the boxes is measured by weighing the whole box as shown in Figure 5. The measured moisture increase of 1 percent is close to the increase of 0.5-1 percent reported by Kirkpatrick [26]. The values of Kirkpatrick are for a PE-coated corrugated fiberboard boxes measured at 20°C after 8 days cyclic (60%/90% RH) moisture treatment. In Cases D-E, the high variation in the moisture increase is due to the difficulty in drying the excess water before weighing. These cases are left out of further discussion.

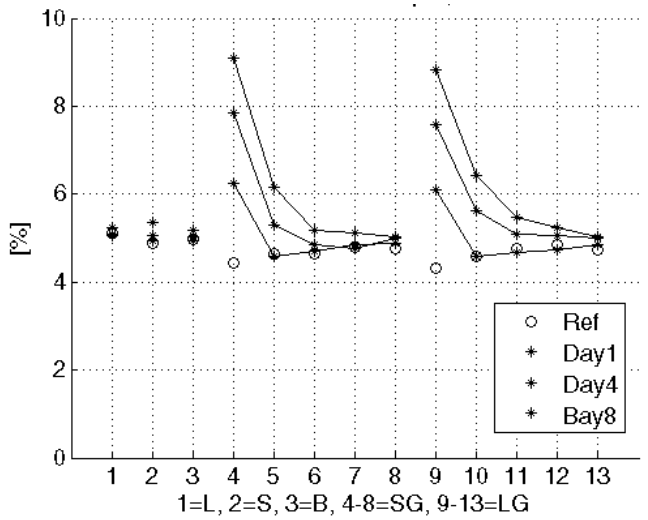

Figure 4. Development of moisture content at different locations of the box during climate treatment: short panel (S), long panel (L), bottom panel (B), gradient measurement from the short edge (SG), gradient measurement from the long sheet edge (LG). The location on the box is shown on the x-axis. Moisture contents are measured from samples taken in days 1, 4, and 8, average value (n=2, n = number of averaged data points).

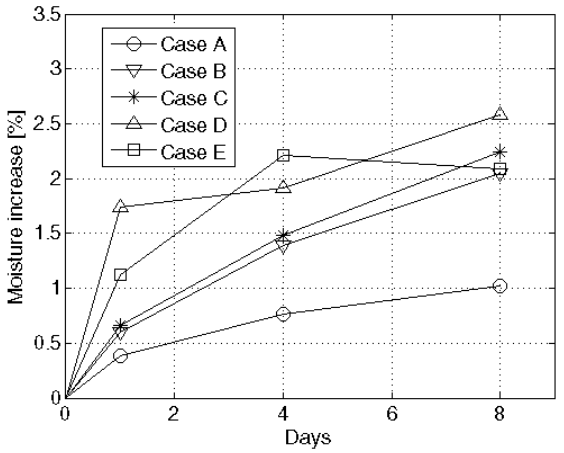

Figure 5. Moisture increase of boxes during climate treatment measured by weighing the whole box, average value (n=3).

The moisture content increase of a transport box due to humidity is often reported as the average increase in container weight [27], average value taken from several boxes [20], or as a relative humidity measurement taken from the outer and inner side of the material [27]. For corrugated boxes these techniques are justified because there is no additional moisture barrier slowing down the moisture sorption. There is no difference in the moisture transport rate in-plane and through-plane. Polyethylene coating slows down the transverse moisture transport considerably, and leads to uneven moisture distribution of the box. This effect was seen as there was relatively little moisture intake in the boxes during the climate treatment. A 100 mm wide strip near the open material edges has considerably higher moisture content than the middle of the box panels. The average moisture content of a box does not provide a reasonable basis for comparing the strength properties. Instead the moisture content of the load bearing parts should be used. However, the average moisture by weighing the whole box is a quick, reliable, and non-intrusive measurement. In the following discussion this measurement description technique is used.

Impact of moisture content on box compression strength

Figure 6 shows the box compression strength as a function of average moisture content. The original moisture content was defined as the average of the three measurements from the middle of the panels (Figure 3, locations L, S and B). The moisture increase is taken from the data presented in Figure 5. In Cases B and C, the moisture penetration of pre-dried boxes was measured. Ventilation conditions during the drying affect the moisture content. The boxes for Cases B and C and for the reference cases RefB and RefC (see Table 2) were dried in different batches, and thus the compression strength values in Figure 6 are only indicative.

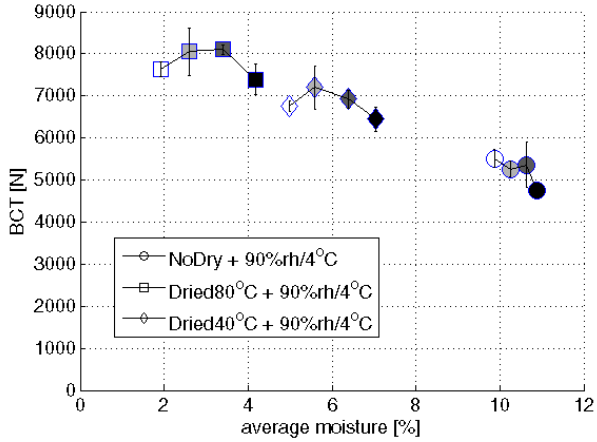

Figure 6. Box compression strength as a function of average moisture content. Marker types: ‘o’ = non-pretreated boxes (Case A), ‘◊’ = pre-dried in 40°C (Case B), ‘□’ = pre-dried in 80°C (Case C), Marker colors: white = references, gray = day 1, dark gray = day 4, black = day 8. Average and standard deviation (n=3).

The decrease of BCT values in Figure 6 is almost linear with respect to the moisture content, as also reported by Kellicut [18]. By omitting the reference, the compression strength decreases 380N per moisture content percent. The polyethylene coated solid fiberboard boxes lost 15% (from 5500N to 4700N) of their compressive strength by being exposed to high humidity in eight days. During that time, the moisture content increased by 1 percent. According to [28], corrugated containers typically lose 10%-20% of their compressive strength at 50% RH in high humidity environments. Data presented by Kellicut [18] shows that an increase in moisture content from 6% to 7% decreases the compression strength of uncoated corrugated boxes by 9%. An increase from 6% to 18% in moisture content would result in 56% reduction in compression strength. The decrease of 15% in compression strength for PE coated boxes is in line with the results by Kellicut [18], keeping in mind the moisture barrier role of the polyethylene. The results seem to hold even for the atypical box design studied.

Displacement at compression strength

Hansson [19] found out that the deformation of corrugated panels at failure when loaded in in-plane direction depends only on the geometry and the boundary conditions of the panels. Deformation does not depend on moisture content of the plates, deformation rate, or the dead-load in the creep test. In the current work, the displacement does not depend on the moisture content of the boxes, as Figure 7 shows. In the range of 2%-11% moisture content, the displacement is constant, approximately 10mm. The result indicates that Hansson's observation can be extended to PE coated boxes with complex design. Failure criterion for a specific box type in compression can be based on vertical displacement, and that it is independent of moisture content.

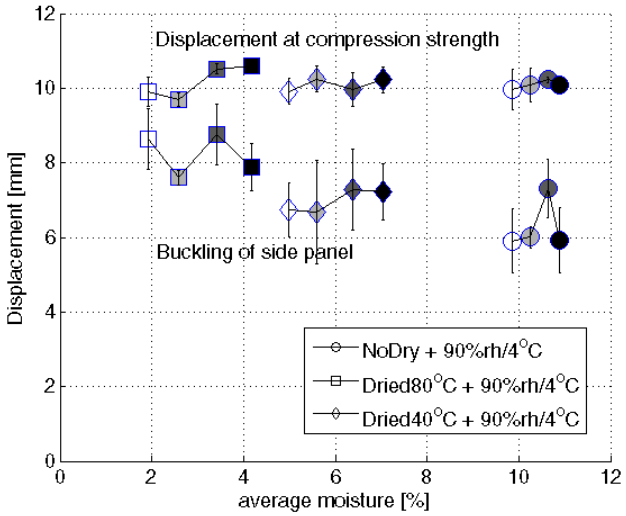

Figure 7. Vertical displacement at compression strength. Marker types: 'o' = non-pretreated boxes (Case A), '◊' = pre-dried in 40°C (Case B), '□' = pre-dried in 80°C (Case C), Marker colors: white = references, gray = day 1, dark gray = day 4, black = day 8. Average and standard deviation (n=3). Also the horizontal buckling of the side panel middle point at compression strength is shown.

Deformation of boxes

The stack of three boxes was compressed only 0.7mm after the immediate fast compression due to placing the dead-load on top. Kirkpatrick [26] studied creep of polyethylene coated corrugated fiberboard boxes, and also noticed the low creep rate of the boxes. The displacement during secondary creep of one box was 1 mm when the box was exposed to cyclic 60%/90% RH and 20°C for 8 days [26].

Figure 8 shows the box compression test curves of the creep tested boxes. BCT curves for boxes without the dead-loading, but with the same climate treatment are shown as reference. The exposure to dead-load has flattened the curve in the range of 1-5 mm, which is probably due to the crushing of crease lines. The effects of creep testing are to reduce the displacement at compression strength by approximately two millimeters.

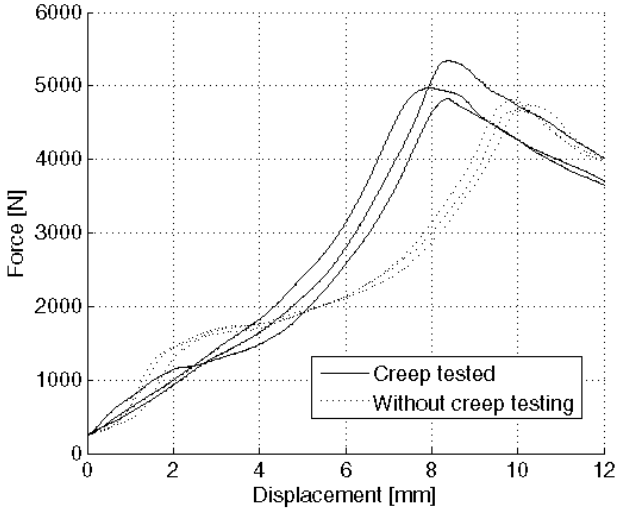

Figure 8. BCT curves of creep tested boxes (—), and boxes that were not creep tested (···) after humidity treatment.

Cyclic compression tests were done to interpret the BCT curves of the creep tested boxes, and to study the vertical deformation due to repetitive loading more closely. The typical cyclic BCT curves (Figure 9) show that loads greater than 3000N-4000N follow a straighter curve than lower loads. Drying of the box does not chance the shape of the BCT curves. When the boxes are loaded to over 2000N, the material starts gradually to yield and BCT curves similar to creep tested boxes are obtained. By comparing the slopes of cyclic BCT curves, it can be anticipated that the creaselines are not completely crushed during the creep test.

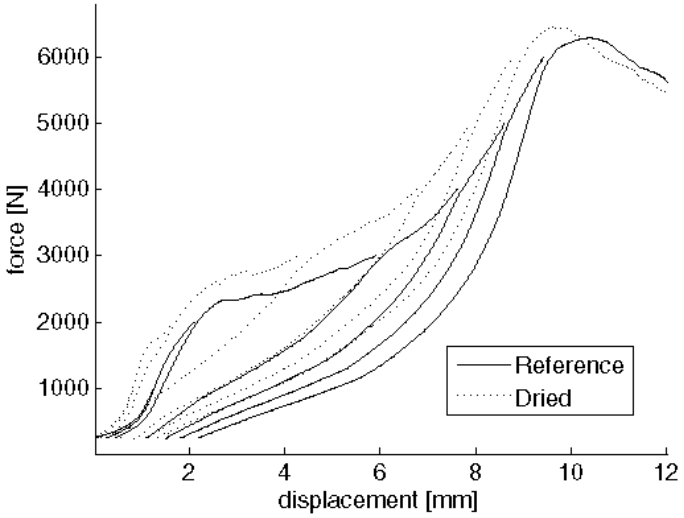

Figure 9. The cyclic BCT curves for a reference boxes (Ref) (—) and a pre-dried box (RefB) (···).

A box deforms permanently due to yielding of the material in each loading cycle. The duration of one loading-unloading cycle was between 30 s and 120 s. Permanent deformation was plotted as a function of total deformation for each loading cycle (Figures 10 and 11). Drying the boxes reduces the permanent deformation. The subsequent moistening increases the deformation, more so in the case where the boxes were dried before the exposure to humidity. Three boxes were also tested with 15 minutes hold time between each cycle. The permanent effect did not dependent on the hold time between the loading cycles.

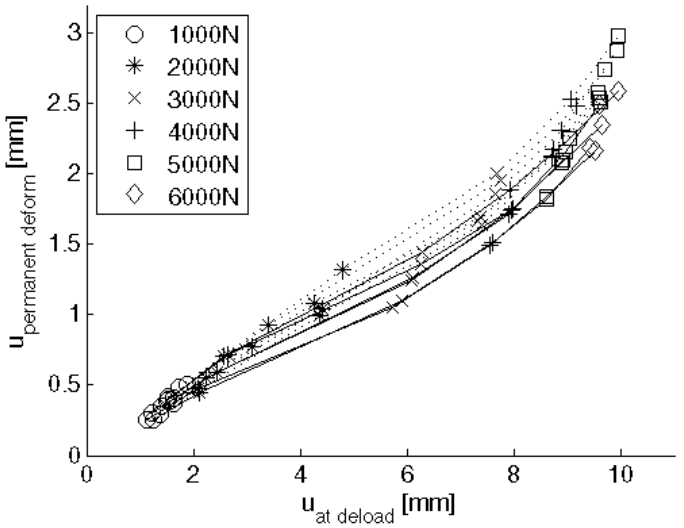

Figure 10: Permanent deformation of a box as a function of total deformation at unloading. (—) reference boxes (Ref), (···) humidity treated boxes (Case A).

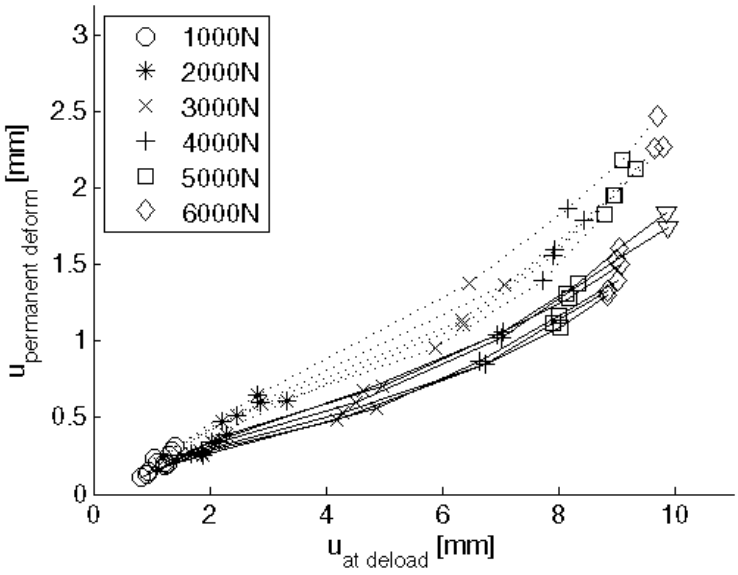

Figure 11: Permanent deformation of a box as a function of total deformation at unloading. (—) reference boxes (RefB), (···) humidity treated boxes (Case B).

The BCT curves of creep tested boxes are clearly different from the non-creep tested boxes. Curves were straighter, and the deformation at fracture was reduced by 2 mm. The compression strength was unaffected. The reduction of the deformation can be interpreted with the cyclic loading data. At the load level 2440 N, the permanent deformation is approximately 1.5 mm (see the curves after humidity treatment in Figure 10). The reduction of displacement in the creep test (2 mm) can be explained by the effect of creep (0.23 mm) and permanent deformation (1.5 mm). In the end-use situation, the load on the lowest box in a stack is approximately the same as in the creep test. During the usage of transport boxes, most of the displacement in box compression is due to plastic deformation of the creases. Thus at the conditions 90% RH, 4°C, and 40% of BCT load, the creep deformation accounts for less than 3% of the total deformation at failure. The 15 min hold time between the cycles of the cyclic testing produced similar results to the immediate loading results, which further confirms that the boxes do not show strong viscoelastic responses.

Buckling of the long box panel

Figure 12 shows the typical shape of the box compression curve and the outward buckling of the mid-point point of the outer long side panel. The BCT curve starts quite flat due to the imperfections of the boxes. After a displacement around 0.5 mm, the slope increases, probably due to the initiation of compression and rotation of the upper and lower crease lines. At 3-4 mm displacement, the force stops increasing, and the side panel starts buckling. At this point, the yielding of the creases is finished, and the stiffer panels strain. The slope of the buckling-displacement curve increases when the compression strength has been reached. At that point, visible kneeling lines 70-80 mm long appeared in the corners of the long panels, as has been reported earlier [8, 13, 14].

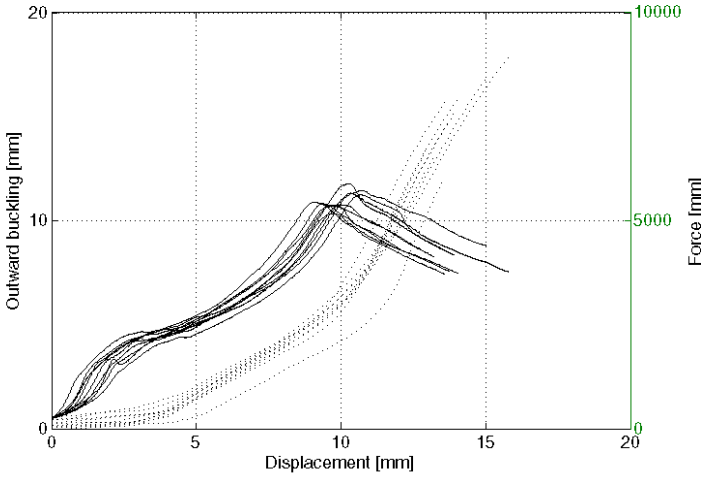

Figure 12. BCT curve (—) and outward buckling (···) of the middle point of outer long side panel.

The buckling of the panel mid-point as a function of average moisture is shown in Figure 7. The data shows a slight decreasing trend, although there is a large variation in the results. The horizontal buckling of side panel decreases with increasing moisture content (R^2 = -0.75 for mean of buckling readings, R^2 = -0.58 for three parallel buckling readings). The vertical movement of the panel mid-point due to the outward buckling during the BCT testing is not accounted for in the data. In the BCT tests, the panels started to buckle after the first plateau had been reached. This also indicates that the first part of the loading causes the creases to yield. The buckling increased rapidly after the maximum force had been reached. The buckling of panels at the compression strength was found to decrease as the boxes got wetter. The results show that the fraction of plasticity deformation increases as the material moisture increases. Thus wetter the box wall is, the more it will deform vertically before it begins buckling.

CONCLUSION

The results show that average moisture content is not well suited to describe moisture distribution of polyethylene coated boxes. PE restricts the moisture transport and leads to higher or lower moisture contents close to the open material edges. The compression strength was observed to decrease linearly at the rate of 380 N per one percent change in moisture content. During eight days of exposure to a high humidity environment (90% RH; 4°C), the boxes lost 15% of their compression strength and moisture content increased by 1%. The decrease of the BCT value in relation to the change in moisture content is comparable to earlier results for uncoated boxes. It takes longer for moisture content to change with PE coatings. Failure of the boxes in this study, can be expressed as a critical vertical displacement independent of moisture content. The viscoelastic effects were found to be small compared to the permanent deformation during the top-to-bottom loading. The magnitude of the permanent deformation increases with

increasing moisture content. As a result, buckling decreased as moisture content increased.

ACKNOWLEDGEMENTS

The tests were done at Innventia in Stockholm, Sweden. The help of Lic. Eng. Thomas Trost on practical test arrangements and the discussions with Dr. Johan Alfthan were valuable and are greatly appreciated. The materials for the test were provided by Peterson Emballege, Trondheim, Norway. Ms Gunvor Levang is appreciated for the box shipments to Stockholm. The Research Council of Norway, Peterson AS, Eka Chemicals AB, and the Foundation of Paper and Fiber Reserch Institute in Trondheim, Norway (PFI) are greatfully acknowledged for the financial support.

REFERENCES

1. Salmen, L., *Responses of paper properties to changes in moisture content and temperature*, in *Tenth fundamental research symposium at Oxford, Vol.1*. 1993, Pira International: Surrey, UK. p. 369-430.
2. Kellicutt, K.Q. and E.F. Landt, *Development of design data for corrugated fiberboard shipping containers.* Tappi, 1952. **35**(9): p. 398-402.
3. Kellicutt, K.Q., *Compressive strength of boxes.* Package Engineering, 1960. **5**(2): p. 94-96.
4. Carlson, D.A., *Box compression variation.* Corrugating Int, 2002. **4**(2): p. 7-9.
5. Kellicutt, K.Q., *Effect of contents and load bearing surface on compressive strength and stacking life of corrugated containers.* Tappi, 1963. **46**(1): p. 151A-154A.
6. Kellicutt, K.Q., *Compressive strength of boxes - Part I.* Package Engineering, 1959. **4**(12): p. 88-89.
7. Peterson, W.S. and T.S. Fox, *Workable Theory Proves How Boxes Fail in Compression.* Paperboard Packaging, 1980. **65**(10): p. 136-140, 142-144.
8. Maltenfort, G.G., *Compression load distribution on corrugated boxes.* Paperboard Packaging, 1980. **65**(9): p. 71-72,74,76-78,80.
9. Meng, G., T. Trost, and S. Östlund, *Stacking misalignment of corrugated boxes - a preliminary study*, in *23rd IAPRI Symposium on Packaging, 3-5 September 2007*. 2007: Windsor UK. p. 19.
10. Peterson, W.S. and W.J. Schimmelpfenning, *Panel edge boundary conditions and compressive strengths of tubes and boxes.* TAppi, 1982. **65**(8): p. 108-110.
11. Beldie, L., G. Sandberg, and L. Sandberg, *Paperboard packages exposed to static loads-finite element modelling and experiments.* Packaging Technology and Science, 2001. **14**(4): p. 171-178.
12. *Packaging — Complete, filled transport packages — Compression and stacking tests using a compression tester.* ISO 12048-2:1994.
13. McKee, R.C. and J.W. Gander, *Top-Load Compression.* Tappi, 1957. **40**(1): p. 57-64.
14. Srihiran, J., L. Jarupan, and T. Jinkarn, *The Analysis of Dimensional Changes Impacts on Compression Strength of Corrugated Box by Finite Element Method*,

in *16th IAPRI World Conference on Packaging, June 8-12, 2008*. 2008: Bangkok, Thailand.
15. Popil, R.E., D.W. Coffin, and C.C. Habeger, *Transverse shear measurement for corrugated board and its significance.* Appita Journal, 2008. **61**(4): p. 307-312.
16. Rahman, A.A. *Finite element buckling analysis of corrugated fiberboard panels*. 1997. Evanston, IL, USA: ASME.
17. Marcondes, J.A., *Effect of load history on the performance of corrugated fibreboard boxes.* Packaging technology and science, 1992. **5**(4).
18. Kellicutt, K.Q., *Structural notes for corrugated containers. Note no 13: Compressive strength of boxes - Part III.* Package Engineering, 1960. **5**(2): p. 94-96.
19. Hansson, T., *Deformation based failure criterion for corrugated board panels*, in *Solid Mechanics*. 2008, KTH: Stockholm. p. 31.
20. Harte, B.R., et al., *Compression strength of corrugated shipping containers held in frozen storage.* Boxboard Containers, 1985. **93**(2): p. 17-23.
21. Lyngå, H. and G. Sikö, *Moisture dynamics in corrugated board boxes*, in *Structural mechanics*. 2003, Lund University: Lund. p. 72.
22. Morgan, D.G. *A Mechanistic Creep Model and Test Procedure*. 2003. Melbourne, Vic., Australia: Appita Inc.
23. Leake, C.H. and R. Wojcik, *Humidity cycling rates: how they influence container life spans.* Tappi, 1993. **76**(10): p. 26-30.
24. Fellers, C. and J. Panek, *Effect of relative humidity cycle start point and amplitude on the mechano-sorptive creep of containerboard*, in *61st Appita annual conference and exhibition*. 2007: Gold Coast, Australia, 6-9 May 2007.
25. Coffin, D.W., *The creep response of paper: review*, in *Advances in Paper Science and Technology: 13th fundamental research symposium, Cambridge, 11-16 Sept. 2005, [Pulp and Paper Fundamental Research Society, 2005, 3 vols (ISBN 0954527232)]*, S.J. I'Anson, Editor. 2005. p. vol 2. 651-747.
26. Kirkpatrick, J. and G. Ganzenmuller, *Engineering Corrugated Packages to Survive Cyclic Humidity Environments - A Case Study*, in *3d International Symposium, Moisture and Creep Effects on Paper, Board and Containers*, I.R. Chalmers, Editor. 1997: Rotorua, New Zealand, 20-21 February 1997. p. 257-264.
27. Bronkhorst, C.A., *Towards a more mechanistic understanding of corrugated container creep deformatino behaviour.* Journal of Pulp and Paper Science, 1997. **23**(4): p. J174-J181.
28. Considine, J.M. and T.L. Laufenberg, *Literature Review of Cyclic Humidity Effects on Paperboard Packaging*, in *Cyclic Humidity Effects on Paperboard Packaging*, T.L. Laufenberg and C.H. Leake, Editors. 1992, TAPPI, USDA: Madison, Wisconsin, USA. p. 1-10.
29. Singh, S.P., *Stability of Stacked Pallet Loads and Loss of Strength in Stacked Boxes Due to Misalignment*, in *4th International symposium - Moisture and Creep Effects on Paper, Board and Containers*, J.-M. Serra-Tosio and I. Vullierme, Editors. 1999, E.F.P.G.: Grenoble, France, 18-19 March, 1999. p. 16-25.

Paper IV

Effect of polyethylene coating on in-plane hygroexpansion of solid fiberboard

Summary

Solid fiberboard is a rigid, heavy containerboard grade specially designed for packaging applications where wet or greasy products are transported in humid environment. The combined board studied here (1120 g/m^2) has four paperboard middle layers and two kraft paper layers that have polyethylene coating. The effect of the polyethylene (PE) coated kraft paper on the in-plane hygroexpansion of the combined board was investigated by measuring the hygroexpansion of the board with and without the PE layer. The PE coated kraft papers were manually peeled off the kraft paper. One sorption-desorption cycle was studied (50 → 100 → 50 % RH). Humid air was generated in a climate chamber and fed to a sealed cabinet that had micrometer-type tester unit. Significant differences in CD and MD strain development rate in sorption and desorption were observed. The development of CD strain in sorption is considerably slower than strains in desorption and the MD strain sorption. The results show that the polyethylene layer permanently restricts the expansion and contraction of the multi-layer paperboard 13 % in CD and 34 % in MD. Tests without polyethylene coating show that the phenomena at the board/surrounding air surface are masked out with other features arising from the bulk structure of the combined board.

Addresses of the authors: **Sara Paunonen** (*), (sara.paunonen@chemeng.ntnu.no) and **Øyvind Gregersen** (oyvind.gregersen@chemeng.ntnu.no): Norwegian University of Science and Technology, Department of Chemical Engineering, NO-7491 Trondhem, Norway. (*) Corresponding author

Keywords: hygroexpansivity, moisture, paper laminates, container boards

1. Introduction

Solid fiberboard is a rigid, puncture-resistant and water resistant material normally used for transport packaging, Kirwan (2005). It can be finished with a variety of lining papers and optionally polyethylene coating. Multi-layer grades are glued together in an off-line laminator. The solid fiberboard is mainly used in demanding packaging applications where the product is wet, frozen or greasy. Solid fiberboard is used much less than corrugated fiberboard in packaging applications. According to Mies et al. (2006), solid fiberboard boxes account for 0.5 % of U.S. total industry corrugated shipments (m^2).

If the paper material is perfectly homogeneous in structure and composition, changes in moisture content would result in even changes in length, width, and thickness only. When there is variation in structure and composition of the material, the varying directions and magnitudes of hygroexpansion cause large variation on the sheet in out-of-plane direction, e.g., curl, warp, of local buckling (cocle), wavy edges, Gallay (1973). This study concentrates on in-plane effects.

The hygroexpansive properties affect the paperboards ability to be converted and to protect the packaged product. Converting and packaging machines normally require the paperboard sheets to be flat to ensure smooth running of the process. Dimensional instability may cause problems in maintaining the required dimensions when the sheet is cut.

Dimensional changes are also important for paperboard boxes. In the box, two of the vertical edges are oriented in CD and two in MD. The hygroexpansion properties of the material in machine and cross-machine directions affect the stability of the stacked boxes when they experience varying climates during storage and transportation. If the transportation box is to be modelled in detail, the magnitude and rate of the hygroexpansion is one of the phenomena to be considered. Dimensional stability is improved by, e.g., hindering or preventing the moisture transfer by a moisture barrier, for example polyethylene coating.

Hygroexpansion is defined as the relative change in material dimensions due to the added volume of the sorbed moisture to the hygroscopic material. It is challenging to describe how the sorbed moisture is distributed inside the paperboard since the material is inhomogeneous both in composition and in structure by nature. Paperboard grades that need to resist penetration or spreading of liquids through the material are internally sized. The increasing level of sizing increases the non-uniformity of the wetting, Horwarth and Schindler (1985). Combined boards are even more complex grades because they consist of several paper and board layers. The glue between the layers has certainly an effect on the moisture distribution hindering the z-directional moisture transfer. The joint hygroexpansion effect arises from the hygroexpansive properties of all the constituent layers.

This work concentrates on studying the in-plane hygroexpansion of one laminated solid fiberboard grade. After the lamination, the solid fiberboard sheets are converted to boxes that are used for transportation of fresh victuals together with ice. During the eight days transportation, the temperature is held constant at 4 °C and the relative humidity close to 100 % RH. Before this step change in relative humidity, the boxes are stored in an uncontrolled environment from few days to several weeks waiting for the shipment to the customer. The duration and the humidity environment of the transportation are taken as the frame of this study, although hygroexpansion is observed in laboratory temperature.

The aim of the study is to investigate the effect of the polyethylene coating and its substrate paper on the hygroexpansion of the complete solid fiberboard. The effect is studied in one sorption-desorption cycle, since the situation during the end-use of the box is of interest. The results are used for commenting how sorbed moisture affects heavy duty boxes for wet goods transport. The study is done on one solid fiberboard type.

2. Hygroexpansion

Several reviews on hygroexpansion and dimensional stability are available (Gallay (1973), Uesaka (2002)). George (1958) lists several factors that affect the hygroexpansion of a paper sheet, e.g., type of pulp, degree of refining, fiber orientation, and tension during drying.

The hygroexpansion is primarily caused by sorption of moisture into the paper structure. The different mechanisms of moisture sorption include: capillary penetration, diffusion through fibres and bonds, and surface diffusion and vapor phase transport, Swanson (1989). The moisture content of a paper material is a response to environmental moisture. The response is independent of how the material is dried during fabrication, but depends on the history of the environmental humidity, Salmén et al. (1993). One of the fundamental findings is that hygroexpansive strains should be expressed as a function of moisture content that describes the internal state of the paper, and not as a function of the environmental condition causing the changes in dimensions Uesaka et al. (1991).

Fiber-fiber bond properties

Several properties of fibers and fiber networks affect the hygroexpansion. Uesaka and Qi (1994) state that hygroexpansivity of paper depends on both the axial and transverse directional hygroexpansive properties of the fiber through stress transfer from fiber network to fibers, which occurs in fiber-to-fiber bonds. The fibers expand mainly in the transverse direction. Their simulations show that the hygroexpansion in MD is mainly controlled by the longitudinal hygroexpansion of fibers. The CD hygroexpansion of paper is affected by the fiber-fiber bonding and the fiber orientation in the sheet due to the larger contribution of transverse hygroexpansion of fibers. Uesaka and Moss (1997) studied the complex effects of fiber morphology with a michromechanical model, and showed that dimensional stability of restrained-dried sheets is enhanced by increasing fiber length and decreasing fiber width. According to Salmén et al. (1987a), the shrinkage potential of freely dried sheets with curled fibers is larger than with straight fibers. The cellulose microfibril angle (MFA) has a strong positive correlation with hygroexpansion for handsheets made of a specified pine species, Courchene et al. (2006). Larsson and Wågberg (2008) found out that the fiber-fiber joint contact area does not influence the dimensional stability of sheets dried under constraint.

Drying history

Drying conditions have a major impact on the hygroexpansive behavior of the sheet, the effect is greater on hygroexpansion than on other mechanical properties, Salmén et al. (1993) Another important feature of hygroexpansion is its dependence of the humidity history, Uesaka et al. (1989). When the paper sheet has been dried under restraint, which is the case for normal factory made papers, it shows irreversible shrinkage under humidity cycling due to release of stresses that have been introduced during the drying, Uesaka et al. (1991). Salmén et al. (1987b) showed that hygroexpansion depends on the drying restraint conditions over the whole range of solids content 30-100 %. Nanko and Tada (1995) explained the irreversible shrinkage with the behaviour of the microfibrils. Under restrained drying the movement and thus hydrogen bond formation of microfibrils is restricted, and the resulting packing of fibrils is not optimal. During water absorption, water molecules break hydrogen bonds and the fibrils are allowed to

move and reach a more stable position, which causes a large shrinkage of the fibre wall. After the internal strains created during manufacturing are released, the subsequent moisture cycling results in reversible shrinking and expansion of the sheet.

Raw materials

The furnish composition has an effect on hygroexpansion. For restrained-dried sheets, the level of hygroexpansivity is similar for mechanical and chemical pulps, Nanri and Uesaka (1993). Non-filled sheets like solid board medium, show larger hygroexpansion than filled sheets in cross-machine direction due to filler particles interfering the fiber-fider bondig. MD hygroexpansion is not affected by the filling of the sheet, Lyne et al. (1996). Coffin et al. (1999) simulated the recycling process by drying fibres, and found that the sheets from dried fibers show smaller hygroexpansion than those made from virgin fibers. Lamination of paper with inert films restrain the hygroexpansion of paper whether the film is on the outside or between the paper layers, George (1958).

Dynamic hygroexpansion

In some applications the speed of hygroexpansion is of relevance, not only the equilibrium value. Brecht (1962) shows that even a small velocity of air flow around the test piece during the test increases the strain rate. The expansion phase takes longer than the shrinkage phase. The half-value time to reach equilibrium both in expansion and in shrinkage increases when basis weight increases. Same equilibrium expansion or contraction values are reached independent of basis weight, Brecht (1962). Many of these results were later confirmed by the dynamic hygroexpansion studies by Niskanen et al. (1997). Diffusion can be divided in bulk diffusion inside the sheet and surface diffusion through the sheet surface, Niskanen et al. (1997). The bulk diffusion inside the sheet is more important for thick sheets.

Multi-layer/laminate approach

The material studied in this work is a multi-layer paperboard laminate. Carlsson (1981), Nordström et al. (1998) and Bortolin et al. (2002) all studied multi-ply boards, but their interest was out-of-plane hygroinstability. The grades they studied were not laminated. Carlson and Bortolin et al. developed a model based on classical lamination theory where each constituent ply is considered as a macroscopic homogeneous, elastic medium, and the required input data include the elastic and expansional properties as a function of the moisture content for each ply. Bortolin et al. (2002) adds a separate strain model to the main mechanical model to include the effects of process control inputs that contribute to the drying stresses. Nordström et al. (1998) assume large strains. Salmén et al. (1984) has also applied the composite laminate approach to study hygroexpansion. In their work paper is treated as a laminate where the ply properties are retrieved from properties of the constituent wood polymers.

Polyethylene coating

Low density polyethylene (LDPE) branched polymer that is used as a extrusion coating providing moisture barrier properties. The properties of LDPE depend on the co-polymerisation, additives and processing, and testing should be done to describe the material in question. Here are some indicative properties of LDPE, Soroka (2009):

moisture vapor transmission rate (MVTR) 15-20 g/m^2/24 h (0/90 % RH, 38 °C, 25 µm film), tensile strength 6.9 – 15.8 MN/m^2, elongation at break 200-600 %.

For hygroscopic materials, there is an interaction between the specimen and the surrounding air due to the coupling between the diffusion of moisture in paper and the transfer of sorption heat, Niskanen et al. (1997). A surface boundary layer is formed on the sheet surface. During adsorption, the flux of moisture through the surface is reduced because the heat of adsorption raises the temperature on the surface and thus reduces the air humidty. The boundary layer effects the moisture transport also in desorption. Diffusion can be divided to bulk diffusion inside the sheet and surface diffusion through the sheet surface, Niskanen et al. (1997). Bulk diffusion inside the sheet is more important on thick sheets. The simulations of Lavrykov et al. (2004) show how for a copy paper sheet (thickness 0.1 mm), the moisture diffuses primarily through the sheet planes and diffusion through edges can be neglected. All phenomena related to the sheet surface are reduced in magnitude when the paperboard has barrier coating.

3. Experimental

The solid fiberboard grade

The paperboard studied is a unidirectionally stacked heavy-duty solid board. The four middle layers are made of 100 % recycled fiber and they are heavily internally sized. The outer layers on both sides are made of bleached machine finished kraft paper. The kraft papers have a double extrusion coated low-density polyethylene layer. The six paper and paperboard layers are glued together in an industrial lamination process. The glue used in lamination contains poly-vinyl alcohol (PVA) as an active agent, clay, additives and water. The solids content of the liquid glue used in lamination is 24 %.

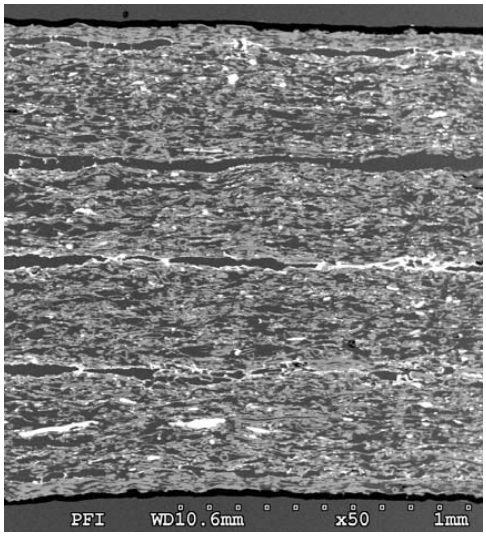

Figure 1. SEM picture of the solid fiberboard.

Figure 1 shows a SEM picture of the cross section of the combined board. For getting the idea of the material geometry, the grammage and the thickness of the layers are given in Table 1. The thicknesses in Table 1 are based on thicknesses measurements of the layers before the lamination taking into account that the lamination process compresses the layers 11 %. No thickness is given for the non-homogeneous adhesive layers.

Table 1. Material parameters of the solid fiberboard. (*) Indicative thicknesses based on thickness measurements of the layers before lamination.

	Name of the layer	Grammage [g/m^2]	Thickness(*) [mm]
1	Polyethylene coating	20	0.02
2	Kraft paper 1	60	0.07
3	Adhesion layer 1	10	
4	Middle layer 1	250	0.39
5	Adhesion layer 2	10	
6	Middle layer 2	250	0.39
7	Adhesion layer 3	10	
8	Middle layer 3	250	0.39
9	Adhesion layer 4	10	
10	Middle layer 4	250	0.39
11	Adhesion layer 5	10	
12	Kraft paper 2	60	0.07
13	Polyethylene coating	20	0.02
	Solid fiberboard	1220	1.73

Hygroexpansion measurement

The hygroexpansion was tested using a Lorentzen & Wettre micrometer system (type 3-2) shown in Figure 2. The system consists of a horizontal support for eight 15 mm × 200 mm test pieces that are clamped at the upper end. A 45 g weight is attached on the lower end of the test stripe. The length of the specimen is measured by lowering it with a micrometer screw. The needle of the weight closes an electric circuit when it touches the frame of the machine.

The hygroexpansion tester is attached to a climate chamber via a 1700 mm long tube (Ø 15 mm) that has a fan in the middle. The chamber is composed of two interconnected cabins (main cabin 700 mm × 700 mm × 1100 mm, side cabin 760 mm × 520 mm × 470 mm). Water vapor (90 ± 3 % RH, 27 °C) is created in the chamber and lead through the tube into the cylinder that encloses the specimens. The devices are located in a standard climate room. Relative humidity inside the cylinder is not controlled directly, but is measured. Measurements show that the humidity was 100±2 % RH. Temperature is not controlled or measured.

Hygroexpansion of MD and CD samples was measured during one relative humidity cycle (50 → 100 → 50 % RH). The test pieces were cut with a knife from A4 size sheets that had been stored at standard climate for months after lamination. To create the step change from 50 % RH to 100 % RH, the cylinder is put around the samples while the climate inside the chamber was maintained at 90 % RH/27 °C. To create the

opposite step in relative humidity, the climate preserving cylinder is removed from the hygroexpansion tester. The humidity drops immediately.

Figure 2. The micrometer tester used in hygroexpansion tests without the climate preserving cylinder around the clamps.

To observe the effect of the extruded polyethylene on the hygroexpansion, the polyethylene coated kraft paper was manually peeled off, and the remaining board was tested (three MD, four CD strips). As Figure 1 shows, there are voids in the glue layer that joins the kraft paper and the paperboard layer beneath. The white colored kraft paper could be separated with only traces of white fibers on the brown paperboard. Removing the coated krat papers drops the grammage from the remaining combined board from 1220 g/m^2 to 1060 g/m^2.

4. Results

The polyethylene coating acts as a barrier material against moisture transfer through the planes. The mechanisms of permeation through the coating include (a) flow through pores, capillaries, pinholes, and other defects; (b) activated diffusion through the intact polymer films, Stannett (1973). For water vapor, the diffusion through the film provides the main flux. Water vapor transmission rate (WVTR) for a 23 μm thick polyethylene film is 2.8 g/m^2/24 h (driving force 1.3 kPa), Piergiovanni et al. (1995). The corresponding diffusivity value is $8 \cdot 10^{-11}$ m^2/s. Hashemi et al. (1997) reports in-plane diffusivity values of $2.5 \cdot 10^{-7}$ – $17.5 \cdot 10^{-7}$ m^2/s for kraft handsheets (grammage 60 g/m^2, moisture content range 0.2-1 kg(water)/kg(fiber), temperature 25 °C). The materials and thicknesses are not completely comparable to the solid fiberboard studied here. Comparison of the diffusivities show that major part of the moisture penetrates through the open edges of the board.

After a step change from 50 % RH to 90 % RH, the moisture content of a 15 mm × 210 mm size PE coated board sample is stable after 17 hours (Figure 3). For the samples where the polyethylene is peeled off, the penetration occurs not only through the edges but also in the transverse direction through the planes, and the moisture content stabilizes faster than in Figure 3.

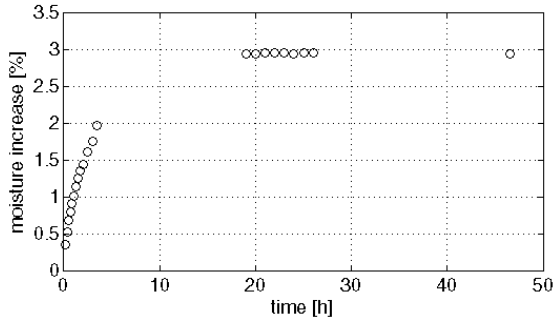

Figure 3. Moisture content increase of a PE coated board sample (size 15 mm × 210 mm) after a step change in relative humidity from 50 % RH to 90 % RH. The equilibrium moisture content at 50 % RH is 8.0 %.

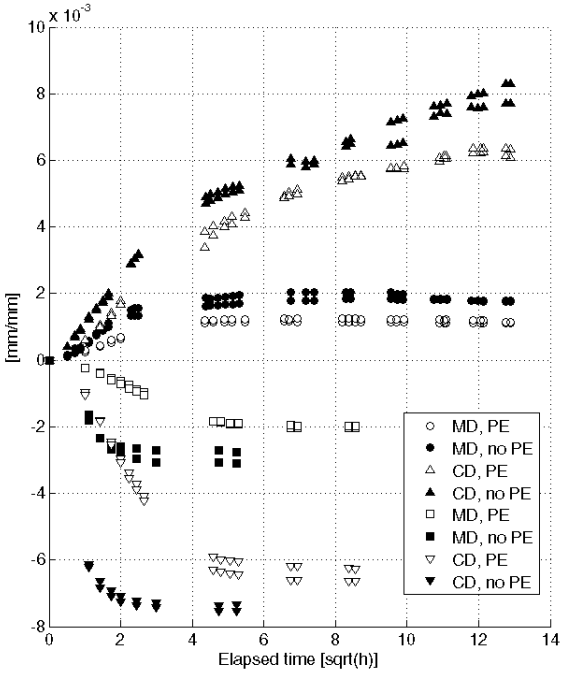

Figure 4. Hygroexpansion of the solid fiberboard with and without polyethylene coating in CD and MD in sorption phase (the curves above the zero displacement) and in desorption phase (the curves below the zero displacement line).

The results of the one-dimensional hygroexpansion tests are shown in Figure 4. After the step change in relative humidity, the rate of change in strain is very fast especially for the desorption samples. By plotting the hygroexpansion against square root of time, these fast initial phenomena are emphasized. The curves describe one humidity cycle from 50 to 100 % RH (sorption) and back to 50 % RH (desorption) with and without polyethylene coating on the solid board. The sorption curves are above, and the desorption curves below the zero hygroexpansion line.

The following parameters were estimated form the data: maximum strain, time elapsed to constant strain (time to equilibrium), and hygroexpansion coefficient. The maximum strain is the average of last three values. The time to equilibrium is approximated from the curves without curve fitting. Results for CD expansion are left out due to large variance in the data.

Table 2. Maximum hygroexpansive strain, approximate time to equilibrium and hygroexpansion coefficient of the solid fiberboard in MD and CD and in sorption and desorption phases. No results are reported for the CD behaviour in sorption due to uncertainties in measurement.

	Max strain [%]		**Time to equilibrium [h]**				**Hygroexpansion coeff. [%/% RH]**	
Solid board	MD	CD	MD sorb	MD des	CD sorp	CD des	MD sorb	CD sorp
With PE	0.12	--	16	27	--	27	0.0023	--
Without PE	0.18	--	16	10	--	10	0.0036	--

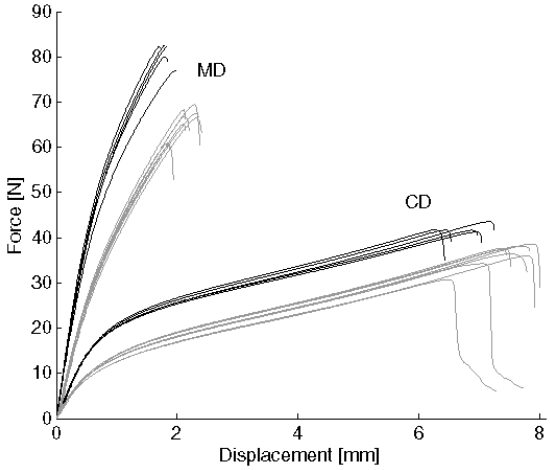

Figure 5. Force-displacement curves of polyethylene coated kraft paper in 50 %RH (black line) and 90 % RH (grey line). Test length 100 mm, test width 15 mm.

Tensile properties of the polyethylene coated kraft paper were measured in 50 % RH and 90 %RH with a Zwick tensile tester according to ISO (1924-2:1994) (test speed 25 mm/min, sample width 15 mm, sample length 100 mm). Samples were conditioned 3 days in 90 %RH prior to testing. Samples were held in a plastic bag, and taken one by

one from testing, which occurred in standard climate (appr. 45 sec/test). Figure 5 shows the force-displacement curve of the PE coated kraft paper. Based on the curves, elastic moduli were calculated for the MD samples: 580 MPa (50 % RH), 360 MPa (90 % RH) and for the CD samples: 210 MPa (50 % RH), 150 MPa (90 % RH). The thickness of the coated paper was 0.10 mm in both humidities.

5. Discussion

This study gives answers to two questions: how much the polyethylene restricts the hygroexpansion of the solid fiberboard, and what is the role of hygroexpansion in during the package life-time. There are many unknown factors concerning the material that limit commenting the fundamental phenomena during hygroexpansion. The glue layer limits the moisture transfer in z-direction. It might have an effect also in in-plane mechanical properties of the combined board since the glue is dried on paperboard surfaces as a layer.

The polyethylene coating slows down the hygroexpansion of the solid fiberboard. The effect is more drastic in desorption than in sorption. Both in MD and CD desorption, the new equilibrium strain is reached almost in one third of the time that was needed when the polyethylene coating was on. Absence of the plastic layer allows the samples to contract 15 % (CD) and 44 % (MD) more. In sorption, the shape of the expansion curve with and without the PE layers seems the same both in both material directions. The permanent MD strain difference with and without PE is 59 % in MD.

For sorption of moisture by PE coated board, the observed time evolution of hygroexpansive strains to their equilibrium value is different in CD vs. MD. The MD strains develop considerably faster than the CD strains, and approximately in pace with the moisture content. CD strains need more than five times more time to reach equilibrium length. Time evolution of the strains doesn't thus occur in pace with the moisture content. In desorption of PE coated board, the MD and CD strains need approximately equal time, 30 hours, to develop to the equilibrium.

The difference in MD and CD stain development was observed by Brecht (1962). Niskanen et al. (1997) adds a fiber-level explanation to the same observation. They present that the bonding geometry affects the slow expansion in CD direction. A typical fiber lying in CD direction has been shrunk during drying and makes quite large bonded areas with the contacting fibers. The expansion of that kind of fiber bond involves plastic flow of the contracted fiber section in the bonds, which slows down the expansion compared to a straight MD fiber bond. The other explanation Niskanen et al. give is that rapid release in internal stress in MD fibers. Also Lavrykov et al. (2004) verifies the phenomenon experimentally and explains it simply by introducing a compressive residual stress into a simulation model. The compressive residual stress is released during the hygroexpansion, which leads to lower equilibrium strain and decreased strain rate in MD. The results presented here don't provide basis for commenting fiber level phenomena.

Niskanen et al. (1997) and Lavrykov et al. (2004) report a sigmoid shape in their data from measurements of single fluting and linerboards sheets ranging from 127 to 336 g/m^2, when the relative hygroexpansion is plotted agaist square root of time. According to Lavrykov et al. (2004), the sigmoid behavior is due to the interplay of diffusion with the pore and fiber system, boundary layers and the humidity changes in the surrounding air.

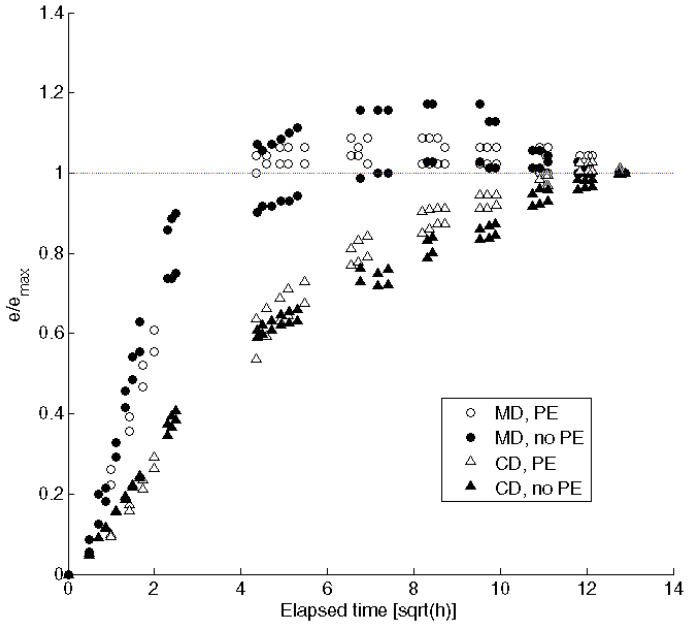

Figure 6. Transient relative hygroexpansion of solid fiberboard in CD and MD with and without PE coated paper in sorption.

Figure 6 shows the relative hygroexpansion of the solid board for the sorption phase. There are readings exceeding the limit value one, since the hygroexpansion was normalized by the last measurement value of the series in question. There is very little sigmoidal shape seen in the curves, even when the board is not PE coated. It seems that the phenomena occurring at the interface between the material surface and surrounding air are insignificant compared to the sorption lengths. In-plane moisture transport is significant in this material grade. In in-plane direction the external mass transfer resistances are insignificant compared to the internal mass transfer resistance of the material itself.

Typical in-plane hygroexpansion coefficients for paper materials are in the ranges of 0.002–0.004 %/% RH (MD) and 0.008–0.02 %/% RH (CD) according to Rutland (1987). Kajanto and Niskanen (1996) report similar ranges 0.002–0.003 %/% RH (MD) and 0.009–0.02 %/% RH (CD) for paper webs. The coefficient measured in this work, 0.0023 %/% RH (MD with PE) fit within the same range.

During the transportation, the box experiences mainly the sorption phase. The boxes are converted and stored in temperature and humidity close to standard climate, and used in the climate of 100 % RH/ 4 °C. In theory, box continues to expand six days out of the eight days of transportation. Temperature effects were not studied.

6. Conclusion

Hygroexpansion of multilayer solid board with and without the polyethylene coating was measured with a micrometer tester. One moisture cycle from 50 % RH to 100 % RH and back to 50 % RH was observed. The polyethylene layer restricts the solid board approximately 13 % in CD contraction, insufficient data on expansion), and 34 % in MD contraction and expansion. Without PE layers in desorption, the equilibrium contraction is reached in one third of the time required when PE layer is on. No difference in time to equilibrium expansion was observed in sorption. For PE coated samples in sorption, the moisture content stabilises in pace with MD strains, but CD strains needed ten times more time to reach the full strain. The tests without PE coating, show that the phenomena at the board/surrounding air surface are masked out with other features arising from the bulk structure of the combined board.

6. Acknowledgements

The Research Council of Norway, Peterson AS, Eka Chemicals AB, and the Foundation of Paper and Fiber Reserch Institute in Trondheim, Norway (PFI) are greatfully acknowledged for the financial support.

References

Bortolin, G., Gutman, P. O. & Nilsson, B. (2002) Modeling of out-of-plane hygroinstability of multi-ply paperboard. *Proceedings Fifteenth International Symposium on Mathematical Theory of Networks and Systems.* Notre Dame, IN, USA, Univ. Notre Dame.

Brecht, W. (1962) Effect of structure on major aspects of paper behaviour with fluids. IN BOLAM, F. (Ed. *The Formation and structure of paper: transactions of the symposium held at Oxford, September 1961.* London, British Paper and Board Makers' Association, Technical Section.

Carlsson, L. (1981) Out-of-plane hygroinstability of multi-ply paperboard. *Fibre Science and Technology,* 14(3)**,** 201-212.

Coffin, D. W., Habeger, C. J. & Waterhouse, J. F. (1999) Effect of recycling fibers on accelerated creep. *IPST Technical paper series, number 829.* Atlanta, Georgia, IPST Technical paper series, number 829, Institute of paper science and Technology.

Courchene, C. E., Peter, G. F. & Litvay, J. (2006) Cellulose microfibril angle as a determinant of paper strength and hygroexpansivity in Pinus Taeda L. *Wood and Fiber Science,* 38(1)**,** 112-120.

Gallay, W. (1973) Stability of dimensions and form of paper. *Tappi,* 56(11)**,** 54-63.

George, H. O. (1958) Methods of affecting the dimensional stability of paper. *Tappi,* 41(1)**,** 31-33.

Hashemi, S. J., Gomes, V. G., Crotogino, R. H. & Douglas, W. J. M. (1997) In-plane diffusivity of moisture in paper. *Drying Technology,* 15(2)**,** 265-294.

Horwarth, P. & Schindler, M. K. (1985) The areal distribution of liquid penetration of paper. *Papermaking raw materials. Their interaction with the production processes and their effect on paper properties.* . Oxford, UK.

Iso (1924-2:1994) Paper and board — Determination of tensile properties — Part 2: Constant rate of elongation method.

Kajanto, I. M. & Niskanen, K. J. (1996) Optical measurment of dimensional stability. *1996 Progress in paper physics - A seminar proceedings.* Stockholm, Sweden.

Kirwan, M. J. (2005) Solid fibreboard packaging. IN KIRWAN, M. J. (Ed.) *Paper and paperboard packaging technology.* Oxford, Wiley-Blackwell Publ.

Larsson, P. A. & Wågberg, L. (2008) Influence of fibre-fibre joint properties on the dimensional stability of paper. *Cellulose,* 15(4)**,** 515-525.

Lavrykov, S. A., Ramarao, B. V. & Lyne, O. L. (2004) The planar transient hygroexpansion of copy paper: Experiments and analysis. *Nordic Pulp and Paper Research Journal,* 19(2)**,** 183-190.

Lyne, A. L., Fellers, C. & Kolseth, P. (1996) The effect of filler on hygroexpansivity. *Nordic Pulp & Paper Research Journal,* 11(3)**,** 152-152.

Mies, W., Potter, J., Miller, D. & Kenney, J. (Eds.) (2006) *Global Pulp & Paper Fact & Price Book 2006*, RISI.

Nanko, H. & Tada, Y. (1995) Mechanisms of hygroexpansion of paper. *International Paper Physics Conference 1995.* Niagara-on-the-lake, Ontario, Canada, CPPA and Tappi.

Nanri, Y. & Uesaka, T. (1993) Dimensional stability of mechanical pulps - drying shrinkage and hygroexpansivity. *Tappi,* 76(6)**,** 62-66.

Niskanen, K. J., Kuskowski, S. J. & Bronkhorst, C. A. (1997) Dynamic hygroexpansion of paperboards. *Nordic Pulp & Paper Research Journal,* 12(2)**,** 103-110.

Nordström, A., Gudmundson, P. & Carlsson, L. A. (1998) Influence of sheet dimensions on curl of paper. *Journal of Pulp and Paper Science,* 24(1)**,** 18-25.

Piergiovanni, L., Fava, P. & Siciliano, A. (1995) Mathematical model for the prediction of water vapour transmission rate at different temperature and relative humidity combinations. *Packaging Technology and Science,* 8(2)**,** 73-83.

Rutland, D. F. (1987) Dimensional stability and curl - a review of the causes. IN AL, K. E. (Ed.) *Design criteria for paper performance, STFI-meddelande A 969,1987.*

Salmén, L., Boman, R., Fellers, C. & Htun, M. (1987a) The implications of fiber and sheet structure for the hygroexpansivity of paper. *Nordic Pulp and Paper Research Journal,* 2(4)**,** 127-131.

Salmén, L., Carlsson, L., Ruvo, A. D., Fellers, C. & Htun, M. (1984) A treatise on the elastic and hygroexpansional properties of paper by a composite laminate approach. *Fibre Science and Technology,* 20(4)**,** 283-296.

Salmén, L., Fellers, C. & Htun, M. (1987b) The development and release of dried-in stresses in paper. *Nordic Pulp & Paper Research Journal,* 2(2)**,** 44-48.

Salmén, L., Fellers, C. & Htun, M. (1993) The in-plane and out-of-plane hygroexpansional properties of paper. *Products of Papermaking.* Cambridge, UK, Pira Int.

Soroka, W. (2009) Common packaging plastics (Ch. 10). IN EMBLEM, A. & EMBLEM, H. (Eds.) *Fundamentals of packaging technology.* Leichestershire, UK, The Institute of Packaging, First published 1995 by IOPP, USA.

Stannett, V. T. (1973) Fundamentals of barrier properties. *Fundamental Properties of Paper Relating to Its Uses, Symposium Transactions.*

Swanson, S. W. (1989) Mechanisms of paper wetting. IN REYNOLDS, W. F. (Ed.) *The Sizing of Paper, 2nd ed.* Atlanta, GA, USA, TAPPI Press.

Uesaka, T. (2002) Dimensional stability and environmental effects on paper properties. IN MARK, R. E., HABEGER, C. C., BORCH, J. & LYNE, M. B. (Eds.) *Handbook of Physical Testing of Paper.* New York Basel, Marcel Dekker Inc.

Uesaka, T., Kodaka, I., Okushima, S. & Fukuchi, R. (1989) History-dependent dimensional stability of paper. *Rheologica Acta,* 28(3)**,** 238-245.

Uesaka, T. & Moss, C. (1997) Effects of fibre morphology on hygroexpansivity of paper - A micromechanics approach. IN BAKER, C. G. (Ed. *The fundamentals of Papermaking Materials.* Cambridge, United kingdom, Pira International Ltd.

Uesaka, T., Moss, C. & Nanri, Y. (1991) The characterization of hygroexpansivity of paper. *1991 International Paper Physics Conference.* 22-26 Sept. 1991 at Kona, Hawaii.

Uesaka, T. & Qi, D. (1994) Hygroexpansivity of paper - Effects of fibre-to-fibre bonding. *Journal of Pulp and Paper Science,* 20(6)**,** J175-J179.